INTERDISCIPLINARY DOCTORAL SCHOOL

Faculty of Mechanical Engineering

Gheorghe Alexandru VĂRDARU

Contributions to increasing the efficiency of solar collectors

SUMMARY

Scientific supervisor

Prof. Dr. Habil. Gabriela HUMINIC

BRAȘOV, 2025

ACKNOWLEDGEMENTS

This doctoral thesis is the result of an intense and dedicated period of work conducted at the Faculty of Mechanical Engineering, Transilvania University of Brașov. As I reflect on this journey, centered around an innovative and challenging subject for the academic community in Romania, I realize that it would not have been possible without the support and trust of several remarkable individuals.

First and foremost, I would like to express my deepest gratitude to my supervisor, Professor Dr. habil. Eng. Gabriela Huminic, for her steadfast guidance and patience throughout the entire process. Her expertise and openness to new ideas gave me a clear vision and continuously motivated me, even during challenging times. I am also grateful for the opportunity to contribute to her research project, which provided the foundation for my entire doctoral thesis.

Access to the appropriate research infrastructure was crucial for the successful completion of my research and for this, I extend my thanks to Professor Angel Huminic (Transilvania University of Brașov).

I would also like to sincerely thank researchers Claudiu Fleacă, Florian Dumitrache and Ioan Morjan (National Institute for Laser, Plasma and Radiation Physics) for preparing the multiphase fluids used in the experiments for this thesis. Without their assistance, the completion of these experiments and the overall progress of this work would not have been possible.

I wish to express my gratitude to the members of the Academic Integrity and Advisory Committee for their support, as well as for their valuable feedback on this work.

Lastly, I want to express my profound gratitude to my parents, who have always stood by my side and supported me unconditionally throughout this entire journey. I thank my father for his guidance, patience and the trust he placed in me at every step. I am deeply grateful to my mother for her love, unwavering support and the sacrifices she has made for me over the years. I would also like to thank my brother for his constant encouragement and support, which have meant the world to me.

With gratitude,

Vărdaru Gheorghe Alexandru

TABLE OF CONTENTS

Abbreviations

Al_2O_3 – aluminum oxide

γ-Al_2O_3 – gamma alumina, a specific form of aluminum oxide

ASHRAE – American Society of Heating, Refrigerating and Air-Conditioning Engineers

CNT – carbon nanotubes

CuO – copper oxide

EG – ethylene glycol

Fe – iron

Fe_3O_4 – iron oxide or magnetite

GNP – graphene nanoparticles

LSPR – localized surface plasmon resonance

MgO – magnesium oxide

MWCNT – multi-walled carbon nanotubes

NIST – National Institute of Standards and Technology

Pt – platinum

PV/T – photovoltaic/thermal

SiC – silicon carbide

wt - mass concentration

1. TABLE OF CONTENTS OF THE DOCTORAL THESIS

2. THE DOCTORAL THESIS TOPIC AND ITS RELEVANT FIELD

Against the backdrop of decreasing conventional energy resources and the growing demand for sustainable solutions, identifying efficient methods for energy production and usage has become a global necessity. Climate change and the environmental impact of fossil fuels have accelerated interest in renewable sources, such as solar energy, which presents a promising alternative for a sustainable future.

This thesis, titled "Contributions to the Enhancement of Solar Collector Efficiency", falls within the field of solar energy and focuses on the use of multiphase fluids in Direct Absorption Solar Collectors (DASCs). Solar collectors, essential for capturing and converting solar energy into heat, require efficiency improvements and nanotechnology offers innovative solutions.

Multiphase fluids consist of solid nanoparticles dispersed in a base fluid (water, ethylene glycol (EG), or water-EG mixtures). These fluids, which may contain one or more types of nanoparticles, exhibit superior properties, such as enhanced thermal conductivity and high solar radiation absorption capacity-characteristics that make them ideal for use in DASCs.

The growing interest in multiphase fluids, both in research and industry, is due to their potential to improve the efficiency of solar equipment and reduce environmental impact. Recent advances in this field provide new insights into the mechanisms that enhance heat transfer and improve solar energy conversion.

The main arguments justifying the choice of this topic are:

- **Global energy crisis**: In the context of the global energy crisis, improving the efficiency of energy production, transfer and storage systems has become essential. Multiphase fluids represent an innovative solution that can help reduce energy consumption and carbon emissions, a crucial aspect in the fight against global warming.
- **Rapid evolution of nanotechnology**: The rapid advancement of nanotechnologies, particularly in the area of multiphase fluids, offers new opportunities in fields such as energy. Multiphase fluids, which combine various types of nanoparticles, exhibit enhanced performance and are of significant interest in solar energy capture and utilization applications.
- **Global interest in multiphase fluid research**: On a global scale, research on multiphase fluids benefits from substantial resources, including government funding, private sector investments, modern research infrastructure, access to cutting-edge laboratory equipment and interdisciplinary collaborations between universities and research institutes. Various funding programs, such as those supported by the European Union through FP7 and Horizon 2020, have supported the development of nanotechnologies, including multiphase fluids, for a wide range of energy applications. This interest highlights the potential of multiphase fluids to contribute to future energy efficiency improvements.
- **Impact and potential**: Multiphase fluids offer significant benefits in terms of energy efficiency, cost reduction and minimizing negative environmental impacts, opening new perspectives for the use of solar energy.

3. OBJECTIVES OF THE DOCTORAL THESIS

The experimental research aims to enhance the efficiency of solar collectors by identifying and implementing innovative solutions to optimize heat transfer. These solutions include the development and optimization of working fluids used in energy systems, with the goal of improving thermal performance and enhancing sustainability in the capture and utilization of solar energy.
This thesis proposes the development of multiphase fluids, consisting of a base fluid (water and a water-EG mixture) and a solid phase made up of metallic and oxide nanoparticles with nanometric-scale dimensions.
An innovative aspect of the research is the use of silver (Ag) nanoparticles combined with reduced graphene oxide (rGO), iron oxide (Fe_2O_3), iron carbide (FeC) and titanium dioxide (TiO_2). These combinations are chosen for their ability to significantly increase thermal conductivity, thereby optimizing heat transfer efficiency.

The overall objective of the thesis is to develop multiphase fluids with enhanced thermophysical, optical and photothermal conversion properties, making them effective for thermal applications, particularly in Direct Absorption Solar Collectors (DASCs).

The study thoroughly analyzes the behavior of multiphase fluids, aiming to determine their performance and potential for application in optimizing energy efficiency.

The specific objectives of the thesis are:

- To develop experimental techniques for characterizing thermophysical properties (thermal conductivity, viscosity, density and surface tension).
- To experimentally investigate the optical properties (transmission and extinction coefficients) of heat transfer fluids.
- Carrying out an experimental study on the photothermal conversion efficiency of heat transfer fluids.

The main stages of the research presented in the thesis are:

- Theoretical and experimental study of the thermophysical properties of multiphase fluids based on Ag nanoparticles with rGO, Fe_2O_3, TiO_2 and FeC in water and in a water+EG mixture.
- Development of empirical models to estimate thermophysical properties based on nanoparticle concentration and temperature.
- Theoretical and experimental study of the optical properties of multiphase fluids.
- Theoretical and experimental study of the photothermal conversion properties of multiphase fluids.
- Comparative analysis of the results obtained for multiphase fluids based on water and those with a water+EG mixture.

4. STRUCTURE OF THE DOCTORAL THESIS

The doctoral thesis is organized into seven chapters.

Chapter 1: Introduction provides an overview of the thesis topic, highlighting the importance of multiphase fluids in various application fields. It also presents the research objectives, which aim to deepen the understanding of the phenomena involved and develop multiphase fluids with enhanced properties for use in Direct Absorption Solar Collectors (DASCs).

Chapter 2: Current state of the field of multiphase working fluids reviews recent research in this field, emphasizing the fundamental aspects of multiphase fluids. The first section defines the concept of multiphase fluids, highlighting their complexity and importance in various energy applications.

This chapter also examines the thermophysical properties of these fluids, such as thermal conductivity, dynamic viscosity, density, surface tension and specific heat. Understanding these properties is essential for evaluating the behavior of multiphase fluids under different temperature and concentration conditions, as well as for assessing their impact on performance in DASCs.

Additionally, the chapter analyzes theoretical studies related to the optical properties and photothermal conversion of multiphase fluids-critical aspects in energy applications.

It provides a general overview of recent progress in the field, laying the foundation for the subsequent research and discussions in the thesis.

Chapter 3: Preparation and investigation methods of multiphase fluids provides a description of the process of preparing these fluids, presenting the materials used, their characteristics and the role of surfactants in ensuring the stability and homogeneity of the mixtures.

This chapter also includes a detailed description of the methods employed to investigate the thermophysical, optical and photothermal conversion properties of the multiphase fluids studied, as well as the equipment used in the experiments.

Chapter 4: Experimental study of thermophysical properties focuses on analyzing key thermophysical properties, such as thermal conductivity, dynamic viscosity, density, surface tension and specific heat.

Experimental results are presented for both the base fluids and the multiphase fluids, with the aim of assessing the influence of nanoparticle concentration on the properties of the base fluids (water and a water-EG mixture in a 1:1 ratio, each containing 0.4 g/l and 4 g/l of CMCNa, respectively).

Comparing the experimental results with those obtained from theoretical models allows for an evaluation of their consistency, while comparisons with empirical models help highlight the differences between single-component and two-component multiphase fluids. This comparison illustrates the improvements brought by two-component multiphase fluids over their single-component counterparts.

The conclusions obtained from these analyses highlight the improvements made by the most efficient combinations of Ag-rGO, Ag-Fe_2O_3, Ag-FeC and Ag-TiO_2 nanoparticles on the thermophysical properties of the base fluids, the capability of the theoretical models used to predict these properties and the advantages of these nanoparticle combinations compared to others studied by other researchers.

Chapter 5: Experimental study of the optical properties of new multiphase fluids focuses on analyzing the optical behavior of these fluids, with particular attention to the influence of nanoparticle concentration on solar radiation absorption and transmission.

The study compares the base fluids with the multiphase fluids to assess the impact of nanoparticles on their optical performance. These comparisons specifically aim to evaluate the efficiency of the solar radiation absorption process, which is a crucial factor in improving the performance of solar collectors. Through comparative analysis, the nanoparticle combinations that provide the best optical characteristics, such as extinction coefficients and solar absorption, for use in DASCs are identified. This comparison process helps select the most effective multiphase fluids, contributing to the improvement of solar system performance.

The extinction coefficients and solar power absorption spectra for the fluids analyzed are calculated based on experimentally obtained transmission measurements.

Chapter 6: Experimental study of photothermal conversion characteristics focuses on assessing the performance of multiphase fluids in the photothermal conversion of solar radiation, emphasizing the influence of nanoparticle concentration on this process.

The effects of different nanoparticle combinations (such as Ag-rGO, Ag-Fe_2O_3, Ag-FeC and Ag-TiO_2) at various concentrations on the base fluids (water and a water-EG mixture) in the process of converting solar energy into heat are investigated. The improvements brought by nanoparticles are highlighted, providing a clearer understanding of their influence on photothermal conversion efficiency.

Chapter 7: Conclusions, personal contributions and research directions summarizes the main results obtained in the thesis, emphasizing their significance in the field of multiphase fluids used in DASCs. The author's contributions are presented, along with future research directions focusing on the use of the studied multiphase fluids in DASCs under real operating conditions.

In conclusion, this work makes significant contributions to the field of multiphase fluids used in DASCs. The experimental studies conducted have demonstrated the positive effects of nanoparticle combinations on the thermophysical, optical and photothermal conversion properties of multiphase fluids, showing their potential to improve the performance of solar collectors.

5. RESEARCH METHODOLOGY

The research methodology is based on an integrated approach, combining bibliographic analysis, laboratory experiments and the development of empirical models. The experimental results are then compared with both those obtained from theoretical models and those reported by other authors for similar fluids containing one or two of the components of interest.

Initially, a detailed analysis of 251 bibliographic references was conducted, selected from academic sources, specialized journals and relevant research papers in the fields of multiphase fluids, solar energy and nanotechnology. This analysis facilitated the identification of current trends, experimental methods and theoretical models employed in these fields.

Subsequently, experimental studies were carried out to evaluate the thermophysical properties (thermal conductivity, viscosity, density and surface tension), optical properties (transmittance and absorbance) and photothermal conversion characteristics of the base fluids (water and a water+EG mixture, with surfactants at concentrations of 0.4 and 4 g/l CMCNa), as well as the multiphase fluids (Ag-rGO, Ag-Fe_2O_3, Ag-FeC and Ag-TiO_2).

The experimental data obtained were used to develop empirical models to determine the thermophysical properties of the studied multiphase fluids. Each property was correlated with both temperature and concentration and the results from the empirical models were compared with those generated by existing theoretical models in the literature to validate their accuracy in estimating the thermophysical properties (thermal conductivity, viscosity and density) of two-component multiphase fluids.

Additionally, the experimental results were compared with those obtained from empirical models developed by other authors for the thermophysical properties (thermal conductivity, viscosity, density and surface tension) of multiphase fluids containing one or two of the components of interest. This comparison allowed for the evaluation of the improvements brought by the studied nanoparticle combinations (Ag-rGO, Ag-Fe_2O_3, Ag-FeC, Ag-TiO_2) in the same base fluids.

The specific heat of the multiphase fluids was calculated based on density measurements, using the theoretical model proposed by Takabi and his collaborators. The results obtained were compared with values derived from empirical models available in the literature for multiphase fluids containing one or two of the analyzed components.

Based on transmittance measurements, the extinction coefficients for both the base fluids and the multiphase fluids were calculated using Beer-Lambert's law. Using standard values from the AM1.5 solar spectrum and the transmittance of the fluids, the absorbed solar power spectra were determined.

Finally, to assess the photothermal conversion efficiency of the analyzed fluids, the equation $\eta = Q / (Gs*A*\Delta\tau)$ was used, where Q represents the total energy stored by the working fluid, Gs is the solar irradiance, A is the exposed surface area and $\Delta\tau$ is the exposure time to solar radiation. The results obtained were compared with existing data on photothermal conversion efficiency for other multiphase fluids containing one or more of the components of interest.

Thus, by combining these approaches-literature analysis, laboratory experiments, developed empirical models and comparisons with theoretical and empirical models from the literature-an in-depth understanding of the studied phenomena is achieved, significantly contributing to the enhancement of solar energy conversion system performance.

6. INTRODUCTION

6.1 The concept of multiphase working fluids

In recent years, research on multiphase working fluids has made significant advances in improving heat transfer and reducing environmental impact. These fluids play a crucial role in a variety of applications, from heating and cooling systems to industrial processes for photothermal energy conversion. The key characteristic of multiphase fluids is the simultaneous presence of two or more phases (liquid, gas, solid) (Figure 6.1), which allows them to enhance heat and mass transfer [1-3].

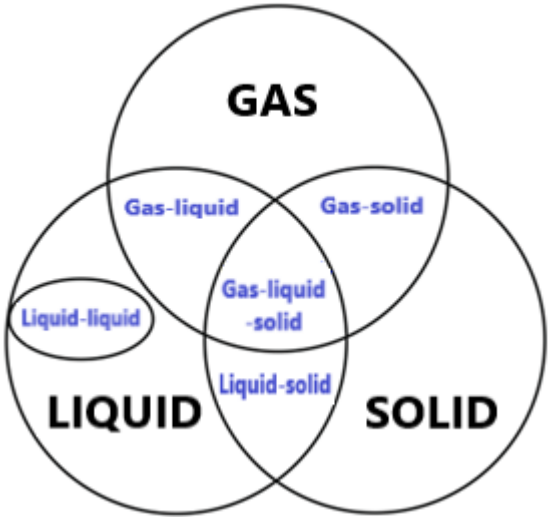

Figure 6.1 The component phases of a multiphase working fluid

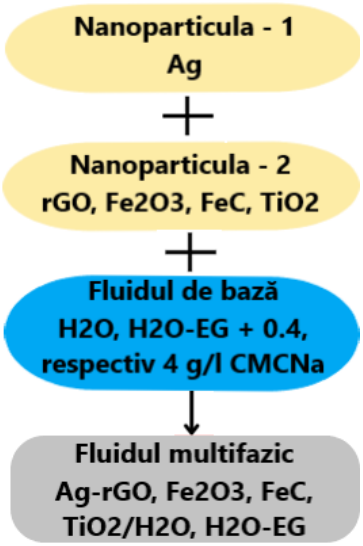

Figure 6.2 Components of the studied multiphase working fluids

Among the new research directions are multiphase fluids composed of metallic, oxide, or carbon-based nanoparticles dispersed in liquids such as water or water-EG mixtures. Silver nanoparticles combined with rGO, Fe_2O_3, FeC and TiO_2 (Figure 6.2) enhance the thermophysical properties of base fluids, increasing thermal conductivity and heat transfer efficiency. Additionally, their use reduces the size of cooling or heating equipment, saving space and costs, while also contributing to the reduction of carbon emissions.

6.2 Applications of multiphase fluids

In 1959, Richard Feynman paved the way for nanotechnology with his speech "There's Plenty of Room at the Bottom," where he anticipated the possibility of manufacturing materials at the atomic scale [4]. Today, nanotechnology is a rapidly expanding field with applications in both industry and research and multiphase fluids represent an important outcome of this development. These fluids have superior thermal properties compared to conventional fluids, making them ideal for heat transfer. By incorporating various combinations of nanoparticles into conventional fluids (water, EG, or water-EG mixtures), their optical properties are significantly enhanced. Examples of nanoparticle combinations include MgO-MWCNT, Al_2O_3-CNT, Ag-CNT, Fe_2O_3-CNT, etc. [5]. These combinations show great potential in applications such as solar collectors [6], where photothermal conversion efficiency is crucial.

Due to their thermal and optical performance, multiphase fluids are used in industrial applications such as heat pipes [7], radiators [8] and plate heat exchangers [9]. They are also used in thermal energy storage systems and contribute to increased efficiency in PV/T systems [10]. Nanotechnology promises innovative solutions for the energy challenges of the future, improving heat transfer efficiency, reducing costs and minimizing environmental impact.

6.3 Thermophysical properties of multiphase fluids

The main thermophysical properties that characterize multiphase fluids, as outlined in the literature, are:

- **Thermal conductivity**: This refers to the ability of a mixture composed of distinct phases (liquids, gases, or solids) to transfer heat through conduction. It reflects the efficiency with which thermal energy is transferred between the constituent phases when a temperature gradient is present [11]. By incorporating nanoparticles, the thermal conductivity of these fluids significantly increases compared to conventional fluids, which is crucial in heat dissipation applications such as cooling systems [12].
- **Dynamic viscosity**: This measures the resistance of a fluid to flow, influenced by the interactions between the multiple phases present (e.g., liquid-solid, liquid-gas), determining the flow behavior of the mixture under the action of external forces [13].
- **Density**: This represents the total mass of all the phases in the mixture relative to the volume occupied. It depends on the density of each constituent phase and can improve the fluid's ability to store and transfer thermal energy, but it can also affect the flow behavior in heat transfer systems [14].
- **Surface tension**: This is the force acting at the surface of a liquid, causing it to behave like an elastic film and resist the penetration of objects, due to the attractive forces between its molecules [15]. Modifying the surface tension by incorporating nanoparticles can enhance performance in applications such as micro-cooling and microfluidics [16].
- **Specific heat**: This refers to the amount of energy required to raise the temperature of one unit mass of a multiphase mixture by one degree Celsius or Kelvin, considering the specific heat of each phase and the thermal exchanges between them [11]. It determines how efficiently a multiphase fluid can store heat [17], having a significant impact on applications involving thermal energy storage and release [18].

Analyzing these properties is essential for improving the performance of multiphase fluids in fields that require thermal stability and high heat transfer efficiency.

6.4 Optical properties of multiphase working fluids

The most commonly used fluids for heat transfer, such as water, glycols and oils, do not efficiently absorb light in the ultraviolet (UV) and visible spectrum, absorbing only 13% of the received solar energy, according to recent studies [19]. Adding nanoparticles in very small quantities (less than 0.01 vol%) significantly improves the optical properties of these transparent fluids. The amount of nanoparticles incorporated into a fluid depends on the specific application and their presence results in increased light absorption. For instance, while water and many organic liquids are transparent in the

300-1500 nm wavelength range, they may exhibit significant absorption outside of this range [20, 21]. Multiphase fluids need to absorb a considerable amount of solar radiation to achieve optimal performance. Single-component multiphase fluids, such as carbon nanotubes, exhibit excellent optical properties [22, 23], but they are costly and present challenges in achieving uniform dispersion [24]. In contrast, ceramic oxides (Al_2O_3, CuO, TiO_2, SiC) show good dispersion and high absorption in the visible range (380-780 nm), but lower absorption in the near-infrared (780-1500 nm) [25]. The solar spectrum contains 53% of its energy in the visible range and 42% in the near-infrared, making it crucial to enhance absorption in both the visible and infrared spectra to optimize the efficiency of multiphase fluids. To overcome the limitations of single-component multiphase fluids, multiphase fluids made of two or more nanoparticles have been developed, offering superior optical properties [26, 27]. These fluids can ensure more efficient solar thermal absorption across a broad range of wavelengths by utilizing the complementary properties of different nanoparticles [28, 29]. Multiphase fluids can be optimized to capture solar radiation in both the visible and near-infrared regions, which are essential for solar collectors. The main optical properties that characterize multiphase fluids, according to the literature, are:

- **Transmittance**: This represents the ability of a fluid to allow light to pass through it, quantifying the fraction of incident light that is transmitted without being absorbed or scattered [26].
- **Absorbance**: This represents the ability of a fluid to absorb incident radiation and this property is essential in fields such as optics and photothermal energy conversion [27].

6.5 Photothermal conversion characteristics

The photothermal conversion of multiphase fluids involves the transformation of light energy into thermal energy through suspended particles or various phases within the fluid. The key characteristics that influence this photothermal conversion and are specific to multiphase fluids include [30]:

- **Light Absorption**: The ability of multiphase fluids to absorb radiation depends on the composition and structure of the phases, as well as the presence of nanoparticles.
- **Thermal Conductivity**: This plays a crucial role in the heat transfer generated by photothermal conversion. Depending on the constituent phases (solid, liquid, gas), this property varies and impacts the fluid's ability to dissipate heat.
- **Conversion Efficiency**: This varies depending on the absorption and thermal conductivity of the phases and nanoparticles can significantly enhance this process.
- **Specific Heat**: This affects the amount of thermal energy stored, with multiphase fluids exhibiting different specific heat values depending on the constituent phases.

The concept of the Direct Absorption Solar Collector (DASC) was proposed by Minardi and Chuang in 1975 [30]. The main characteristic of a DASC is the direct absorption of incident solar radiation by the working fluid volume within the system.

7. THERMOPHYSICAL PROPERTIES – EXPERIMENTAL RESULTS

The effects of temperature and concentration on the thermophysical properties of base fluids and multiphase fluids (thermal conductivity, dynamic viscosity, density, specific heat and surface tension) are presented and discussed. Measurements were carried out for distilled water, distilled water with 0.4 and 4 g/l CMCNa, a distilled water+EG (50:50) mixture, with and without CMCNa, as well as for multiphase fluids Ag-rGO, Ag-Fe_2O_3, Ag-FeC and Ag-TiO_2, in water and water+EG, at three nanoparticle concentrations and temperatures ranging from 293.15 to 323.15 K.

7.1 Thermal conductivity

7.1.1 Thermal conductivity of base fluids

In the first stage, the thermal conductivity of base fluids-water and a water+EG (1:1) mixture, with and without surfactant (0.4 and 4 g/l CMCNa) was measured at temperatures ranging from 293.15 to 323.15 K. The results were compared with reference data provided by NIST [31] and ASHRAE [32].
Figure 7.1 (a) shows the thermal conductivity of water, both with and without surfactant, in comparison to the NIST values. The thermal conductivity of water increases with temperature and the experimental values for water without surfactant closely match the NIST data, with a maximum deviation of only 0.552%. Furthermore, adding surfactant to the water (0.4 and 4 g/l CMCNa) had a minimal effect on thermal conductivity, with an average increase of 0.703% and 1.360%, respectively [33].
Figure 7.1 (b) presents the thermal conductivity values for the water+EG mixture, with and without surfactant and compares the experimental data to the values provided by ASHRAE. The thermal conductivity of the water+EG solution without surfactant is very close to the ASHRAE data, with a maximum deviation of 1.319% [34]. The addition of surfactant (0.4 and 4 g/l CMCNa) resulted in a significant increase in conductivity by 5.756% and 9.647%, respectively.
This behavior, where thermal conductivity increases with temperature, is characteristic of liquids.

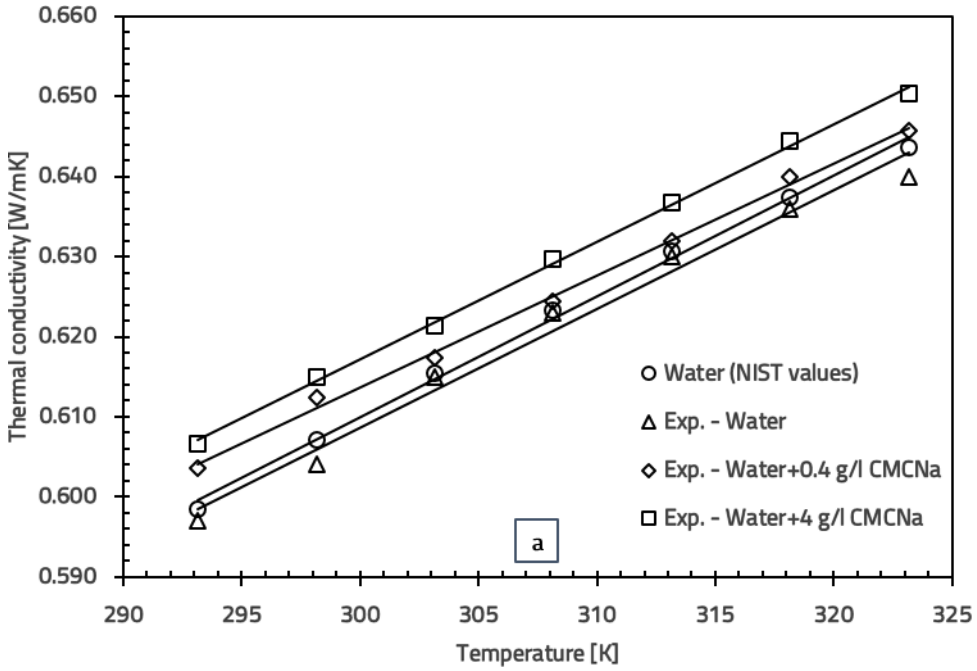

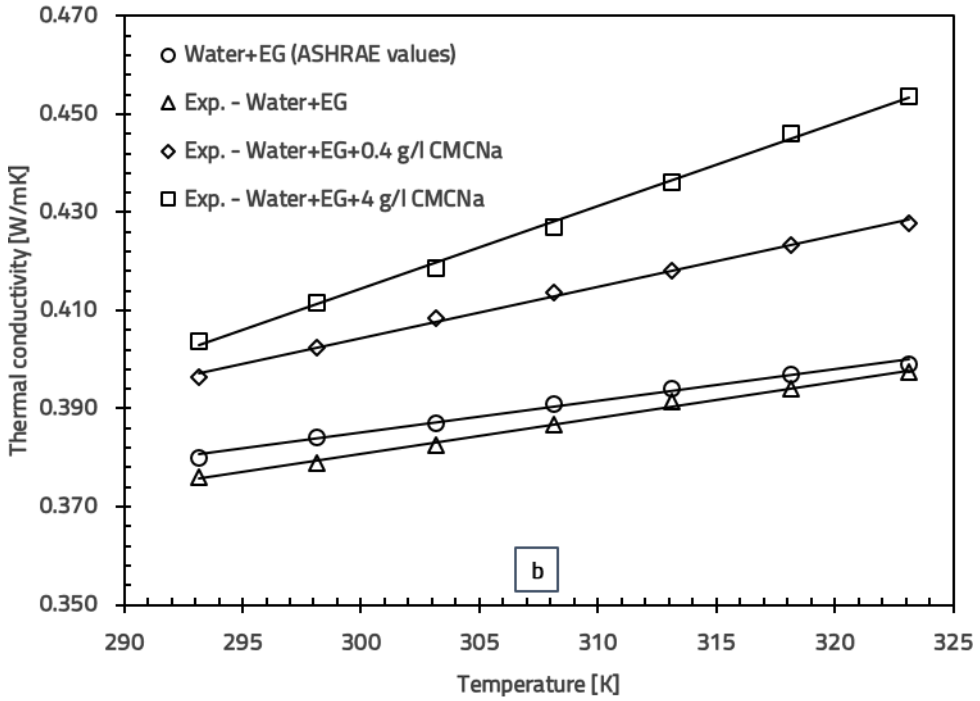

Figure 7.1. Validation of the thermal conductivity measurements for: a) water; b) water+EG

7.1.2 Thermal conductivity of multiphase fluids

In the second stage, the thermal conductivities of multiphase fluids were measured. Figure 7.2 shows the variation in thermal conductivity (TC) of the multiphase fluids Ag-rGO, Ag-Fe_2O_3, Ag-FeC and Ag-TiO_2 based on water, at different mass concentrations as a function of temperature. To provide a comprehensive overview, the TC values of the multiphase fluids were compared to those of the base fluid (water with 0.4 and 4 g/l CMCNa). As shown in Figure 7.2, the maximum TC value for the water-based multiphase fluids was obtained at concentrations of 0.1 and 1.0 wt% and a temperature of 323.15 K.

The effect of temperature on the TC of the Ag-rGO/water multiphase fluid at different concentrations is shown in Figure 7.2 (a). At a concentration of 0.050 wt%, temperature causes an 11.68% increase in TC between 293.15 and 323.15 K. At higher concentrations (0.075 and 0.1 wt%), the temperature effect is less pronounced, with increases of 9.55% and 9.22%. The increase in nanoparticle concentration (0.050-0.1 wt%) improves the TC of the base fluid (water + 0.4 g/l CMCNa) by 1.66%, 5.25% and 8.39% at 293.15 K and by 6.14%, 7.80% and 10.69% at 323.15 K. This indicates that the effect of concentration is amplified at higher temperatures [33].

The effect of temperature on the TC of the Ag-Fe_2O_3/water multiphase fluid at concentrations of 0.5, 0.75 and 1.0 wt% is shown in Figure 7.2 (b). At a concentration of 0.5 wt%, a TC increase of 6.90% was observed in the temperature range from 293.15 to 323.15 K. At higher concentrations (0.75 and 1 wt%), the increases were 6.95% and 7.03%, suggesting that higher concentrations intensify the temperature effect on TC. Compared to Ag-rGO/water, the influence of concentration on TC in the Ag-Fe_2O_3/water fluid is lower. At concentrations of 0.5, 0.75 and 1 wt%, the TC increases at 293.15 K were 1.10%, 1.92% and 3.13%. At 323.15 K, these values slightly decreased, with increases of 0.82%, 1.69% and 2.97%. These results suggest that, in the case of the Ag-Fe_2O_3/water multiphase fluid, the addition of nanoparticles has a smaller effect on TC, especially at higher temperatures, compared to the Ag-rGO/water fluid.

For the Ag-FeC/water multiphase fluid (Figure 7.2 (c)), the temperature effect on TC becomes more pronounced as the nanoparticle concentration increases. The observed TC improvements are 11.29%, 11.56% and 11.78% for the three concentrations analyzed (0.5, 0.75 and 1.0 wt%) in the 293.15-323.15 K temperature range, indicating that the temperature effect is more significant for Ag-FeC compared to Ag-Fe_2O_3, at the same concentrations. The concentration effect on TC for the Ag-FeC/water fluid is more pronounced than for Ag-Fe_2O_3. At concentrations of 0.5, 0.75 and 1.0 wt%, TC increased by 2.69%, 3.63% and 4.45% at 293.15 K and by 6.61%, 7.84% and 8.92% at 323.15 K, compared to the base fluid (water + 4 g/l CMCNa). Unlike Ag-Fe_2O_3, Ag-FeC nanoparticles have a more significant impact on improving the TC of the base fluid, suggesting that the structure and interactions of the particles in Ag-FeC contribute more effectively to the TC increase.

The Ag-TiO_2/water multiphase fluid (Figure 7.2 (d)) shows TC improvements of 9.16%, 9.84% and 10.59% with the temperature increase from 293.15 to 323.15 K for the analyzed concentrations (0.5-1.0 wt%). These values are lower than those obtained for Ag-FeC but higher than those for Ag-Fe_2O_3, suggesting a lower sensitivity to temperature variations compared to Ag-FeC, but better performance than Ag-Fe_2O_3. Increasing the concentration from 0.5 to 1.0 wt% improves TC by 1.98%, 3.30% and 4.78% at 293.15 K and by 3.84%, 5.84% and 8.10% at 323.15 K. These results highlight that the concentration effect on TC is more pronounced for Ag-TiO_2/water than for Ag-Fe_2O_3, but less than for Ag-FeC/water, except at the 1.0 wt% concentration, where the increase is 4.78% at 293.15 K.

According to the data obtained, Ag-FeC/water exhibited the highest TC improvement with temperature. In contrast, Ag-rGO/water at a concentration of just 0.050 wt% provided a significant TC improvement comparable to that of Ag-FeC at 1.0 wt%. These results suggest that Ag-rGO/water (0.05 wt%) could be a viable option for applications requiring high temperatures. Regarding the concentration effect, Ag-rGO nanoparticles had the most significant impact, improving the TC of the base fluid (water + 0.4 g/l CMCNa) by 8.39% at 293.15 K and by 10.69% at 323.15 K.

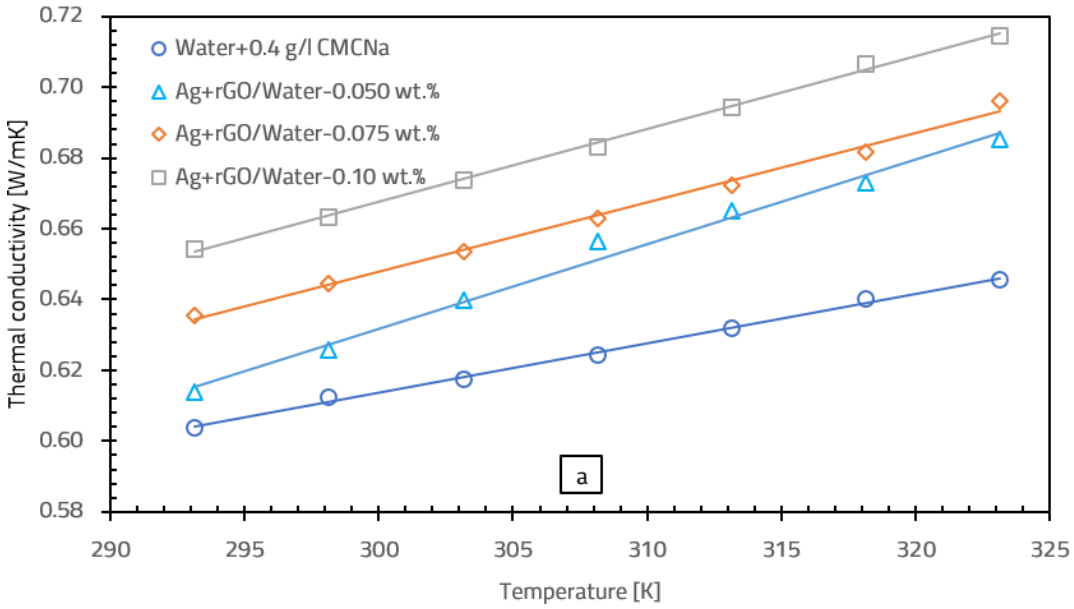

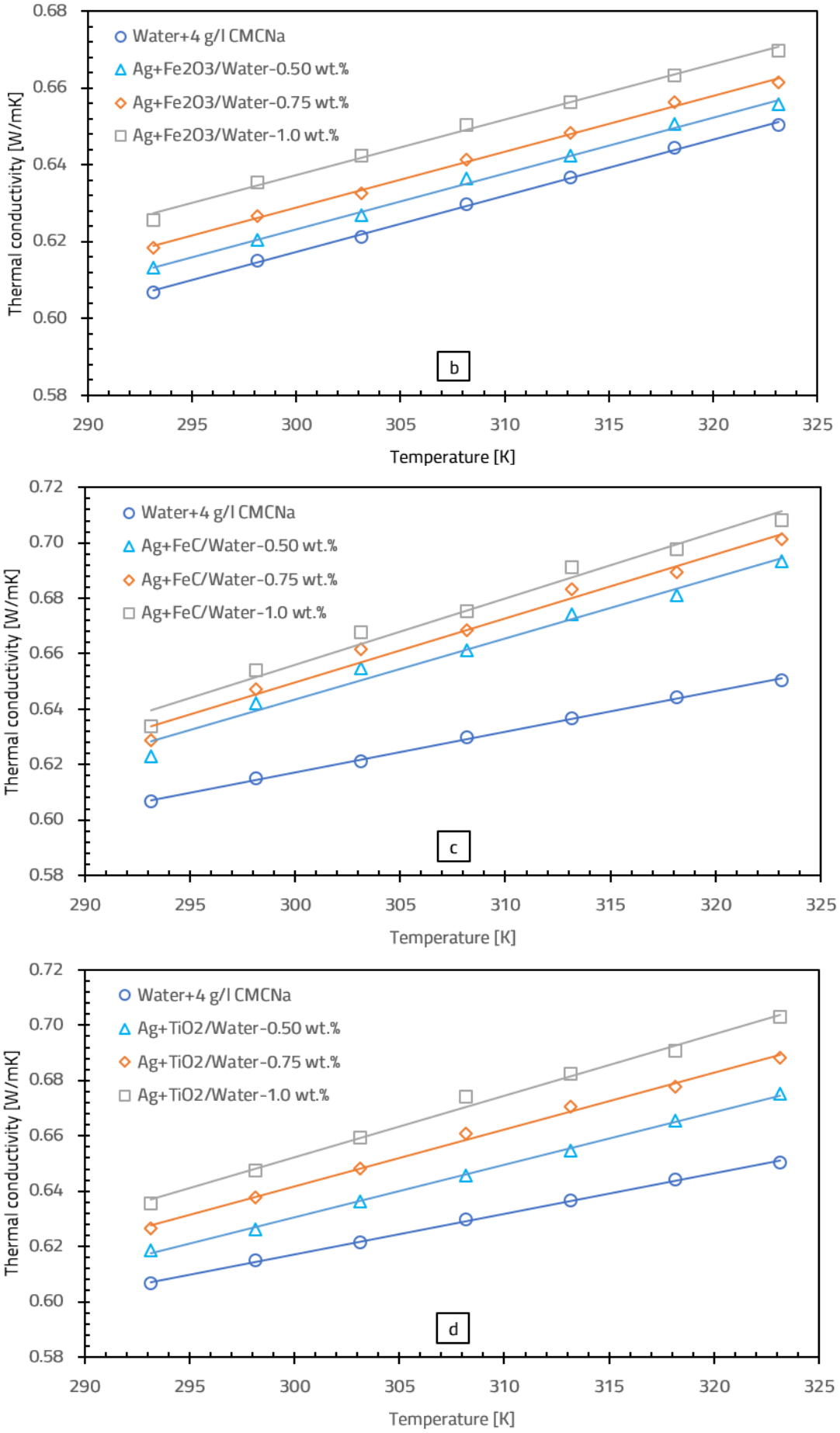

Figure 7.2. Variation of thermal conductivity with temperature for water-based multiphase fluids: a) Ag-rGO; b) Ag-Fe_2O_3; c) Ag-FeC; d) Ag-TiO_2.

The variation in TC for water+EG-based multiphase fluids, including Ag-rGO, Ag-Fe_2O_3, Ag-FeC and Ag-TiO_2, at different mass concentrations as a function of temperature is shown in Figure 7.3. Similar to the water-based multiphase fluids, the TC of the studied multiphase fluids increased with both temperature and concentration. It was also observed that the maximum TC value was reached at a concentration of 0.1 wt% for Ag-rGO and 1.0 wt% for the other multiphase fluids at a temperature of 323.15 K.

Figure 7.3 (a) illustrates the effect of temperature on TC for Ag-rGO/water+EG at different concentrations. At a concentration of 0.050 wt%, increasing the temperature from 293.15 to 323.15 K results in an 11.29% increase in TC, while for concentrations of 0.075 and 0.1 wt%, the increases are 11.22% and 11.54%, respectively, indicating that higher concentrations amplify this effect [34]. Regarding the influence of nanoparticle concentration, at 293.15 K, the addition of nanoparticles (0.050, 0.075 and 0.1 wt%) improves TC by 5.80%, 7.23% and 9.34%, respectively. At 323.15 K, the temperature effect is more pronounced, with increases of 9.12%, 10.52% and 13.02%. These results indicate that higher concentrations of Ag-rGO nanoparticles significantly improve TC, with the effect being more pronounced at higher temperatures.

The effect of temperature on TC for the Ag-Fe_2O_3/water+EG multiphase fluid is shown in Figure 7.3 (b). Increasing the concentration from 0.5 to 1 wt% leads to a more pronounced temperature effect on TC, with increases of 12.56%, 13.06% and 13.20% in the 293.15–323.15 K temperature range. These results suggest that a higher concentration of nanoparticles intensifies the temperature effect on TC. Regarding the influence of concentration, increasing the concentration of Ag-Fe_2O_3 nanoparticles from 0.5 to 1.0 wt% leads to a TC improvement of 1.24%, 2.39% and 3.88% at 293.15 K and 1.40%, 3.01% and 4.63% at 323.15 K. However, these increases are smaller compared to those observed for the Ag-rGO multiphase fluid.

For the Ag-FeC/water+EG multiphase fluid (Figure 7.3 (c)), it is observed that at concentrations of 0.5 and 0.75 wt%, the temperature effect on TC is more pronounced, with increases of 11.58% and 11.98%. At a concentration of 1.0 wt%, the temperature effect is smaller, with a 10.75% increase in TC, suggesting a limitation in effective thermal interactions, possibly due to nanoparticle agglomeration. Regarding the influence of concentration, at 293.15 K, the TC increases by 1.98%, 3.39% and 5.20%, while at 323.15 K, the increases are smaller, with values of 1.25%, 3.01% and 3.67%. This indicates that the concentration effect is more pronounced at lower temperatures. Compared to Ag-Fe_2O_3, the Ag-FeC multiphase fluid exhibits better thermal conductivity at 293.15 K but lower conductivity at 323.15 K. These observations highlight that the concentration effect depends on temperature and that the choice of nanoparticles plays a crucial role in the multiphase fluid's performance.

For the Ag-TiO_2/water+EG multiphase fluid (Figure 7.3 (d)), the effect of temperature on TC becomes more pronounced as the concentration increases from 0.5 to 1.0 wt%, with increases of 11.49%, 11.61% and 12.54% in the 293.15–323.15 K range. Regarding the influence of concentration, increasing from 0.5 to 1.0 wt% improves TC by 2.06%, 3.88% and 5.37% at 293.15 K and by 1.25%, 3.16% and 5.51% at 323.15 K. At higher temperatures, the effect of concentration is less pronounced, except at 1 wt%. Compared to other multiphase fluids (Ag-Fe_2O_3 and Ag-FeC in water+EG), Ag-TiO_2/water+EG exhibits higher TC.

Based on the obtained results, it can be concluded that the Ag-Fe_2O_3/water+EG multiphase fluid exhibited the best performance regarding the effect of temperature on TC increase, suggesting that at a concentration of 1.0 wt%, it could be ideal for high-temperature applications. In terms of TC

improvement due to concentration, the Ag-rGO/water+EG multiphase fluid showed the greatest enhancement, followed by Ag-TiO_2, Ag-FeC and Ag-Fe_2O_3.

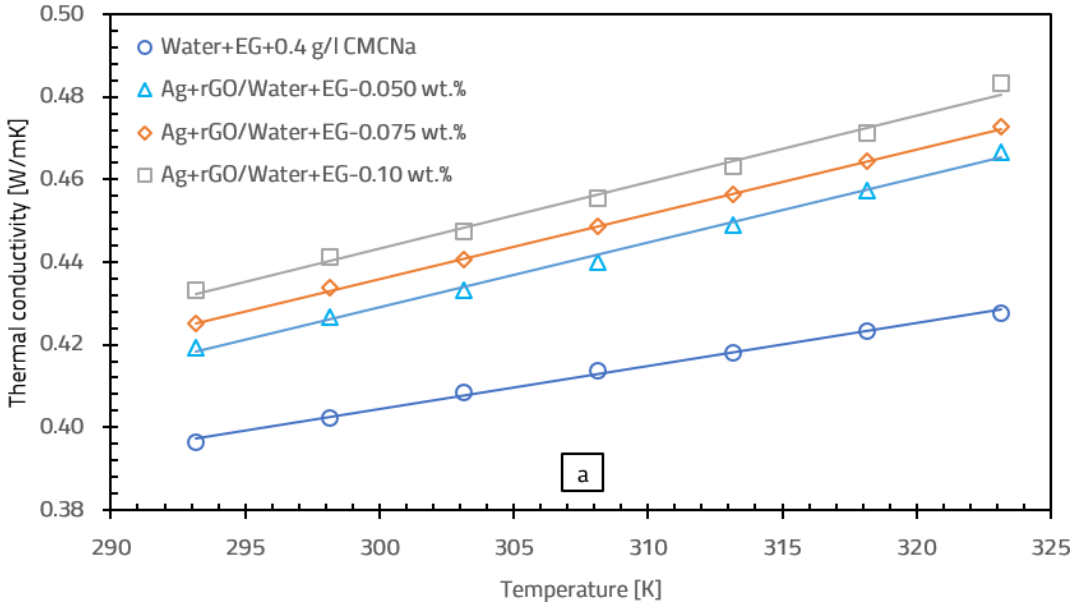

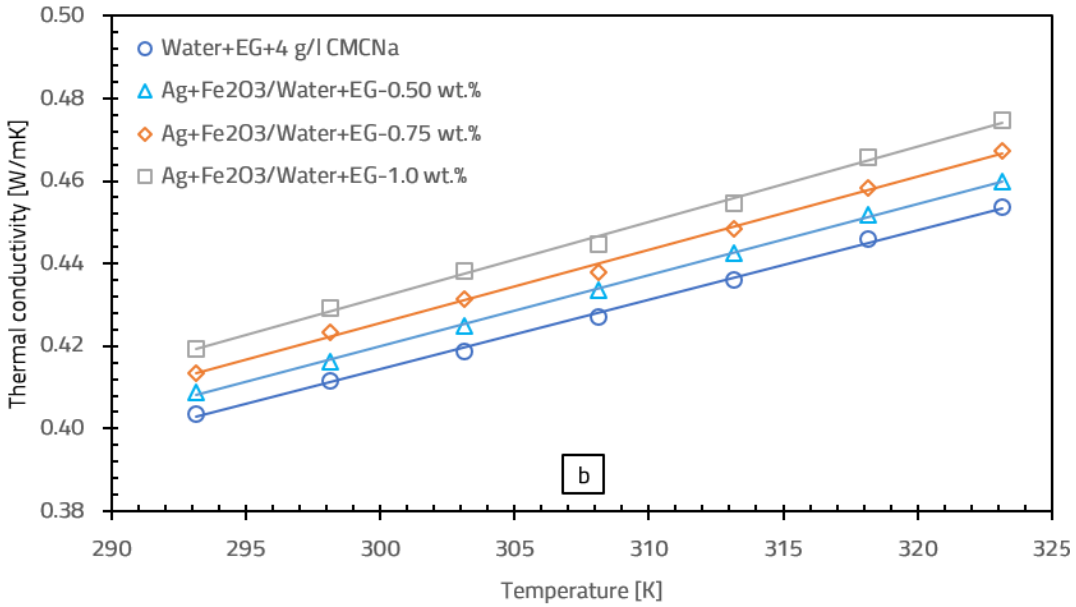

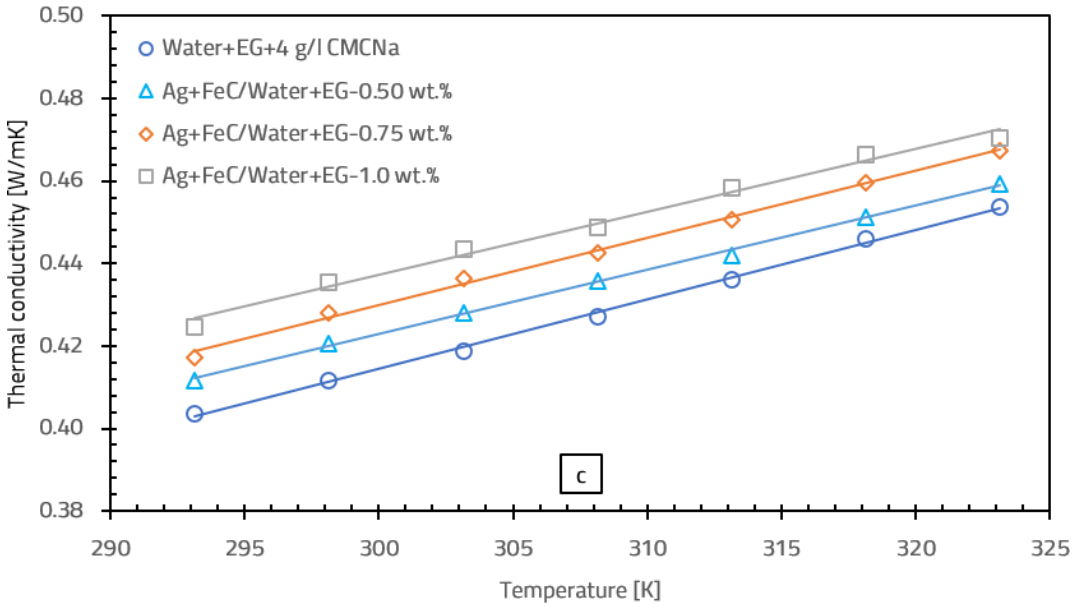

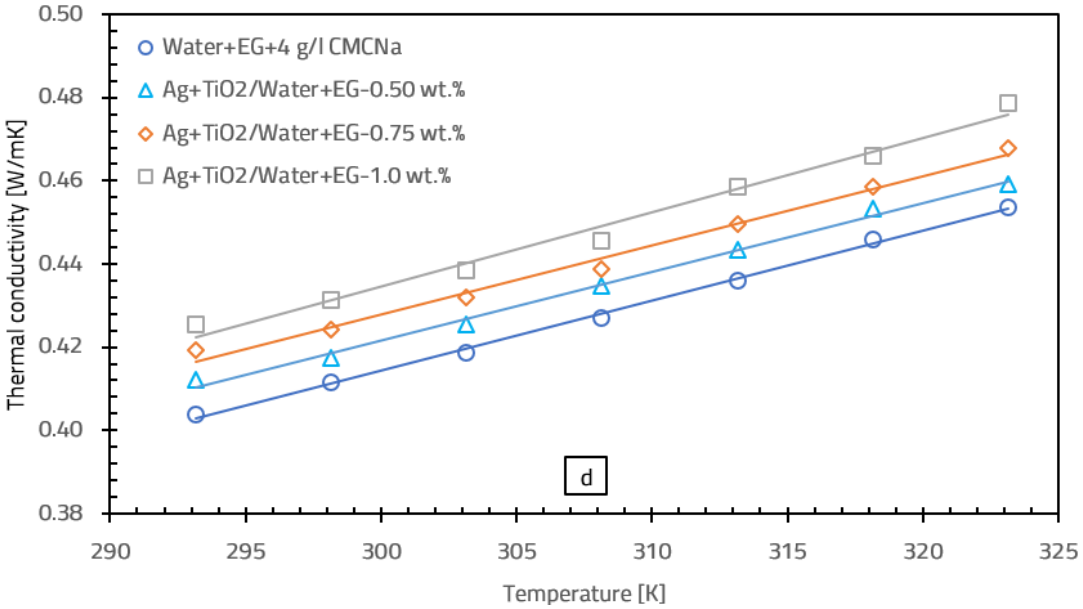

Figure 7.3. Variation of thermal conductivity with temperature for water+EG-based multiphase fluids: a) Ag-rGO; b) Ag-Fe_2O_3; c) Ag-FeC; d) Ag-TiO_2

The thermal conductivity of all the studied multiphase fluids increased with temperature and the use of higher nanoparticle concentrations significantly enhanced it. This phenomenon is caused by the Brownian motion of the particles within the multiphase fluid, where the small particle size and the low viscosity of the base fluid – which decreases as the temperature increases – lead to uncontrolled motion. As the temperature rises, the frequency of collisions increases, improving heat transfer [35]. Thus, the increase in thermal conductivity is closely related to the average particle velocity and, consequently, to the energy exchange between the particles [36]. Additionally, the Brownian motion of the particles can be influenced by the inertia of the base fluid [37]. The movement of a particle generates vortices in the fluid, which affect the dynamics of the particles and may influence thermal conductivity [38].

7.1.3 Conclusions on the study of thermal conductivity of multiphase fluids

- The Ag-rGO/water+EG multiphase fluid with a concentration of 0.10 wt% showed the maximum increase in thermal conductivity of 13.02% compared to the base fluid (water+EG with 0.4 g/l CMCNa) at a temperature of 323.15 K.
- For water-based multiphase fluids, the Ag-rGO/water multiphase fluid with a concentration of 0.1 wt% exhibited the maximum increase in thermal conductivity of 10.69% compared to the base fluid (water with 0.4 g/l CMCNa).
- The best result regarding the influence of temperature on thermal conductivity was observed for Ag-Fe_2O_3/water+EG with a concentration of 1 wt%, which showed an increase in thermal conductivity of 13.20% in the temperature range of 293.15–323.15 K.
- For water-based fluids, the best performance at high temperatures was observed for Ag-FeC/water with a concentration of 1 wt%, which exhibited an increase in thermal conductivity of 11.78% as the temperature rose from 293.15 to 323.15 K.

7.2 Dynamic viscosity

7.2.1 Dynamic viscosity of base fluids

In the first stage of the experiment, the dynamic viscosity of the base fluids (water and a water+EG (1:1) mixture), both with and without surfactant (0.4 and 4 g/l CMCNa), was measured at temperatures ranging from 293.15 to 323.15 K. The results obtained were compared to reference data from NIST [31] and ASHRAE [32].

Figure 7.4 (a) shows the viscosity of water with and without surfactant, compared to the NIST values. It can be observed that viscosity decreases as the temperature increases and the results for water without surfactant are close to the NIST values, with a maximum deviation of 0.444%. The addition of surfactant (0.4 and 4 g/l CMCNa) increased the viscosity of water by 1.942% and 6.264%, respectively. Figure 7.4 (b) presents the viscosity values for the water+EG mixture, both with and without surfactant, compared to the ASHRAE reference data. The viscosity of the mixture without surfactant is close to the ASHRAE values, with a maximum deviation of 0.307%. The addition of surfactant (0.4 g/l CMCNa) reduced the viscosity by 37.067%, while at 4 g/l CMCNa, it increased by 13.746% [34].

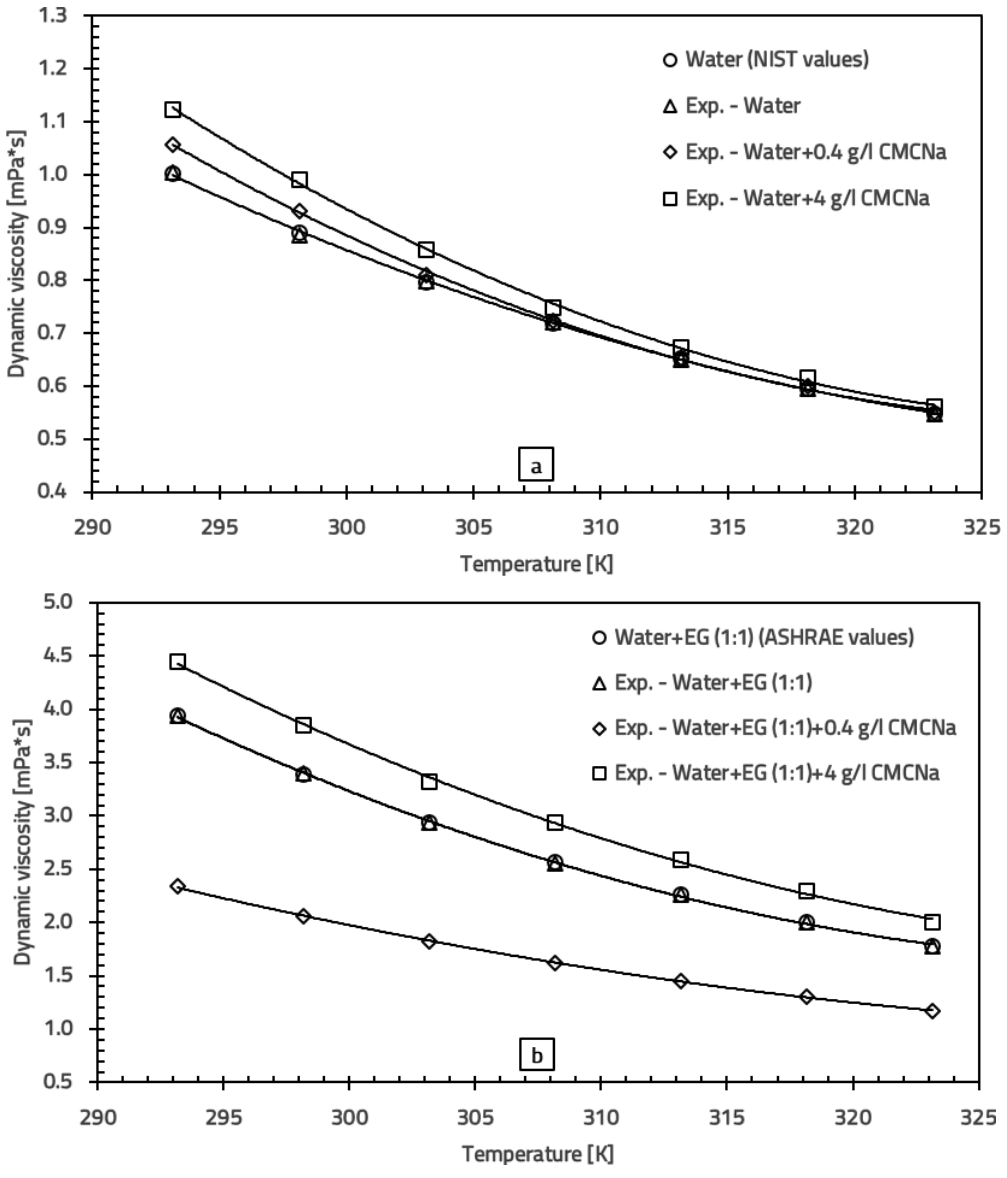

Figure 7.4. Validation of the dynamic viscosity measurements for: a) water; b) water+EG

7.2.2 Dynamic viscosity of multiphase fluids

The effect of temperature on the dynamic viscosity of the multiphase fluids Ag-rGO, Ag-Fe_2O_3, Ag-FeC and Ag-TiO_2 based on water was studied at different mass concentrations. Figure 4.11 shows that the maximum viscosity for water-based multiphase fluids was reached at concentrations of 0.1 wt% (for Ag-rGO) and 1.0 wt% at a temperature of 293.15 K. Additionally, a general trend of decreasing viscosity with increasing temperature was observed for all the multiphase fluids analyzed. This decrease in viscosity can be attributed to the increased kinetic energy of the molecules in the fluid, which move faster at higher temperatures, reducing the attractive forces between them. As a result, the fluid becomes less viscous and the particles move more freely within it.

Furthermore, the reduction in viscosity at higher temperatures facilitates fluid circulation in cooling systems and heat transfer processes, which, in turn, improves the energy efficiency of these processes. Therefore, the temperature-dependent reduction in viscosity is a crucial factor influencing the behavior and applicability of multiphase fluids in areas such as thermal engineering and nanotechnology.

Figure 7.5 (a) illustrates the effect of temperature on the viscosity of the Ag-rGO/water multiphase fluid at different concentrations. At a concentration of 0.050 wt%, viscosity decreases by 49.94% as the temperature rises from 293.15 to 323.15 K. At concentrations of 0.075 and 0.1 wt%, the reductions are 48.44% and 49.78%, suggesting a smaller temperature effect at higher concentrations. The addition of nanoparticles increases the viscosity of the base fluid (water+0.4 g/l CMCNa) by 0.57%, 2.50% and 17.38% for the concentrations of 0.050, 0.075 and 0.1 wt%, respectively, at 293.15 K. At 323.15 K, viscosity decreases by 3.23% at 0.050 wt% and increases by 1.59% and 13.31% at 0.075 and 0.1 wt%. These results suggest that the Ag-rGO/water fluid at 0.050 wt% could be a viable option for DASC systems, as its viscosity is close to that of the base fluid [33].

Figure 7.5 (b) presents the effect of temperature on the viscosity of the Ag-Fe_2O_3/water multiphase fluid at concentrations between 0.5 and 1.0 wt%. At a concentration of 0.5 wt%, viscosity decreases by 52.19% in the 293.15–323.15 K range, while at concentrations of 0.75 and 1.0 wt%, the reductions are 51.67% and 44.44%, indicating a smaller temperature effect at higher concentrations. At lower concentrations, nanoparticles are more mobile and respond more efficiently to higher temperatures, while at higher concentrations, more complex interactions limit this effect. Increasing the nanoparticle concentration from 0.5 to 1.0 wt% results in viscosity increases of 18.75%, 21.13% and 24.95% for the base fluid at 293.15 K. At 323.15 K, the influence of concentration decreases for 0.5 and 0.75 wt% (increases of 13.66% and 17.21%), while at 1 wt%, the viscosity increase reaches 39%.

Figure 7.5 (c) shows the effect of temperature on the viscosity of the Ag-FeC/water multiphase fluid. As the temperature increases from 293.15 to 323.15 K, viscosity decreases by 51.72%, 51.59% and 51.89% at concentrations of 0.5, 0.75 and 1.0 wt%, indicating a significant temperature effect and an amplified effect at higher nanoparticle concentrations. The effect of concentration on viscosity is less pronounced than in the Ag-Fe_2O_3/water multiphase fluid. At 293.15 K, the viscosity of water increases by 12.18%, 12.94% and 14.43% for concentrations of 0.5, 0.75 and 1.0 wt% and at 323.15 K, these increases are smaller, namely 8.44%, 9.46% and 10.23%. Compared to Fe_2O_3 nanoparticles, FeC nanoparticles have a lesser impact on the viscosity of the base fluid due to their specific structure.

Figure 7.5 (d) analyzes the effect of temperature on the viscosity of the Ag-TiO_2/water multiphase fluid at different concentrations. At a concentration of 0.5 wt%, viscosity decreases by 51.52% across the studied temperature range. At 0.75 wt%, the reduction is more pronounced at 53.19% and at 1.0 wt%, the decrease is 51.78%, indicating a smaller temperature effect compared to the 0.75 wt%

concentration. Increasing the nanoparticle concentration from 0.5 to 1.0 wt% leads to viscosity increases of 13.06%, 20.54% and 23.26% at 293.15 K and at higher temperatures, the effect of concentration decreases, with increases of 9.75%, 12.97% and 19.01%. The influence of concentration on viscosity is more pronounced in the case of Ag-TiO_2/water than in Ag-FeC/water, but still less pronounced compared to Ag-Fe_2O_3/water.

The results show that the Ag-TiO_2/water multiphase fluid at 0.75 wt% exhibited the greatest reduction in viscosity, while Ag-Fe_2O_3/water at 1 wt% showed the smallest reduction. These results suggest that Ag-TiO_2/water is effective in reducing viscosity at higher temperatures, while Ag-Fe_2O_3/water is more suitable for maintaining a higher viscosity. At 323.15 K, the Ag-Fe_2O_3/water multiphase fluid at 1 wt% exhibited the highest viscosity increase of 39%, while Ag-rGO/water at 0.050 wt% showed a decrease of 3.23% compared to the base fluid.

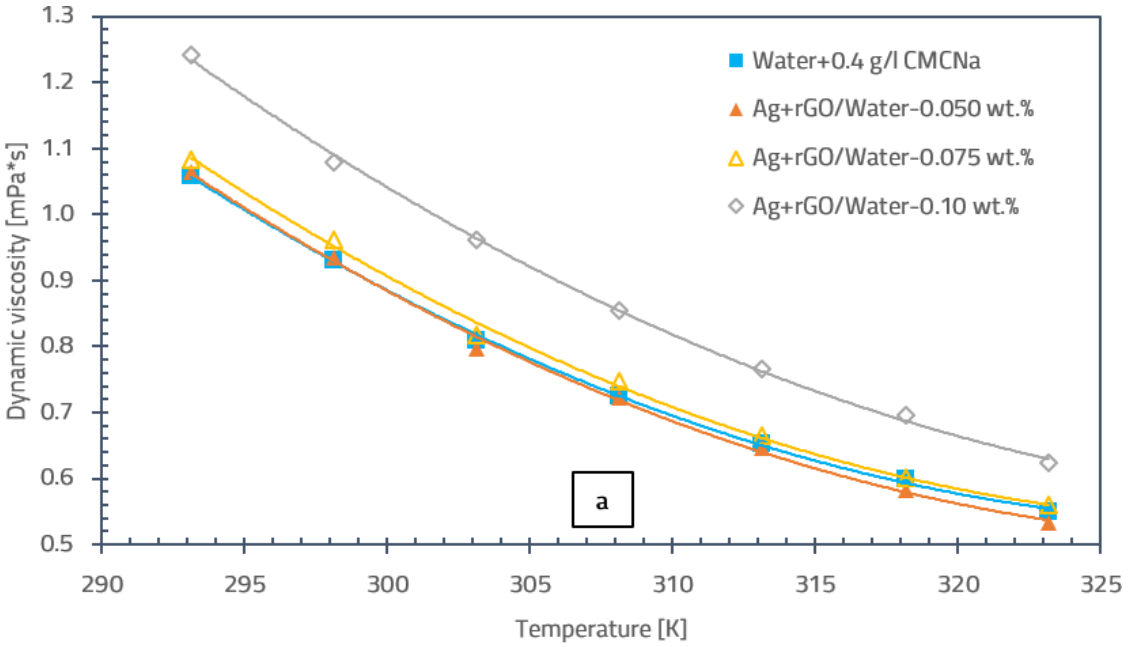

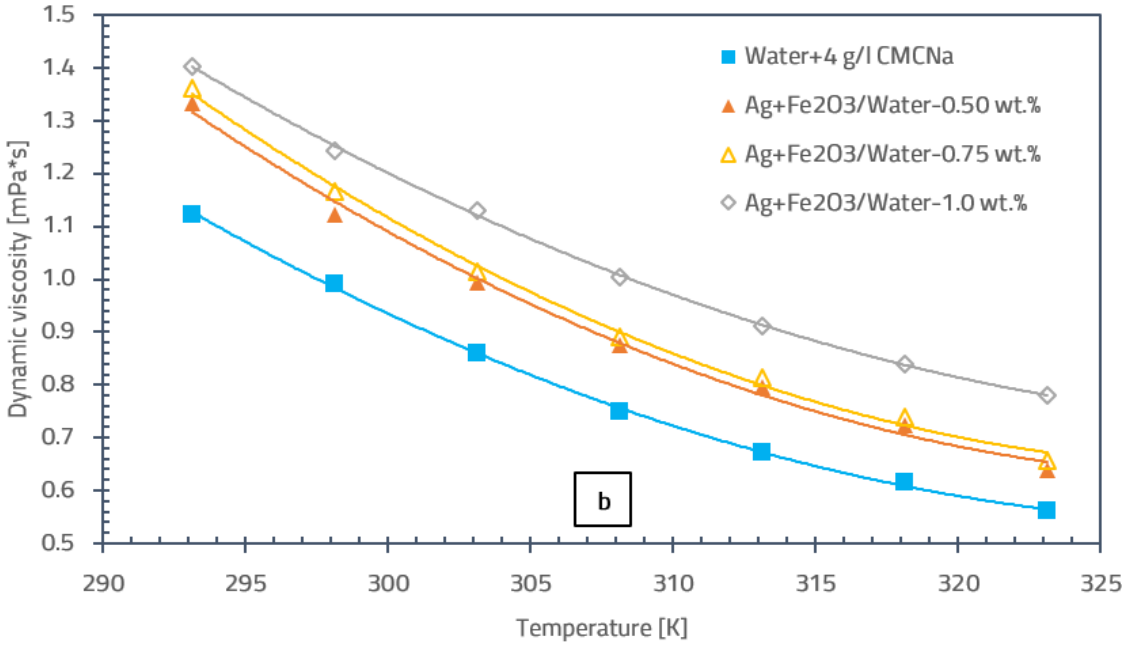

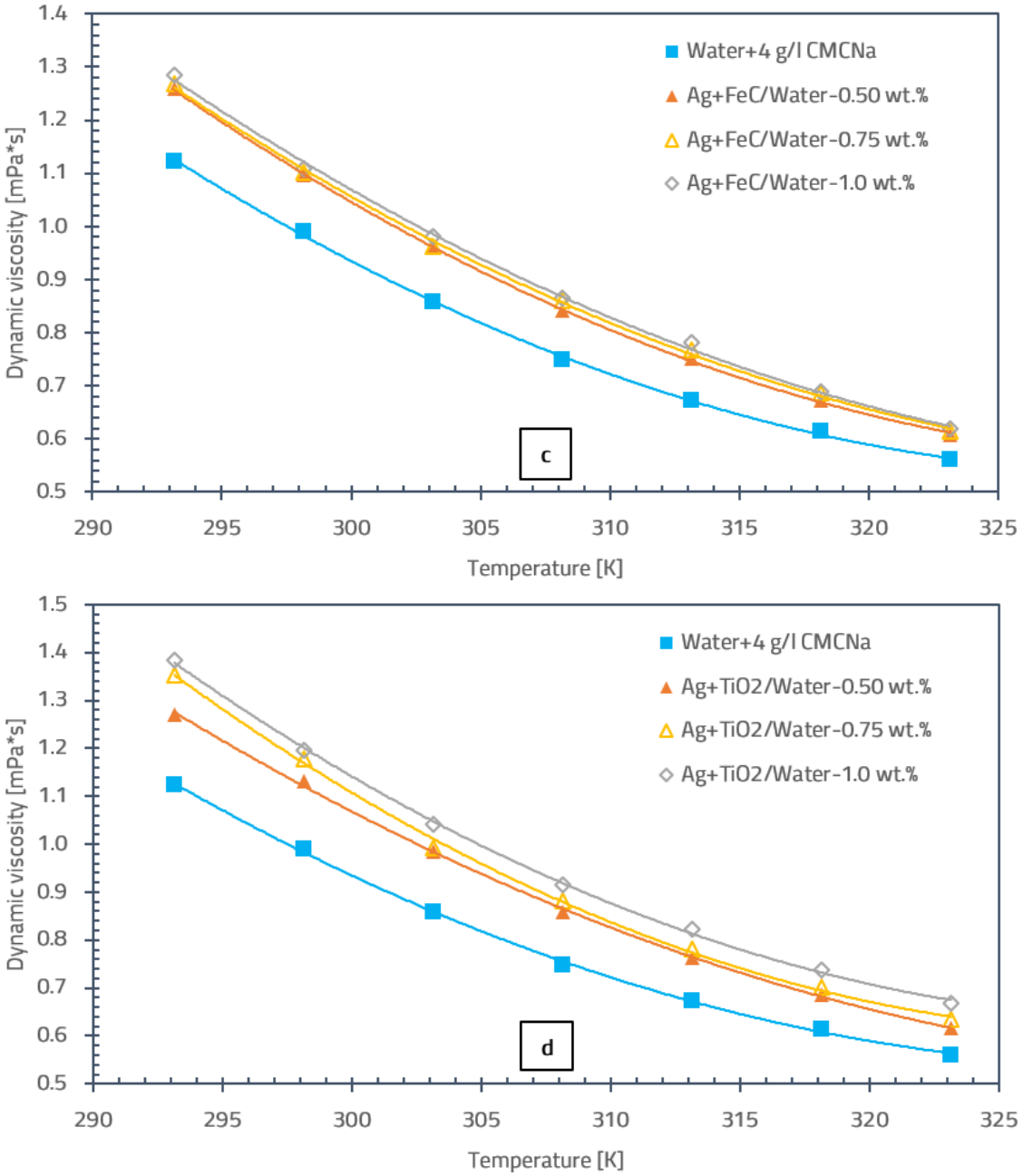

Figure 7.5. Variation of dynamic viscosity with temperature for water-based multiphase fluids: a) Ag-rGO; b) Ag-Fe_2O_3; c) Ag-FeC; d) Ag-TiO_2.

In Figure 7.6, it can be observed that the viscosity of the water+EG-based multiphase fluids decreased with increasing temperature, similar to the water-based multiphase fluids. Additionally, the maximum viscosity was recorded at concentrations of 0.1 wt% for Ag-rGO and 1.0 wt% for the other multiphase fluids at a temperature of 293.15 K.

Figure 7.6 (a) shows the influence of temperature on the viscosity of the Ag-rGO/water+EG multiphase fluid at three different mass concentrations. At a concentration of 0.050 wt%, an increase in temperature from 293.15 to 323.15 K reduces viscosity by 54.34%. At 0.075 wt%, the temperature effect is more pronounced, with a reduction of 55.18%, while at 0.1 wt%, the effect is smaller, with a decrease of 52.06%. These results suggest that higher concentrations reduce the impact of temperature on the viscosity of Ag-rGO/water+EG [34]. Regarding the influence of concentration, at 293.15 K, the viscosity of water+EG with 0.4 g/l CMCNa increases by 77.60%, 83.27% and 133.26% at concentrations of 0.050, 0.075 and 0.1 wt%, respectively. At 323.15 K, these increases are smaller:

62.43%, 64.51% and 124.06%. These data suggest that Ag-rGO nanoparticles have a greater impact on viscosity at lower temperatures, while at higher temperatures, the effect diminishes.

Figure 7.6 (b) analyzes the effect of temperature on the viscosity of the Ag-Fe_2O_3/water+EG multiphase fluid at concentrations between 0.5 and 1.0 wt%. As the concentration increases, the impact of temperature on viscosity becomes more pronounced, with decreases of 54.09%, 54.16% and 55.02% in the 293.15–323.15 K range. Compared to the Ag-rGO/water+EG multiphase fluid, the influence of concentration on viscosity is smaller. Increasing the Ag-Fe_2O_3 nanoparticle concentration from 0.5 to 1.0 wt% results in viscosity increases of 3.64%, 5.64% and 8.65% at 293.15 K. At 323.15 K, the effect of concentration on viscosity becomes more pronounced, with increases of 5.44% and 7.31% at concentrations of 0.5 and 0.75 wt%. At 1 wt%, the effect diminishes and viscosity increases by 8.31%. These data suggest that higher concentrations of Ag-Fe_2O_3 nanoparticles contribute to increased viscosity, but this effect is not as pronounced as with the Ag-rGO/water+EG fluid at lower concentrations.

In Figure 7.6 (c), it is observed that for the Ag-FeC/water+EG multiphase fluid, the influence of temperature on viscosity decreases as the concentration increases, with reductions of 55.30%, 55.11% and 55.02% at concentrations of 0.5, 0.75 and 1.0 wt%. Unlike Ag-Fe_2O_3, where higher concentrations intensify the temperature effect due to uniform particle dispersion, Ag-FeC shows an opposite behavior, reducing temperature sensitivity as concentration increases. Increasing the concentration from 0.5 to 1.0 wt% results in viscosity increases of 8.17%, 9.69% and 11.10% at 293.15 K. At a higher temperature of 323.15 K, the effect of concentration on viscosity is smaller, with increases of 7.16%, 9.14% and 10.75%. Compared to Ag-Fe_2O_3, Ag-FeC shows higher viscosity at all concentrations.

For the Ag-TiO_2/water+EG multiphase fluid presented in Figure 7.6 (d), the effect of temperature on viscosity decreases as the concentration increases from 0.5 to 0.75 wt%, with reductions of 55.09% and 54.97% between 293.15 and 323.15 K. At a concentration of 1 wt%, the temperature effect slightly increases, with a reduction of 55.14%. Increasing the nanoparticle concentration from 0.5 to 1.0 wt% leads to viscosity increases of 7.54%, 12.06% and 13.13% at 293.15 K. At 0.5 wt%, the effect of concentration is more pronounced, with an increase of 9.41% at 323.15 K, while at 0.75 and 1.0 wt%, the effect diminishes, with increases of 11.83% and 12.48%. Compared to Ag-Fe_2O_3 and Ag-FeC, Ag-TiO_2 shows a greater increase in viscosity, except at a concentration of 0.5% at 293.15 K, where Ag-FeC/water+EG records a larger increase.

The analysis indicates that the Ag-FeC/water+EG multiphase fluid at 0.5 wt% exhibited the largest decrease in viscosity (nearly 55%) with an increase in temperature from 293.15 to 323.15 K, while the Ag-rGO/water+EG fluid at 0.1 wt% showed the smallest reduction, approximately 52%. The same Ag-rGO/water+EG multiphase fluid also recorded the largest increase in viscosity (133.26%) at 0.1 wt% and 293.15 K, while Ag-Fe_2O_3/water+EG showed the smallest increase (3.64%) at 0.5 wt% and 293.15 K. These results suggest that the effects of concentration and temperature on viscosity significantly influence the behavior of the multiphase fluid.

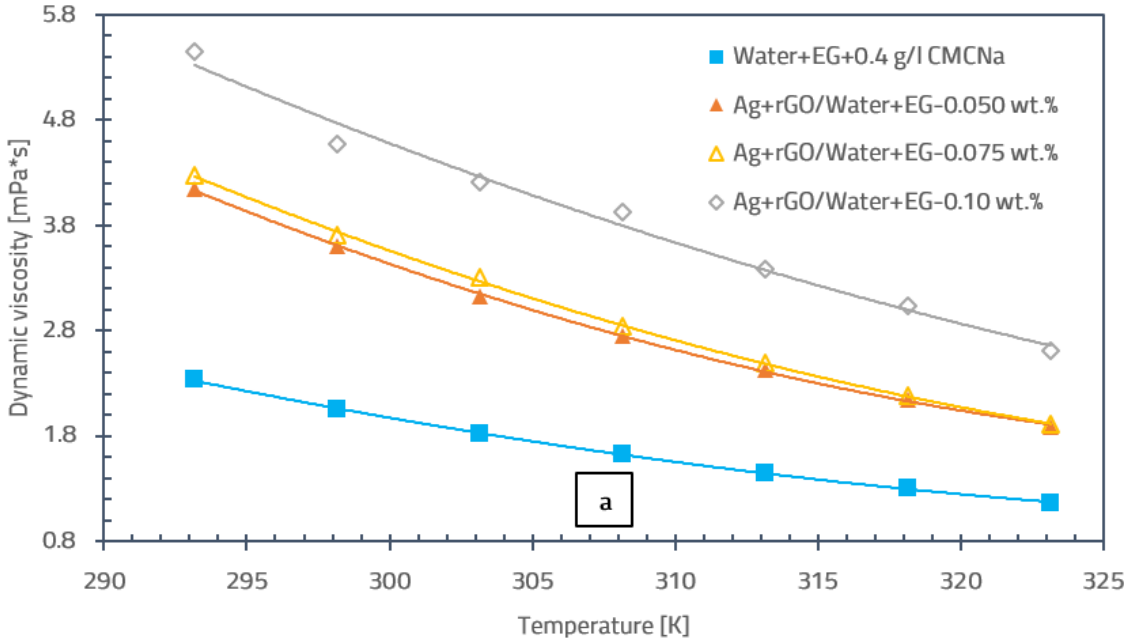
Water+EG+0.4 g/l CMCNa
Ag+rGO/Water+EG-0.050 wt.%
Ag+rGO/Water+EG-0.075 wt.%
Ag+rGO/Water+EG-0.10 wt.%
a
Dynamic viscosity [mPa*s]
Temperature [K]

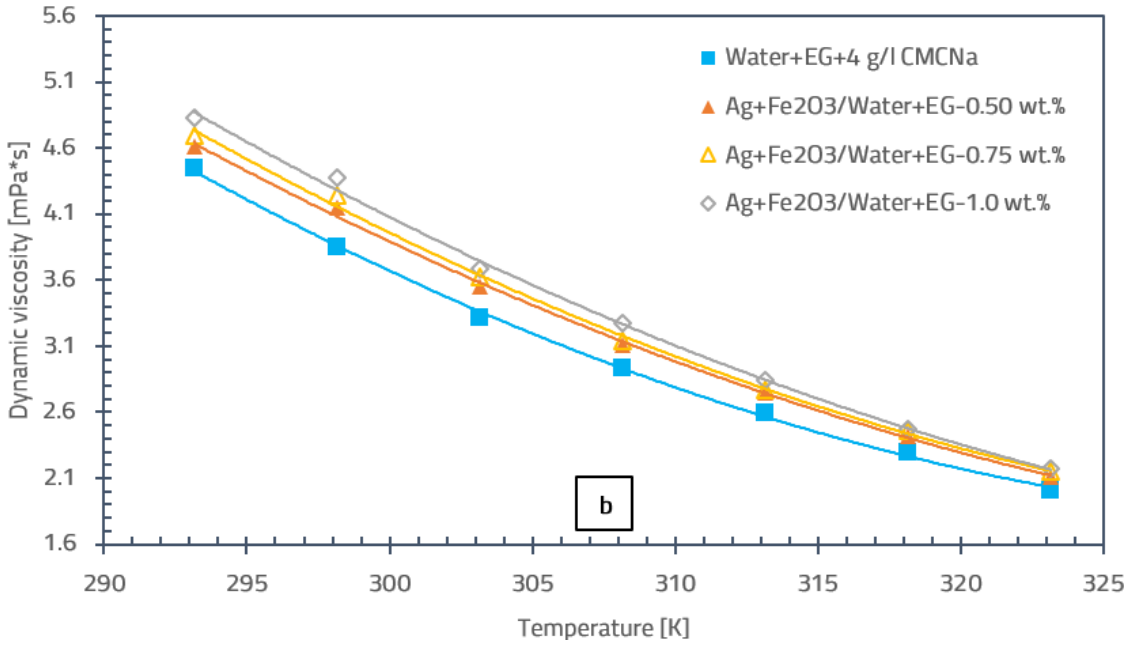
Water+EG+4 g/l CMCNa
Ag+Fe2O3/Water+EG-0.50 wt.%
Ag+Fe2O3/Water+EG-0.75 wt.%
Ag+Fe2O3/Water+EG-1.0 wt.%
b
Dynamic viscosity [mPa*s]
Temperature [K]

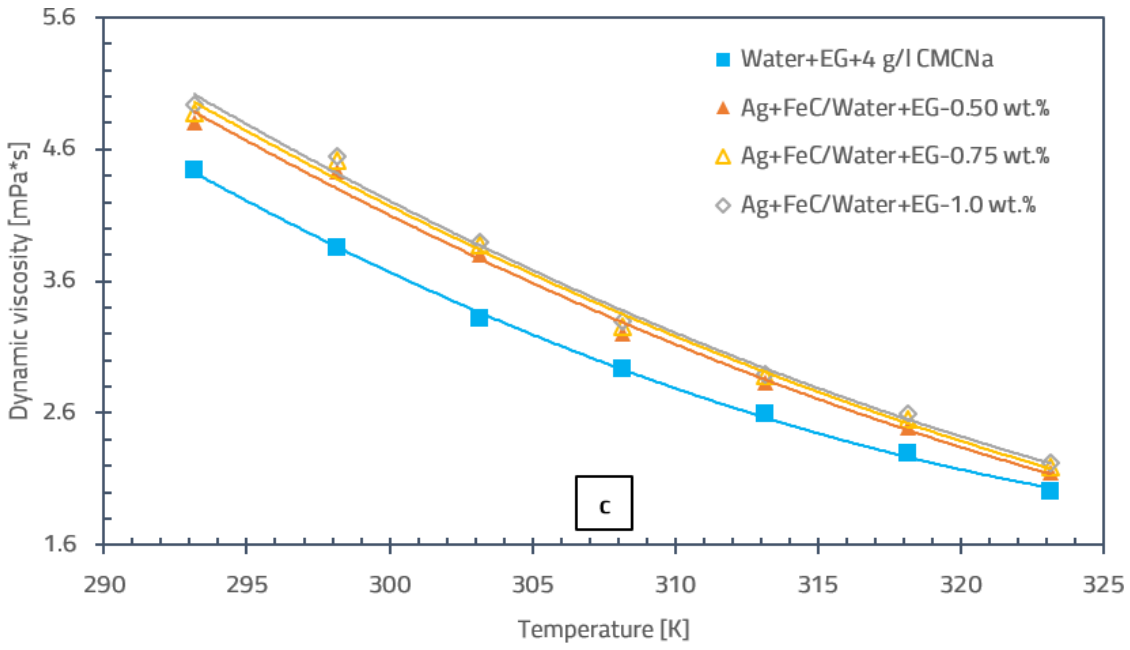
Water+EG+4 g/l CMCNa
Ag+FeC/Water+EG-0.50 wt.%
Ag+FeC/Water+EG-0.75 wt.%
Ag+FeC/Water+EG-1.0 wt.%
c
Dynamic viscosity [mPa*s]
Temperature [K]

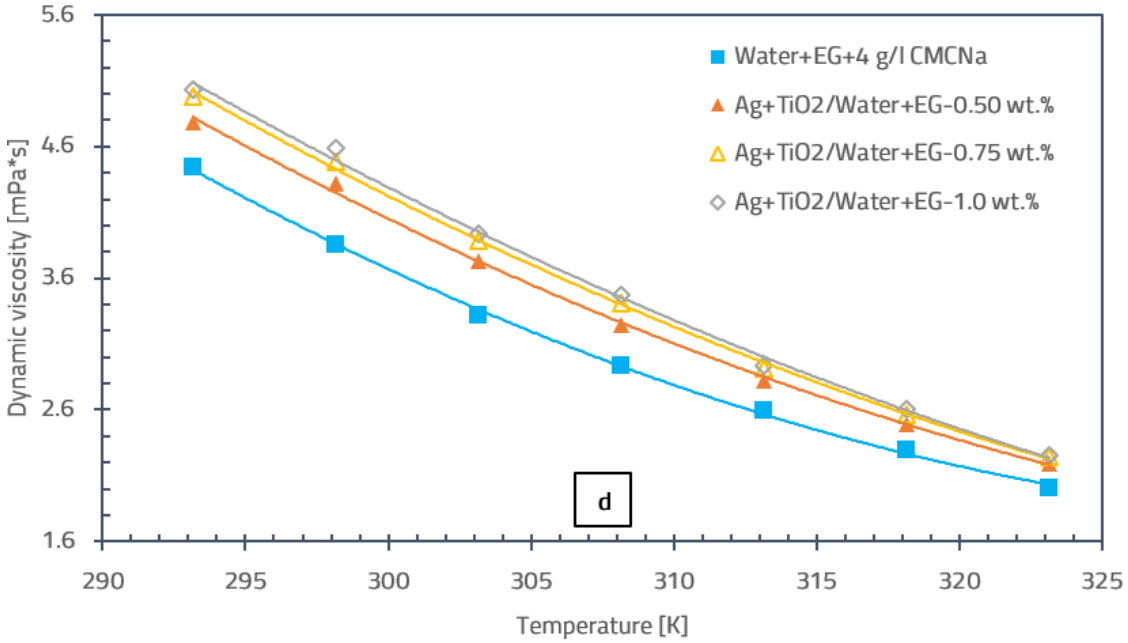

Figure 7.6. Variation of dynamic viscosity with temperature for water+EG-based multiphase fluids: a) Ag-rGO; b) Ag-Fe_2O_3; c) Ag-FeC; d) Ag-TiO_2

7.2.3 Conclusions on the study of the dynamic viscosity of multiphase fluids

- The Ag-FeC/water+EG multiphase fluid, with a concentration of 0.5 wt%, showed the greatest reduction in viscosity (55.30%) as the temperature increased from 293.15 K to 323.15 K.
- Among the water-based fluids, Ag-TiO_2/water at 0.75 wt% had the largest reduction in viscosity (53.19%) over the temperature range of 293.15–323.15 K.
- Ag-Fe_2O_3/water (1 wt%, 323.15 K) had a 39% increase in viscosity compared to the base fluid (water + 4 g/l CMCNa), while Ag-rGO/water (0.05 wt%, 323.15 K) showed a 3.23% decrease compared to the base fluid (water + 0.4 g/l CMCNa).
- For the water+EG-based fluids, Ag-rGO/water+EG (0.1 wt%, 293.15 K) had the highest increase in viscosity (133.26%) compared to the base fluid (water+EG with 0.4 g/l CMCNa), whereas Ag-Fe_2O_3/water+EG (0.5 wt%, 293.15 K) showed a 3.64% increase compared to the base fluid (water+EG with 4 g/l CMCNa).

7.3 Density

7.3.1 Base fluid density

In the first stage, the density of the base fluids (water and water+EG (1:1)) was measured, both with and without surfactant (0.4 and 4 g/l CMCNa), at temperatures ranging from 293.15 to 323.15 K. The experimental results were compared with NIST [31] and ASHRAE [32] data and are presented in Figure 7.7.

In Figure 7.7 (a), it can be seen that the experimental values obtained for pure water are very close to the NIST data, with a maximum deviation of 0.06%. The addition of CMCNa (0.4 and 4 g/l) led to an increase in water density by 0.22% and 0.54%, respectively.

Figure 7.7 (b) shows the density values for the water+EG mixture, with and without surfactant, compared to ASHRAE data. The density values for the solution without surfactant were very close to the ASHRAE data, with a deviation of 1.70%. The addition of 0.4 g/l CMCNa resulted in a 4.83% decrease in density, while 4 g/l had a smaller effect, increasing the density by 0.10% [34].

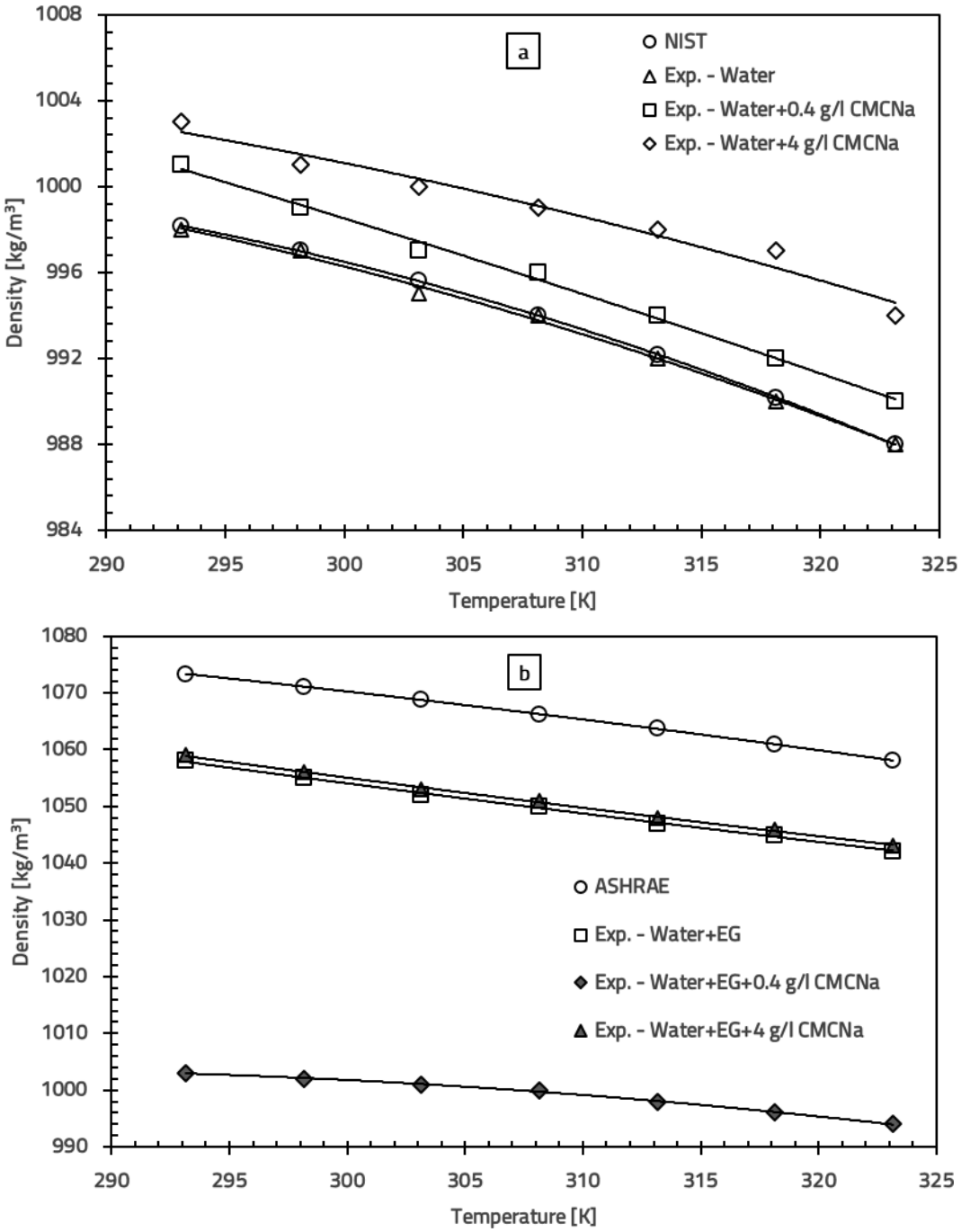

Figure 7.7. Validation of density measurements for: a) water; b) water + EG (1:1)

7.3.2 Density of multiphase fluids

Figure 7.8 presents the densities of water-based multiphase fluids as a function of temperature at different mass concentrations. The results show that density decreases with increasing temperature and increases with concentration. As the temperature rises, the particles gain more energy, move faster and disperse more, which leads to an increase in volume and a decrease in density.

In Figure 7.8 (a), it can be seen that for the Ag-rGO/water multiphase fluid, the maximum density was recorded at a concentration of 0.10 wt% and a temperature of 293.15 K. As the temperature increases to 323.15 K, the density decreases by approximately 0.8% at all concentrations. At concentrations of 0.050 and 0.075 wt%, the densities are close to that of water, with average increases of 0.029% and 0.129%. A higher concentration (0.10 wt%) causes a slight increase in density, with an average rise of 0.259% compared to water+0.4 g/l CMCNa [33]. These results are consistent with those reported by Yarmand et al. [39], who observed similar behaviors for GNP-Ag/water.

The graph in Figure 7.8 (b) shows that the maximum density of the Ag-Fe_2O_3/water multiphase fluid was reached at a concentration of 1.0 wt% and a temperature of 293.15 K. Increasing the temperature to 323.15 K caused a 1.48% drop in density, while for concentrations of 0.5 and 0.75 wt%, the reduction was 1% and 1.29%, respectively. The density of the multiphase fluid at 0.5 wt% was on average 0.086% lower than the base fluid, while at concentrations of 0.75 and 1.0 wt%, it was higher by 0.085% and 0.543%. A similar trend was observed by Askari et al. [40], where the density of the graphene-Fe_3O_4 multiphase fluid increased with concentration and decreased with rising temperature.

For the Ag-FeC/water multiphase fluid (Figure 7.8 (c)), the maximum density was also recorded at 1.0 wt% and 293.15 K. With a temperature increase to 323.15 K, the density decreased by 0.79% and for concentrations of 0.50 and 0.75 wt%, the reduction was 0.89%. At all studied concentrations (0.5, 0.75 and 1.0 wt%), the density values were on average 0.257%, 0.400% and 0.958% higher compared to the base fluid (water+4 g/l CMCNa).

According to the data in Figure 7.8 (d), the maximum density of the Ag-TiO_2/water multiphase fluid at a concentration of 1.0 wt% and a temperature of 293.15 K decreases by 1.18% as the temperature rises to 323.15 K. For concentrations of 0.5 and 0.75 wt%, the density reduction was 1.09% and 0.89%. In the concentration range of 0.5-1.0 wt%, the density of the Ag-TiO_2/water multiphase fluid was higher than that of the base fluid by 0.443%, 0.772% and 1.015%. This behavior is similar to that reported by Shoghl et al. [41] for the TiO_2/water multiphase fluid.

The results indicate that temperature has a minimal impact on the density of water-based multiphase fluids, with the largest decrease being 1.48% for the Ag-Fe_2O_3 multiphase fluid at a concentration of 1.0 wt%. Additionally, concentration does not significantly influence their density.

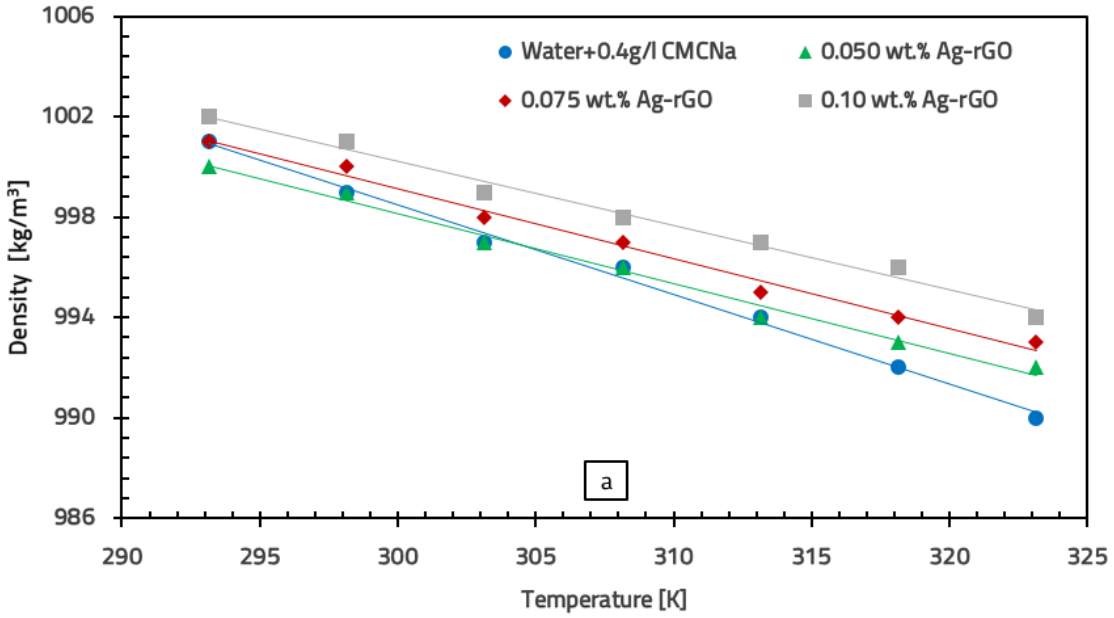

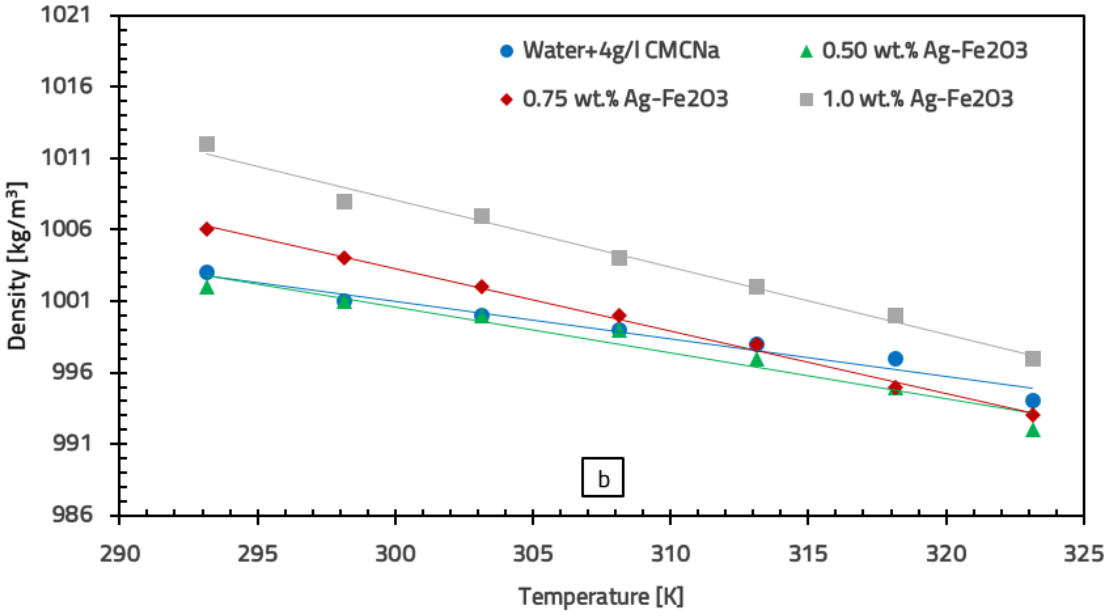

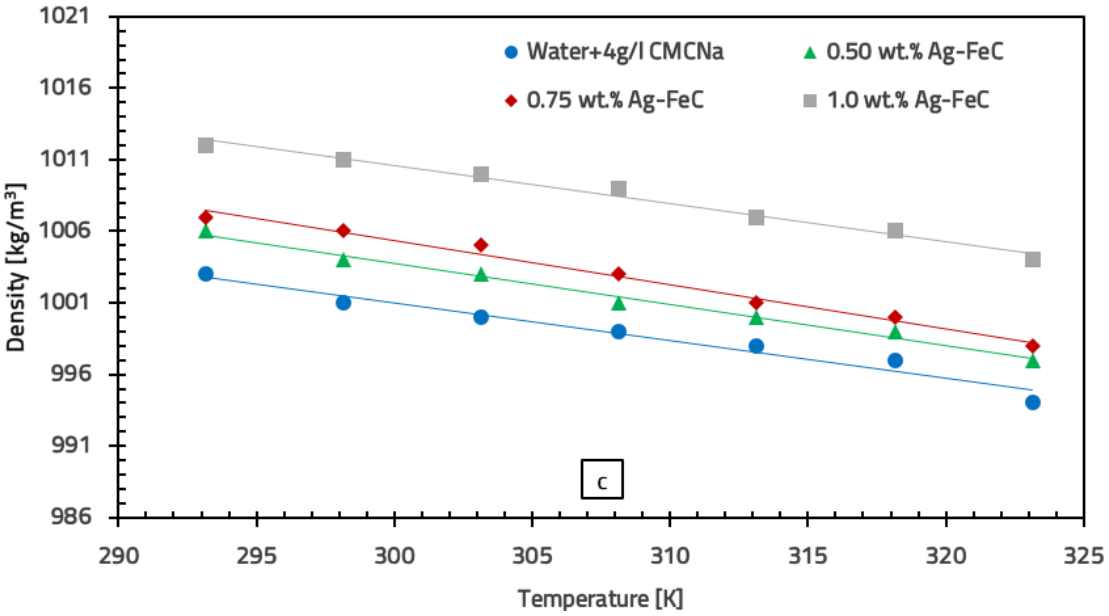

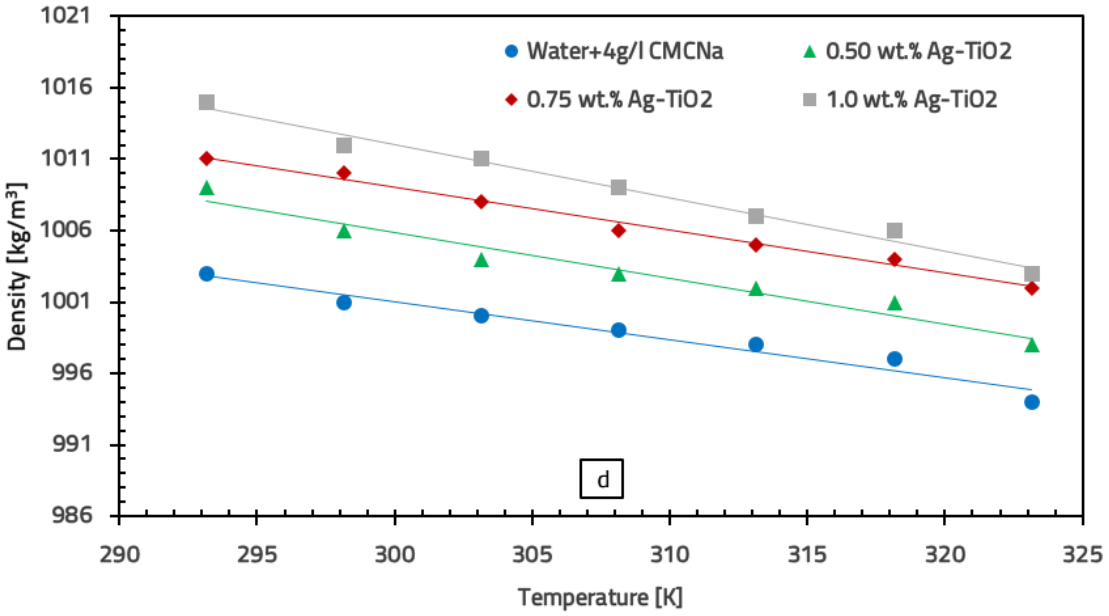

Figure 7.8 Variation of density with temperature for water-based multiphase fluids: a) Ag-rGO; b) Ag-Fe_2O_3; c) Ag-FeC; d) Ag-TiO_2

The variation in the density of water+EG (1:1)-based multiphase fluids with temperature at different mass concentrations is shown in Figure 7.9. These multiphase fluids follow a similar trend to those based on water: density decreases as temperature increases and increases as concentration rises. These multiphase fluids have a higher density than the base fluid at all concentrations and temperatures studied, showing a more pronounced increase in density compared to water-based multiphase fluids.

In Figure 7.9 (a), it can be observed that the maximum density of the Ag-rGO/water+EG multiphase fluid was recorded at a concentration of 0.10 wt% and a temperature of 293.15 K. Increasing the temperature to 323.15 K results in a 1.41% decrease in density, while at concentrations of 0.050 and 0.075 wt%, the reductions are 1.23% and 1.41%, respectively [34]. The density of the base fluid (water+EG with 0.4 g/l CMCNa) increases by 5.376%, 5.561% and 5.676% as the concentration rises from 0.050 to 0.10 wt%. The addition of nanoparticles significantly influences the density, but the change in concentration from 0.050 to 0.10 wt% has a moderate impact on it.

For the Ag-Fe_2O_3/water+EG multiphase fluid (Figure 7.9 (b)), the maximum density was observed at a concentration of 1.0 wt% and a temperature of 293.15 K. When the temperature is increased to 323.15 K, the density decreases by 1.67% and for concentrations of 0.5 and 0.75 wt%, the decreases are 1.95% and 1.76%, respectively. For all concentrations analyzed (0.5-1.0 wt%), the density values exceed those of the base fluid (water+EG with 4 g/l CMCNa) by 1.481%, 1.712% and 1.903%.

According to the graph in Figure 7.9 (c), the maximum density of the Ag-FeC/water multiphase fluid is also reached at 1.0 wt% and 293.15 K. At a temperature of 323.15 K, the density decreases by 1.94% and for concentrations of 0.50 and 0.75 wt%, it decreases by 1.86%. The density of the Ag-FeC/water+EG multiphase fluid increases on average by 1.277%, 1.522% and 1.712% as the Ag-FeC concentration rises from 0.5 to 1.0 wt%. The addition of nanoparticles influences the density, but the change in concentration from 0.50 to 1.0 wt% has a moderate impact.

For the Ag-TiO_2/water+EG multiphase fluid (Figure 7.9 (d)), the maximum density is reached at 1.0 wt% and 293.15 K. As the temperature increases to 323.15 K, the density decreases by 1.57% and for concentrations of 0.50 and 0.75 wt%, the decrease is 1.86%. The density values increase on average by 1.359%, 1.631% and 2.039% as the Ag-TiO_2 concentration rises from 0.5 to 1.0 wt%, although the increase in concentration does not significantly affect the density.

It can be concluded that the density of multiphase fluids decreases as the temperature increases, regardless of the base fluid used. Compared to water-based multiphase fluids, all fluids made with a water+EG mixture show a relatively higher decrease in density with increasing temperature. Concentration significantly influences the density of water+EG-based multiphase fluids, especially for the Ag-rGO/water+EG fluid, which had the highest density compared to the base fluid. The results obtained are consistent with those of other studies [42, 43, 44, 45], which show that nanoparticles have a higher density than the water+EG mixture and that their addition increases the density of the base fluid.

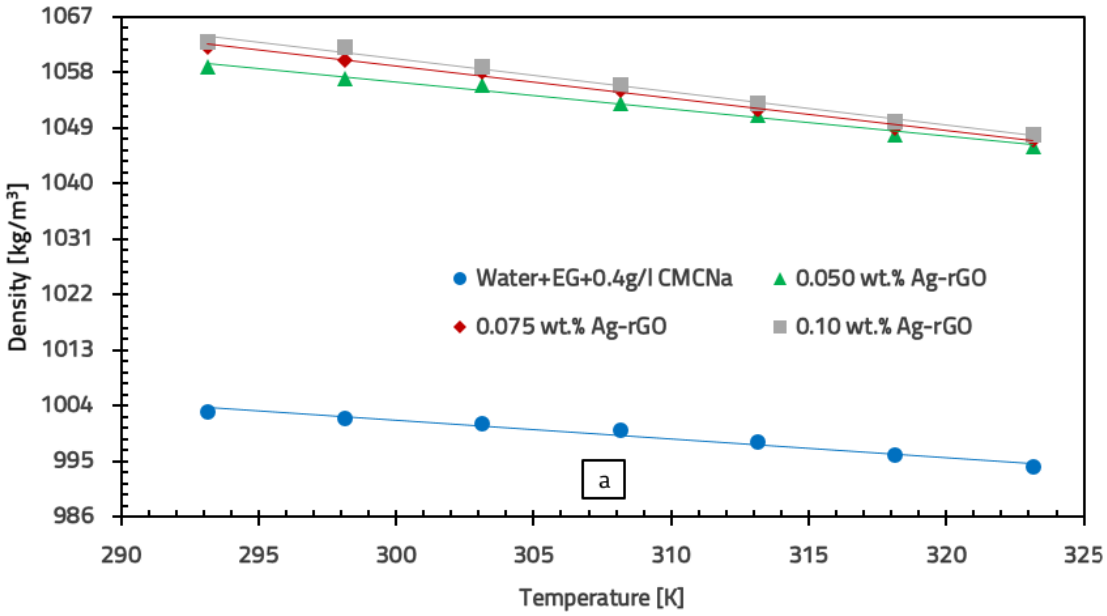
Density [kg/m³]
Temperature [K]
Water+EG+0.4g/l CMCNa
0.050 wt.% Ag-rGO
0.075 wt.% Ag-rGO
0.10 wt.% Ag-rGO
a

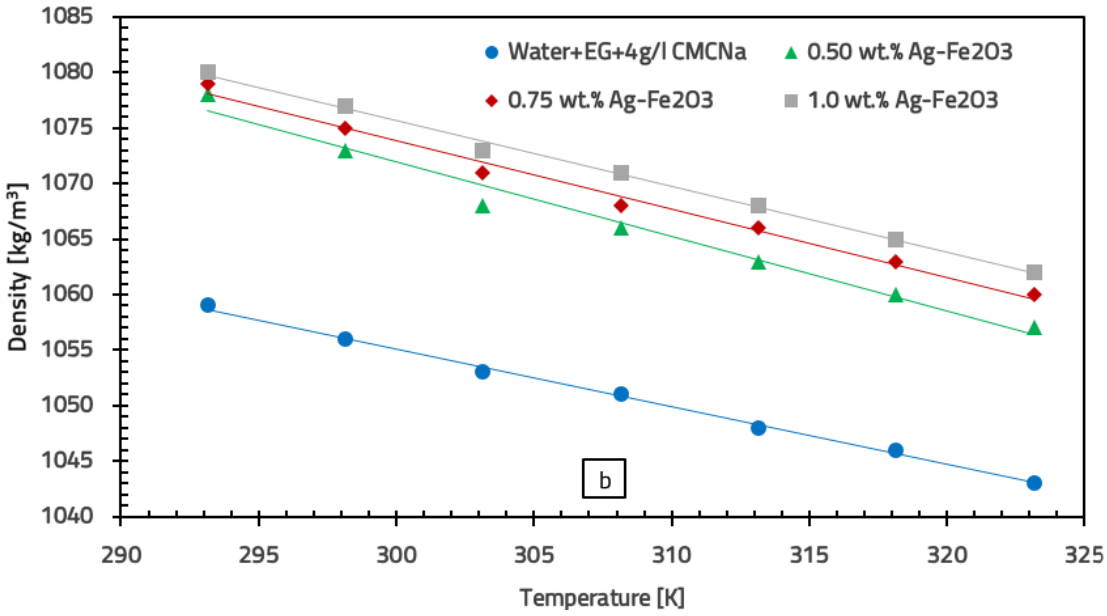
Density [kg/m³]
Temperature [K]
Water+EG+4g/l CMCNa
0.50 wt.% Ag-Fe2O3
0.75 wt.% Ag-Fe2O3
1.0 wt.% Ag-Fe2O3
b

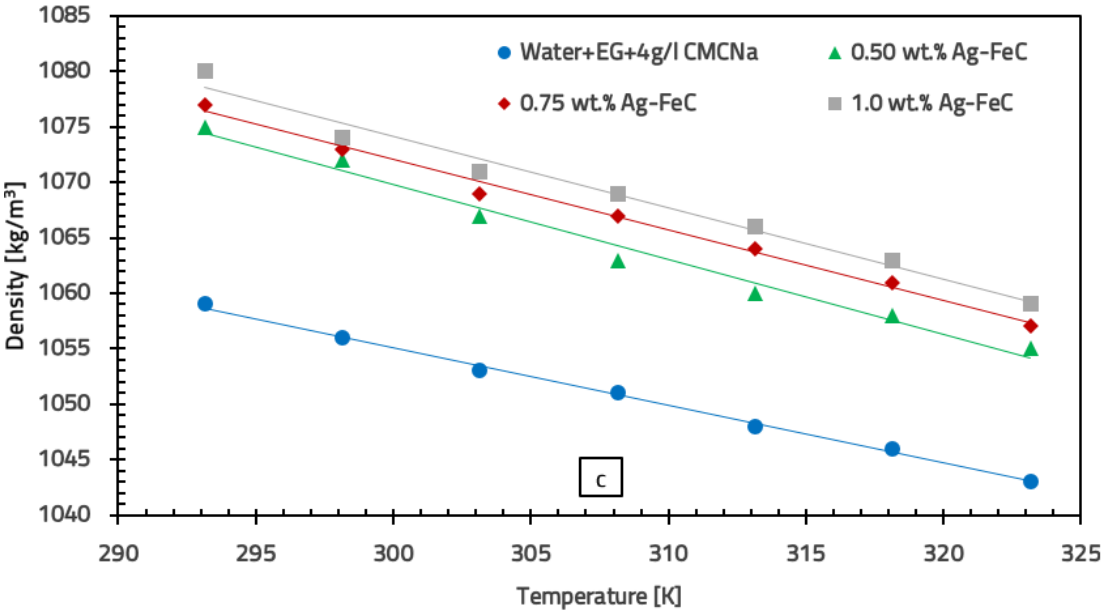
Density [kg/m³]
Temperature [K]
Water+EG+4g/l CMCNa
0.50 wt.% Ag-FeC
0.75 wt.% Ag-FeC
1.0 wt.% Ag-FeC
c

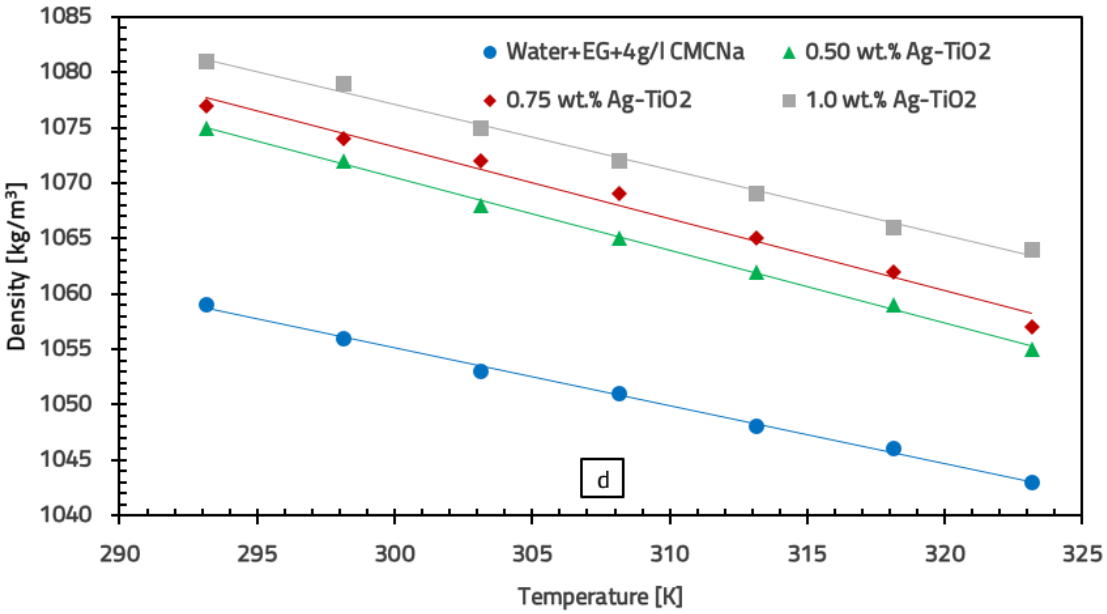

Figure 7.9. Variation of density with temperature for water+EG-based multiphase fluids: a) Ag-rGO; b) Ag-Fe_2O_3; c) Ag-FeC; d) Ag-TiO_2.

7.3.3 Conclusions on the study of multiphase fluid density

- Water-based multiphase fluids showed the best results in terms of density, with the highest average increase of 1% compared to the base fluid, achieved by the Ag-TiO_2/water multiphase fluid at a concentration of 1 wt%.
- The Ag-Fe_2O_3/water multiphase fluid at a concentration of 0.5 wt% demonstrated the best performance, showing a density reduction of 0.086% compared to water + 4 g/l CMCNa.
- Multiphase fluids prepared with a water+EG mixture exhibited the greatest density increases, with Ag-rGO/water+EG at a concentration of 0.1 wt% showing an average increase of 5.37% compared to the base fluid (water+EG with 0.4 g/l CMCNa).

7.4 Surface tension

The investigation of the surface tension of multiphase fluids is in its early stages compared to transport properties such as thermal conductivity or viscosity.

7.4.1 Surface tension of base fluids

In the first stage, the surface tension of the base fluids was measured to establish reference data. Two base fluids were considered: distilled water and a water+EG (1:1) mixture, to which 0.4 and 4 g/l of the surfactant CMCNa were added, respectively.

Figure 7.10 (a) presents the surface tension values for water, with and without surfactant, compared to NIST data [31]. The results confirm that the surface tension decreases as temperature increases, which is consistent with NIST data. The addition of the surfactant (0.4 and 4 g/l CMCNa) reduced the surface tension by 8.66% and 12.04% at 293.15 K and by 6.40% and 7.89% at 323.15 K [46].

Figure 7.10 (b) shows the surface tension for the water+EG solution. The surfactant (0.4 and 4 g/l CMCNa) reduced the surface tension by 4.63% and 7.36% at 293.15 K and by 0.23% and 1.82% at 323.15

K [46]. Experimental data for water+EG were compared with those provided by Jasper [47] and Connors et al. [48]. The maximum deviations from Jasper's and Connors' results were 1.78% and 1.58%, respectively.

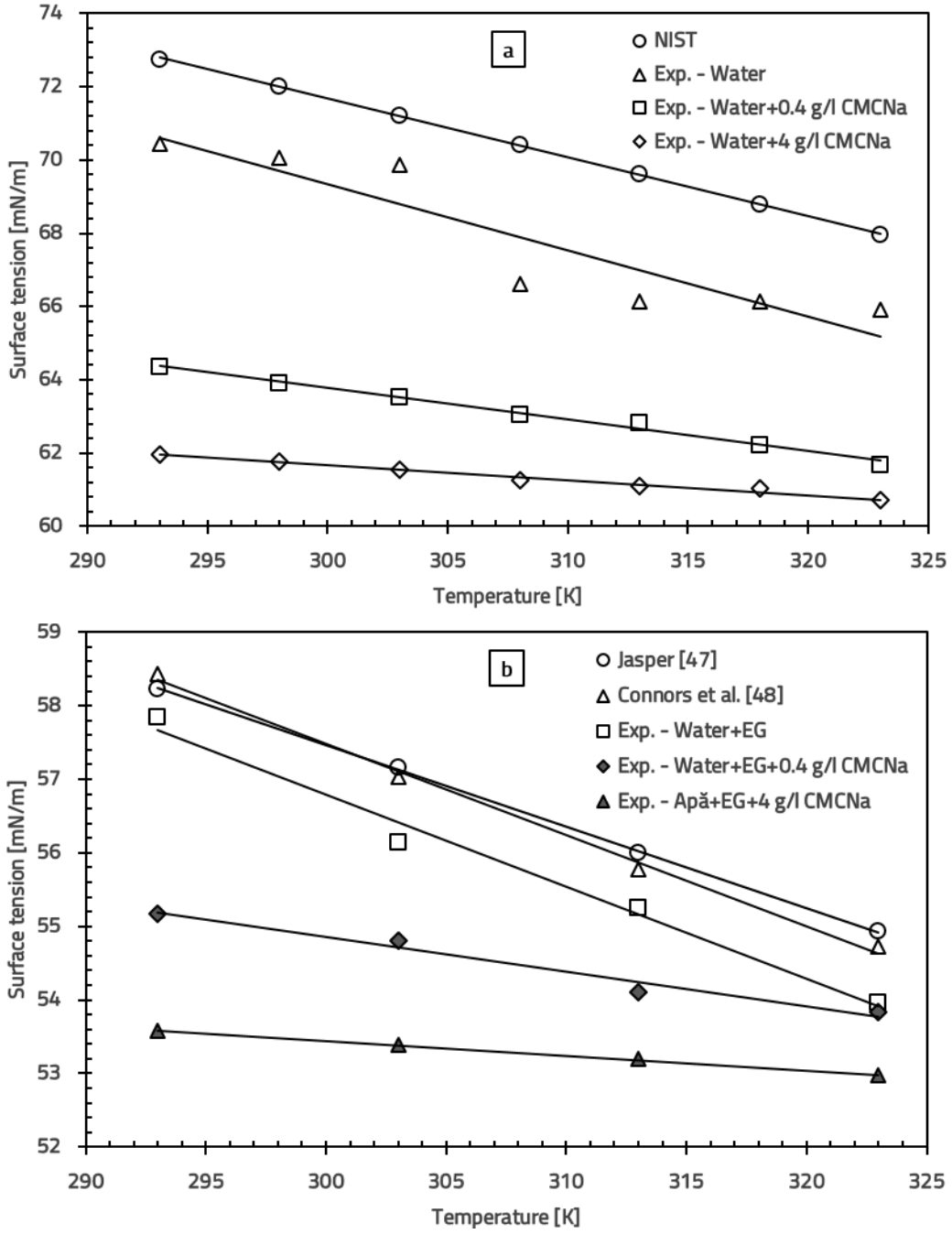

Figure 7.10. Validation of surface tension measurements for: a) water; b) water+EG mixture (1:1)

7.4.2 Surface tension of multiphase fluids

The average values of surface tension for water-based multiphase fluids as a function of temperature at different mass concentrations are shown in Figure 7.11. A decrease in surface tension can be observed for both the base fluid and the multiphase fluids as the temperature increases from 293.15 K to 323.15 K.

The interaction between nanoparticles and surfactants becomes complex due to the numerous interactions occurring at various interfaces [49]. The addition of nanoparticles significantly influences the surface tension and increasing their concentration leads to an increase in surface tension due to the van der Waals forces acting between particles at the liquid-gas interface, which results in an increase in the surface free energy. An increase in concentration reduces the distance between the two nanoparticles and the water molecule, especially at the liquid-gas interface, contributing to a higher surface tension [46]. Additionally, a higher concentration may promote particle aggregation, leading to further increases in surface tension.

In Figure 7.11 (a), the maximum surface tension is recorded for the Ag-rGO/water multiphase fluid at a concentration of 0.10 wt% and a temperature of 293.15 K. As the temperature increases from 293.15 K to 323.15 K, the surface tension decreases by approximately 8.66%. At concentrations of 0.050 and 0.075 wt%, the reduction was 5.16% and 4.74%, respectively. Although surface tension increased with concentration, it remained lower than that of the base fluid, showing reductions of 5.003% and 3.384% for concentrations of 0.050 and 0.075 wt%. At a concentration of 0.10 wt%, the surface tension was 5.006% higher than that of the base fluid [46]. These results are consistent with those reported by Cabaleiro et al. [50], who observed a similar decrease in surface tension for the rGO/water multiphase fluid.

According to the graph in Figure 7.11 (b), the maximum surface tension was observed for the Ag-Fe_2O_3/water multiphase fluid at a concentration of 1.0 wt% and a temperature of 293.15 K. The increase in temperature to 323.15 K led to a decrease of approximately 6.85%. For concentrations of 0.5 and 0.75 wt%, the decrease was 2.10% and 6.27%, respectively. The surface tension of the base fluid decreased on average by 11.948%, 10.020% and 8.743% as the concentration of Ag-Fe_2O_3 nanoparticles increased from 0.50 to 1.0 wt%. The obtained results are in agreement with those reported by Huminic et al. [51], who observed a reduction in surface tension by adding γ-Fe_2O_3 nanoparticles to water.

For the Ag-FeC/water multiphase fluid (Figure 7.11 (c)), the maximum surface tension was recorded at 1.0 wt% and 293.15 K. The increase in temperature to 323.15 K resulted in a decrease of 4.72%, while for concentrations of 0.50 and 0.75 wt%, the reductions were 2.18% and 2.59%, respectively. At a concentration of 0.50 wt%, the surface tension was 5.791% lower than that of the base fluid (water with 4 g/l CMCNa), but it increased at concentrations of 0.75% and 1.0 wt%, surpassing the values of water by 9.807% and 14.144%, respectively. This behavior is similar to that reported by Huminic et al. [52], who observed an increase in the surface tension of water with increasing FeC concentration.

For the Ag-TiO_2/water multiphase fluid (Figure 7.11 (d)), the maximum surface tension was recorded again at 1.0 wt% and 293.15 K. At a temperature of 323.15 K, the surface tension decreased by approximately 7.43%. The reduction was 5.21% at 0.5 wt% and 4.51% at 0.75 wt%. At a concentration of 0.5 wt%, the surface tension was 9.318% lower than that of the base fluid, while at concentrations of 0.75% and 1.0 wt%, it exceeded the values of water by 4.622% and 15.847%, respectively. These results are consistent with those reported by Zhang et al. [53], who observed a decrease in the surface tension of water by adding a smaller amount of TiO_2 nanoparticles.

It can be observed that a higher concentration of nanoparticles (0.1 and 1.0 wt%) leads to significant changes in surface tension as a function of temperature, with the increase being more pronounced at the lower temperature (293.15 K) than at the higher temperature (323.15 K).

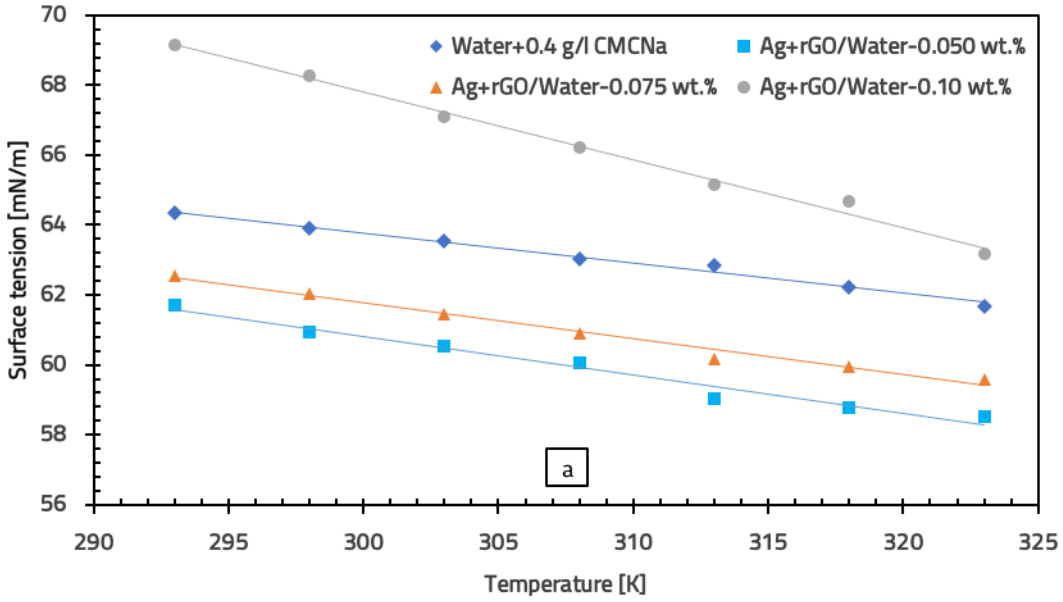
Water+0.4 g/l CMCNa
Ag+rGO/Water-0.050 wt.%
Ag+rGO/Water-0.075 wt.%
Ag+rGO/Water-0.10 wt.%
Surface tension [mN/m]
Temperature [K]
a

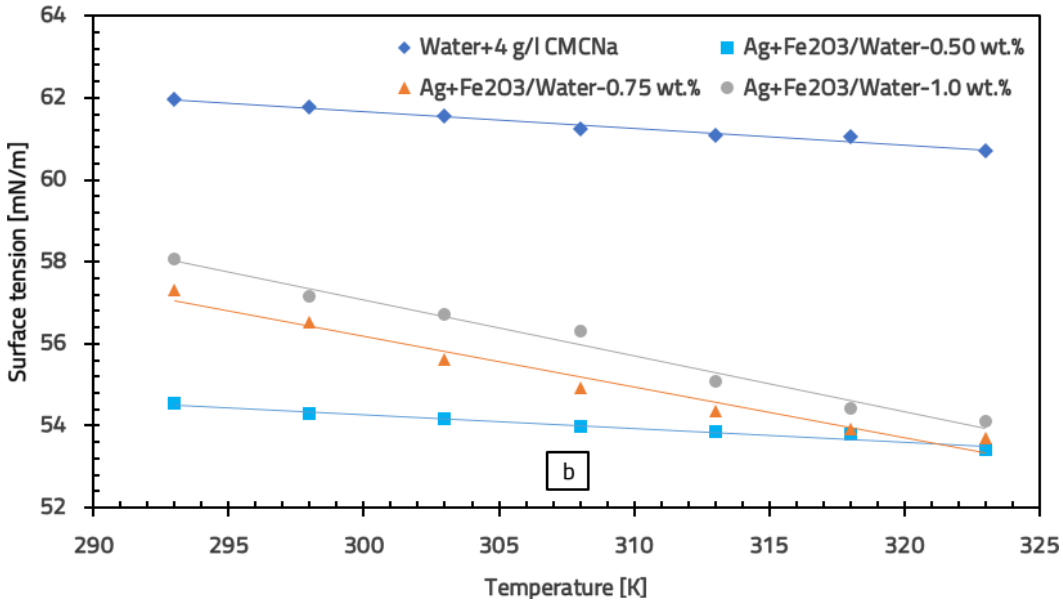
Water+4 g/l CMCNa
Ag+Fe2O3/Water-0.50 wt.%
Ag+Fe2O3/Water-0.75 wt.%
Ag+Fe2O3/Water-1.0 wt.%
Surface tension [mN/m]
Temperature [K]
b

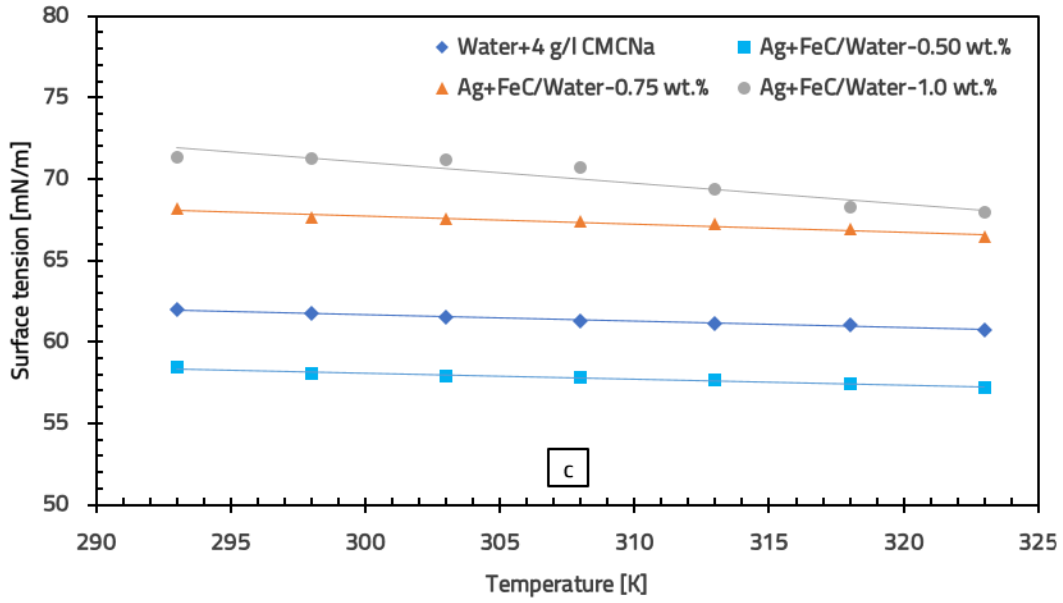
Water+4 g/l CMCNa
Ag+FeC/Water-0.50 wt.%
Ag+FeC/Water-0.75 wt.%
Ag+FeC/Water-1.0 wt.%
Surface tension [mN/m]
Temperature [K]
c

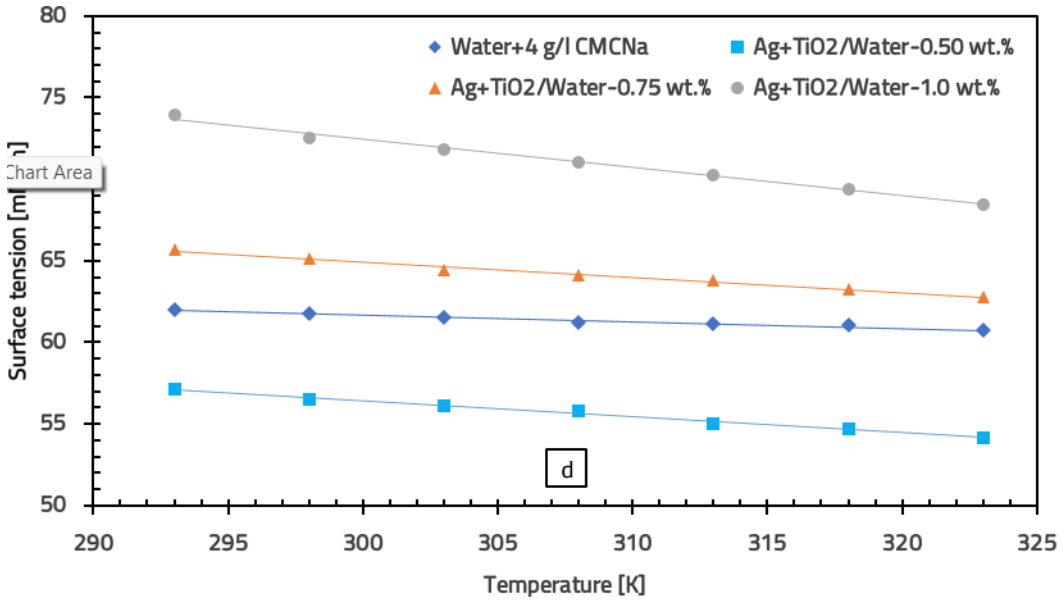

Figure 7.11. Variation of surface tension with temperature for water-based multiphase fluids: a) Ag-rGO; b) Ag-Fe_2O_3; c) Ag-FeC; d) Ag-TiO_2

The variation of surface tension in water+EG-based multiphase fluids with temperature at different concentrations is shown in Figure 7.12. A trend similar to that of water-based multiphase fluids can be observed, characterized by a decrease in surface tension as the temperature increases. The Ag-rGO and Ag-FeC multiphase fluids in water+EG exhibit higher surface tension than the base fluid at all studied concentrations. For Ag-Fe_2O_3 in water+EG, the surface tension is lower at 0.5 wt% and at 0.75 wt%, it is lower only at 323.15 K. The Ag-TiO_2/water+EG multiphase fluid shows lower surface tension values for all nanoparticle concentrations, except for the 1 wt% concentration at 293.15 and 298.15 K. Compared to water-based multiphase fluids, water+EG-based fluids (except for Ag-TiO_2 and Ag-Fe_2O_3 at the 0.5 wt% concentration) show a significant increase in surface tension compared to the base fluid at all concentrations.

In Figure 7.12 (a), it can be observed that the Ag-rGO/water+EG multiphase fluid shows the highest surface tension at a concentration of 0.10 wt% and a temperature of 293.15 K. At 323.15 K, the surface tension decreases by approximately 3.53% and for concentrations of 0.050 and 0.075 wt%, it decreases by 4.08% and 3.19%, respectively. Notably, the surface tension of the base fluid (water+EG with 0.4 g/l CMCNa) increases by 8.125%, 8.824% and 9.369% as the nanoparticle concentration increases from 0.050 to 0.1 wt%. Although adding nanoparticles significantly affects surface tension, increasing the concentration from 0.050 to 0.10 wt% has a moderate impact on it [46].

For the Ag-Fe_2O_3/water+EG multiphase fluid (Figure 7.12 (b)), the maximum surface tension value was observed at a concentration of 1.0 wt% and a temperature of 293.15 K. As the temperature increases to 323.15 K, the surface tension decreases by 3.87% and for concentrations of 0.5 and 0.75 wt%, the reduction is 2.36% and 4.09%, respectively. At a concentration of 0.5 wt%, the surface tension decreases by 1.059% compared to the base fluid and as the Ag-Fe_2O_3 concentration increases to 0.75% and 1 wt%, the surface tension exceeds the base fluid values by 1.248% and 4.733%, respectively.

In the case of the Ag-FeC/water+EG multiphase fluid (Figure 7.12 (c)), the maximum surface tension was recorded at a concentration of 1.0 wt% and a temperature of 293.15 K. At 323.15 K, the surface tension decreases by 3.92% and for concentrations of 0.5 and 0.75 wt%, the reduction was 4.01% and 4.03%, respectively. The surface tension of the water+EG mixture with 4 g/l CMCNa increases by

11.630%, 12.252% and 12.489% as the concentration increases from 0.5 to 1.0 wt%. Adding nanoparticles to the base fluid significantly influences the surface tension, though the impact of increasing the concentration from 0.5 to 1.0 wt% is moderate.

In Figure 7.12 (d), it can be seen that the maximum surface tension for the Ag-TiO_2/water+EG multiphase fluid was recorded at 1.0 wt% and 293.15 K. At 323.15 K, it decreases by approximately 8.25% and for concentrations of 0.50 and 0.75 wt%, it decreases by 6.75% and 8.79%, respectively. The surface tension of the base fluid (water+EG with 4 g/l CMCNa) decreases on average by 8.098%, 4.501% and 1.652% as the concentration increases from 0.50 to 1.0 wt%.

Surface tension decreases with temperature, regardless of the base fluid. The increase in concentration leads to an increase in surface tension, as both the nanoparticles and the water molecules tend to move towards the liquid-gas interface and approach each other.

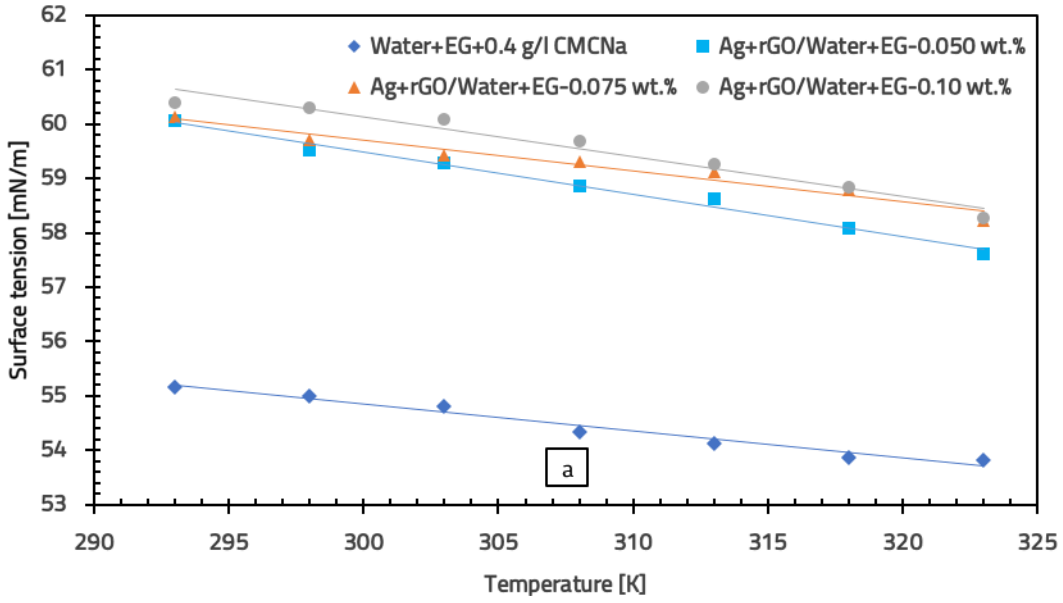

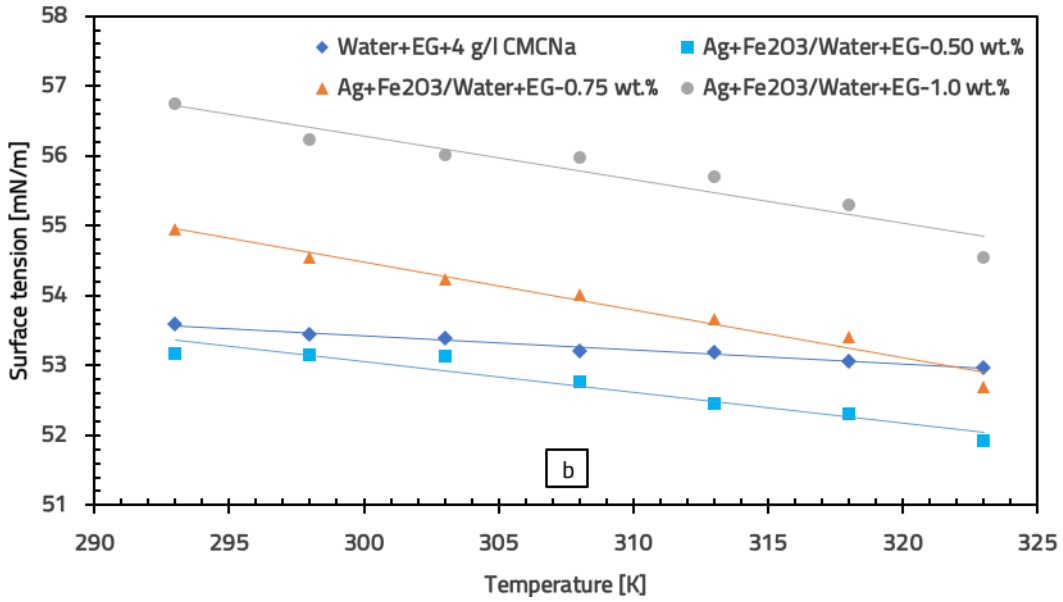

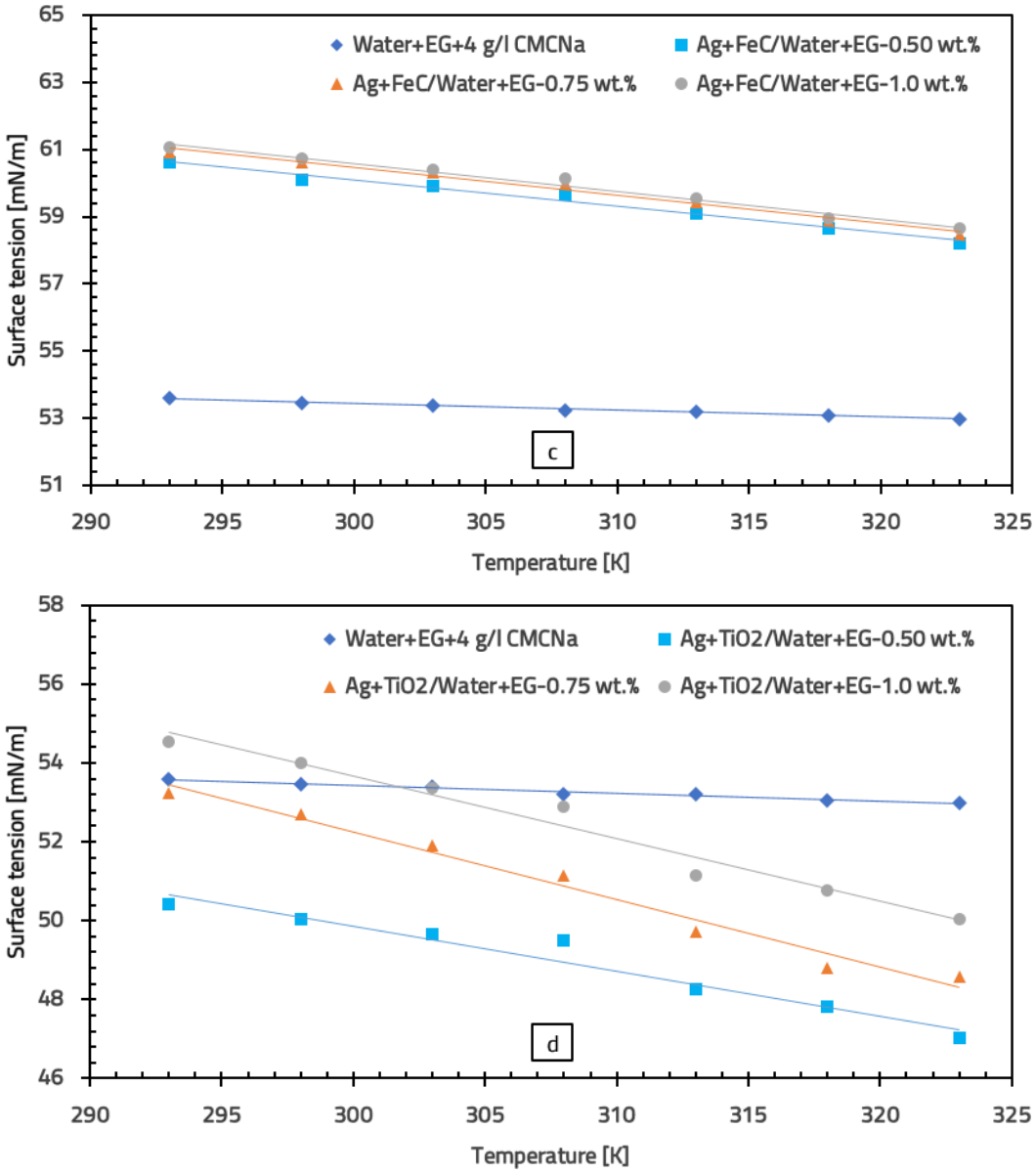

Figure 7.12. Variation of surface tension with temperature for water+EG-based multiphase fluids: a) Ag-rGO; b) Ag-Fe_2O_3; c) Ag-FeC; d) Ag-TiO_2

7.4.3 Conclusions on the surface tension study of multiphase fluids

- For the Ag-rGO/water multiphase fluid, the surface tension decreased by 5.00% and 3.38% at 0.050 and 0.075 wt%, respectively, while at 0.1 wt%, it increased by 5.01% compared to water+0.4 g/l CMCNa.
- For the Ag-rGO/water+EG multiphase fluid, the surface tension is higher than that of water+EG with 0.4 g/l CMCNa. The increases are 8.12%, 8.82% and 9.37% at 0.05, 0.075 and 0.1 wt%, respectively.
- The Ag-Fe_2O_3/water multiphase fluid shows a lower surface tension than water+4 g/l CMCNa at all concentrations (0.5, 0.75 and 1.0 wt%), with reductions of 11.95%, 10.02% and 8.74%.
- The Ag-TiO_2/water+EG multiphase fluid has a lower surface tension than water+EG with 4 g/l, recording decreases of 8.10, 4.50 and 1.65% at concentrations of 0.5, 0.75 and 1.0 wt%.
- As the temperature increases, the surface tension decreases more in water-based multiphase fluids than in water+EG-based fluids.

7.5 Specific heat

Based on the density measurements, the specific heat (SH) values for water-based and water+EG-based multiphase fluids were calculated. The following equation was used to calculate the SH:

$$C_{p,fm} = \frac{\varphi_{np1} * \rho_{np1} * C_{p,np1} + \varphi_{np2} * \rho_{np2} * C_{p,np2} + (1 - \varphi_{np1} - \varphi_{np2}) * C_{p,fb}}{\rho_{fm}} \quad (7.1)$$

Subsequently, the effect of temperature and concentration on the SH of the multiphase fluids was analyzed.

7.5.1 Effect of temperature and concentration on the specific heat (SH) of multiphase fluids

Temperature has a significant impact on the SH of multiphase fluids. It is widely believed that these multiphase fluids have a lower SH than water. Fazeli et al. [54] attributed this phenomenon to the increased thermal diffusivity. The effect of temperature on SH varies slightly and, in some cases, is inconclusive. Nanoparticle concentration is directly proportional to the SH of multiphase fluids. This trend can be attributed to the combined effect of the SH of the nanoparticles and the base fluid. As the concentration of nanoparticles increases, there is a change in the free energy at the interface between the solid phase and the liquid phase. Due to the large surface area of the nanoparticles, the surface free energy significantly influences the overall heat transfer, impacting the SH of nanocomposite materials [55]. Figure 7.13 shows the variation of SH for water-based multiphase fluids as a function of temperature at different concentrations.

For the Ag-rGO/water multiphase fluid (Figure 7.13 (a)), SH increases between 293.15 and 298.15 K, decreases until 318.15 K and then increases again. This behavior is observed for all studied concentrations, but at a concentration of 0.050 wt%, SH keeps decreasing as the temperature rises. The observed trend is similar to the one reported by Devarajan et al. [56] for the CNT-Al_2O_3 multiphase fluid. As the temperature increases from 293.15 to 323.15 K, SH decreases on average by 0.071%, 0.174% and 0.176% for concentrations of 0.05, 0.075 and 0.1 wt%. For Ag-rGO/water, SH decreases by 0.039%, 0.458% and 0.591% at concentrations of 0.05, 0.075 and 0.1 wt%, compared to water. These results align with those reported by Gao et al. [57], who observed a 4% and 7% decrease in SH for Graphene-Al_2O_3/water at concentrations of 0.05 and 0.15 wt% at a temperature of 20 °C, compared to water.

In Figure 7.13 (b), it can be seen that for the Ag-Fe_2O_3/water multiphase fluid at a concentration of 0.5 wt%, SH decreases between 293.15 and 308.15 K, then increases with rising temperature. At 0.75 wt%, SH decreases between 293.15 and 298.15 K, increases until 318.15 K and then decreases again. At 1.0 wt%, SH decreases between 293.15 and 298.15 K, then increases until 303.15 K and decreases once more. SH at a concentration of 0.5 wt% is similar to that of water and increases by 0.033% between 293.15 and 323.15 K. At concentrations of 0.75 and 1.0 wt%, the increases are larger, at 0.331% and 0.525%. The trend observed for Ag-Fe_2O_3/water is similar to that reported by Ahammed et al. [58] for the Graphene-Al_2O_3/water multiphase fluid. At a concentration of 0.5 wt%, SH increased by 0.068% on average, while at concentrations of 0.75 and 1.0 wt%, it decreased by 0.112% and 0.575%, respectively, compared to water. A similar behavior was observed by Sundar et al. [59] for the MWCNT-Fe_3O_4/water multiphase fluid.

For the Ag-FeC/water multiphase fluid (Figure 7.13 (c)), SH at concentrations of 0.5 and 0.75 wt% decreases between 293.15 and 303.15 K, then increases until 318.15 K and decreases again. At 1.0

wt%, SH decreases between 293.15 and 308.15 K, then increases until 318.15 K and decreases once more. The temperature increase from 293.15 to 323.15 K results in a decrease in SH by 0.072% for 0.5 and 0.75 wt% and 0.146% for 1.0 wt%. The trend observed in the effect of temperature on SH for the Ag-FeC/water multiphase fluid is similar to that reported by Fazeli et al. [54]. As the concentration increases from 0.5 to 1.0 wt%, SH decreases by 0.272%, 0.420% and 0.977%. This trend is similar to that observed by Okonkwo et al. [60] for the Al_2O_3-Fe/water multiphase fluid.

In Figure 7.13 (d), it can be observed that for the Ag-TiO_2/water multiphase fluid at 0.5 wt%, SH increases between 293.15 and 303.15 K, decreases until 308.15 K and then increases again. At 0.75 wt%, SH decreases between 293.15 and 298.15 K, increases until 318.15 K and then decreases at higher temperatures. At 1.0 wt%, SH increases between 293.15 and 298.15 K, decreases until 303.15 K and increases again. The temperature increase from 293.15 to 323.15 K results in an increase in SH by 0.126% and 0.220% for 0.5 and 1.0 wt% and a decrease of 0.076% for 0.75 wt%. The same trend was observed by Yarmand et al. [61] for GNP-Pt/water. For concentrations of 0.5, 0.75 and 1.0 wt%, SH decreases by 0.473%, 0.813% and 1.067%, compared to water. A similar trend was observed by Moldoveanu and Minea [62] for Al_2O_3-TiO_2/water.

Based on the results obtained, it can be concluded that temperature and nanoparticle concentration have a small effect on the SH of water-based multiphase fluids.

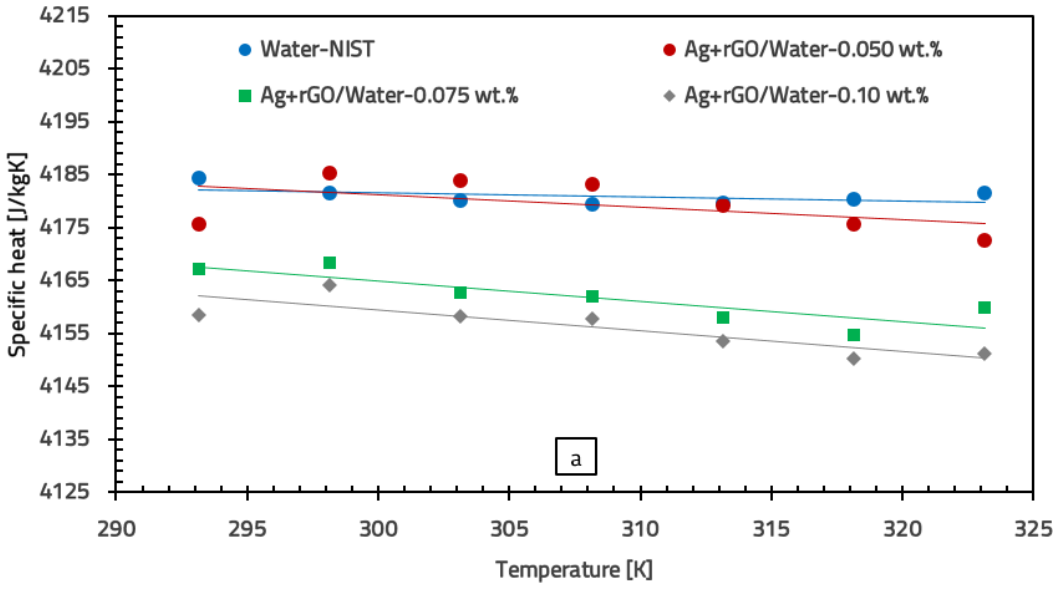

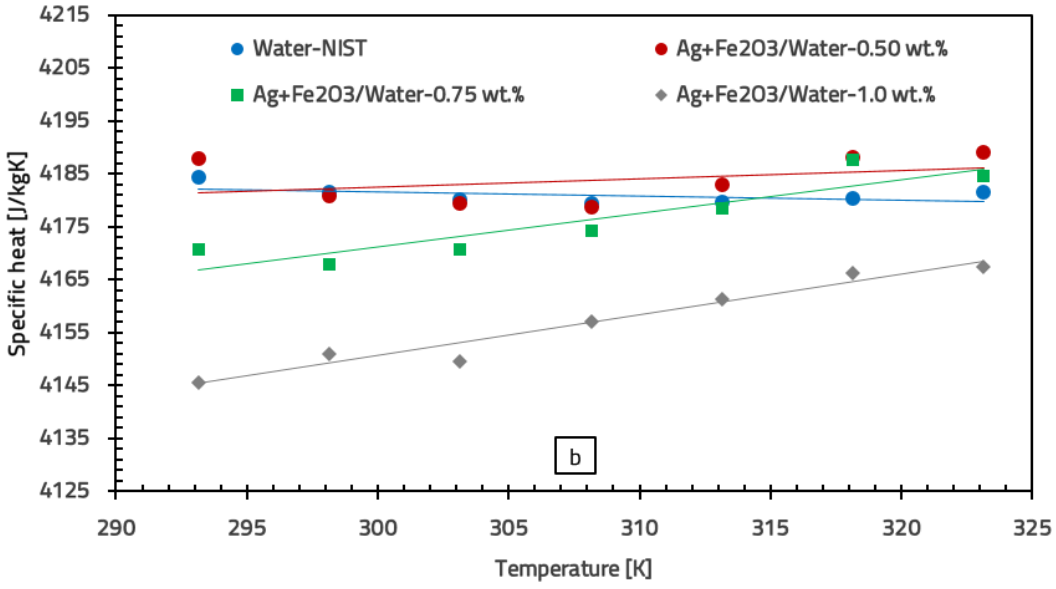

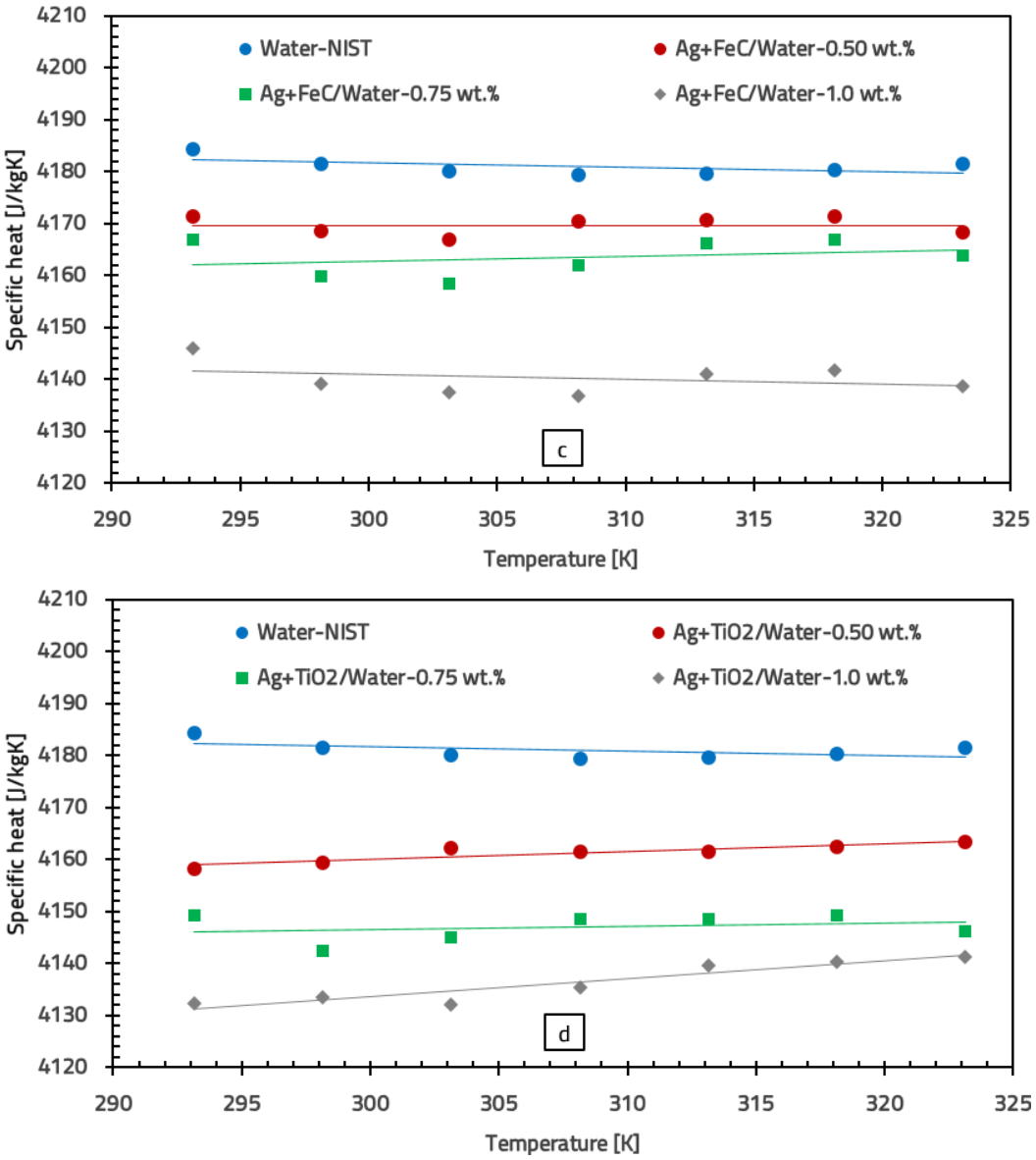

Figure 7.13. Variation of specific heat with temperature for water-based multiphase fluids: a) Ag-rGO; b) Ag-Fe_2O_3; c) Ag-FeC; d) Ag-TiO_2.

The variation of SH of water+EG (1:1)-based multiphase fluids with temperature at different mass concentrations is shown in Figure 7.14. It can be observed that for all the analyzed multiphase fluids, SH increases with temperature. Additionally, the SH values for multiphase fluids based on Ag with rGO, Fe_2O_3, FeC and TiO_2 decrease as the nanoparticle concentration increases, being significantly lower than those of the water+EG solution.

For the Ag-rGO/water+EG multiphase fluid (Figure 7.14 (a)), at concentrations of 0.050, 0.075 and 0.1 wt%, SH increased by approximately 3.851%, 4.046% and 4.044% as the temperature rose from 293.15 to 323.15 K. The increase in concentration from 0.050 wt% to 0.1 wt% resulted in a decrease in SH by 5.109%, 5.280% and 5.387%, compared to the water+EG (1:1) solution [34].

For the Ag-Fe_2O_3/water+EG multiphase fluid (Figure 7.14 (b)), SH increased as the temperature rose from 293.15 to 323.15 K, with increases of 3.965%, 3.767% and 3.667% for the concentrations of 0.5, 0.75 and 1.0 wt%, respectively. Although the trend is similar to the previous one, the reductions were smaller, with decreases of 1.467%, 1.695% and 1.882% at higher nanoparticle concentrations (0.5, 0.75 and 1.0 wt%).

According to the data in Figure 7.14 (c), SH for the Ag-FeC/water+EG multiphase fluid increased by 3.873%, 3.868% and 3.960% at concentrations of 0.5, 0.75 and 1.0 wt%, as the temperature increased from 293.15 to 323.15 K. At the same time, SH decreased on average by 1.267%, 1.508% and 1.695% as the nanoparticle concentration increased from 0.5 to 1.0 wt%, compared to the water+EG solution. For the Ag-TiO_2/water+EG multiphase fluid (Figure 7.14 (d)), SH increased with temperature by 3.872%, 3.868% and 3.567% at concentrations of 0.5, 0.75 and 1.0 wt%. At the same time, SH decreased on average by 1.361%, 1.635% and 2.039% at the same concentrations, compared to the water+EG mixture.

The results show that both temperature and concentration significantly impact the SH of multiphase fluids based on the water+EG (1:1) mixture. An increase in temperature leads to an increase in SH, while a higher nanoparticle concentration results in a decrease in SH. This trend is similar to that observed for water-based multiphase fluids, as the water+EG mixture has a higher SH than the nanoparticles. Furthermore, even at low concentrations, nanoparticles significantly reduce SH, especially at lower temperatures. These observations are consistent with findings in the literature [63, 64].

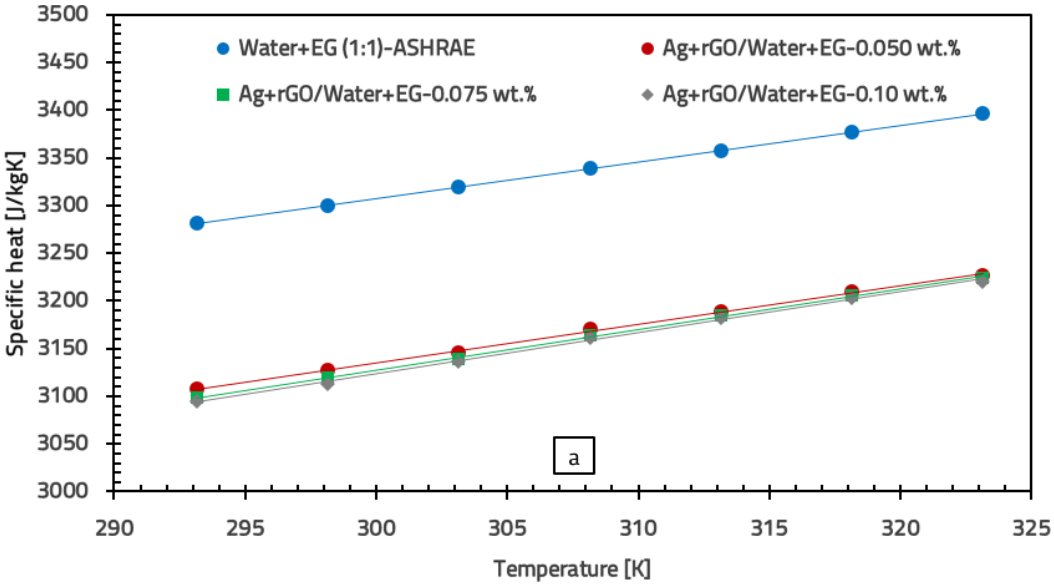

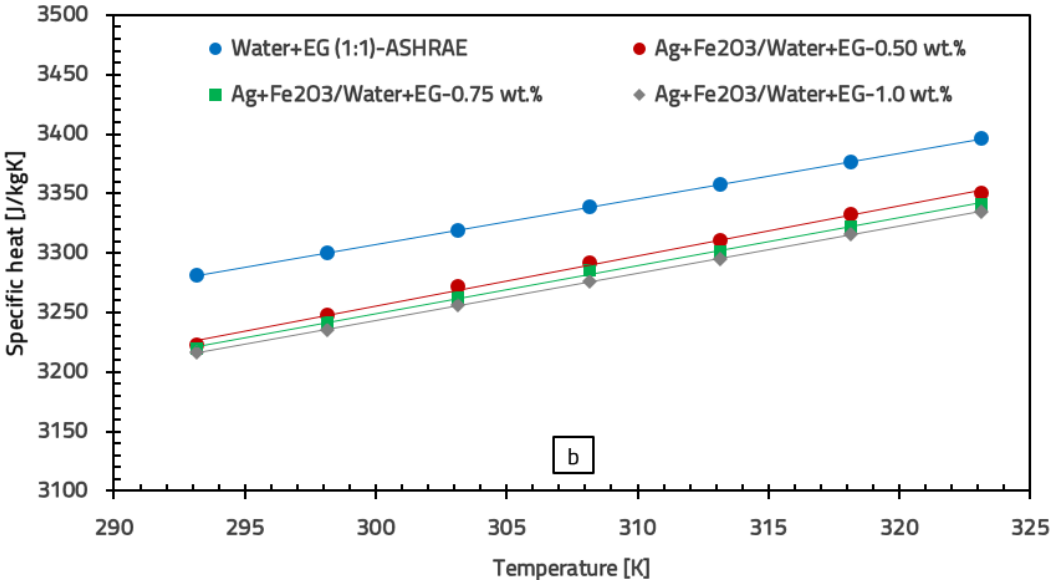

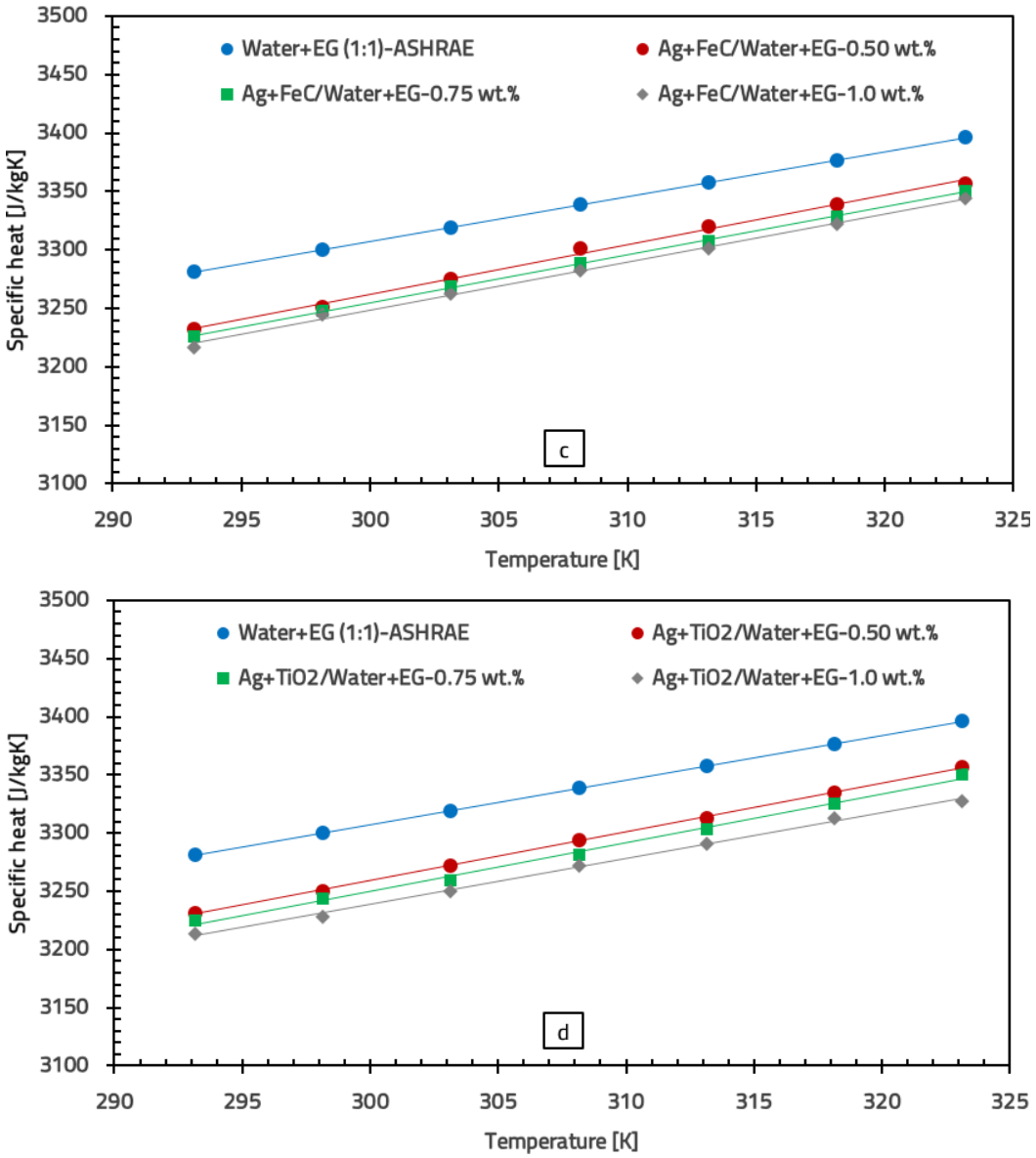

Figure 7.14. Variation of specific heat with temperature for water+EG-based multiphase fluids: a) Ag-rGO; b) Ag-Fe_2O_3; c) Ag-FeC; d) Ag-TiO_2.

7.5.2 Conclusions on the specific heat of multiphase fluids

- The Ag-Fe_2O_3/water multiphase fluid at a concentration of 0.5 wt% showed the best performance, with a 0.068% increase in SH compared to the base fluid.
- The addition of nanoparticles to water led to a decrease in SH, with the maximum reduction of 1.067% observed for the Ag-TiO_2/water multiphase fluid at a concentration of 1 wt%.
- The Ag-rGO/water+EG multiphase fluid showed the largest reduction in SH, 5.387%, at a concentration of 0.1 wt%, compared to the water+EG solution.
- The Ag-FeC/water+EG multiphase fluid at a concentration of 0.5 wt% demonstrated the best results in the water+EG mixture, with a reduction of 1.267%, suggesting that certain nanoparticle combinations can provide a SH close to that of the base fluid.
- Based on the results, it can be concluded that Ag-Fe_2O_3/water exhibits the best SH among the studied multiphase fluids, while Ag-FeC/water+EG showed the best results in the water+EG mixture.

8. OPTICAL PROPERTIES – EXPERIMENTAL RESULTS

8.1 Experimental procedure

This study investigates the transmittance and absorbance values of various multiphase fluids (Ag-rGO, Ag-Al_2O_3, Ag-TiO_2, Ag-FeC), using water and a water+EG mixture as the base fluids, while considering factors such as mass concentration and nanoparticle materials. All multiphase fluids were analyzed at three different nanoparticle mass concentrations.
During the experiment, all measurements were carried out at a constant temperature of 293.15 K. The analysis of the obtained spectra was limited to the 220-1400 nm range, as the absorption of near-infrared light by both water and the water+EG mixture (the primary fluids used) beyond this range is extremely high.

8.2 Interpretation of results for base fluids

Measurements for the base fluids (water and water+EG), with and without surfactant (0.4 and 4 g/l CMCNA), were carried out at room temperature (293.15 K) within the wavelength range of 220-1400 nm.
Figure 8.1 shows that for an optical path length of 1 mm, water exhibits a well-known behavior with high transmittance, being unable to absorb radiation within the studied range. The addition of EG to water does not significantly alter the transmittance values.
Figure 8.1 (a) illustrates the transmittance of water and the surfactant CMCNa mixed in water, while Figure 8.1 (b) shows the transmittance of the water+EG mixture and the surfactant in this mixture. The graph clearly demonstrates that the surfactant has a negligible effect on the optical transmittance of both water and the water+EG mixture. Therefore, any modification of the optical properties of the multiphase fluid, compared to water and the water+EG mixture, will be due solely to the presence of nanoparticles [65].

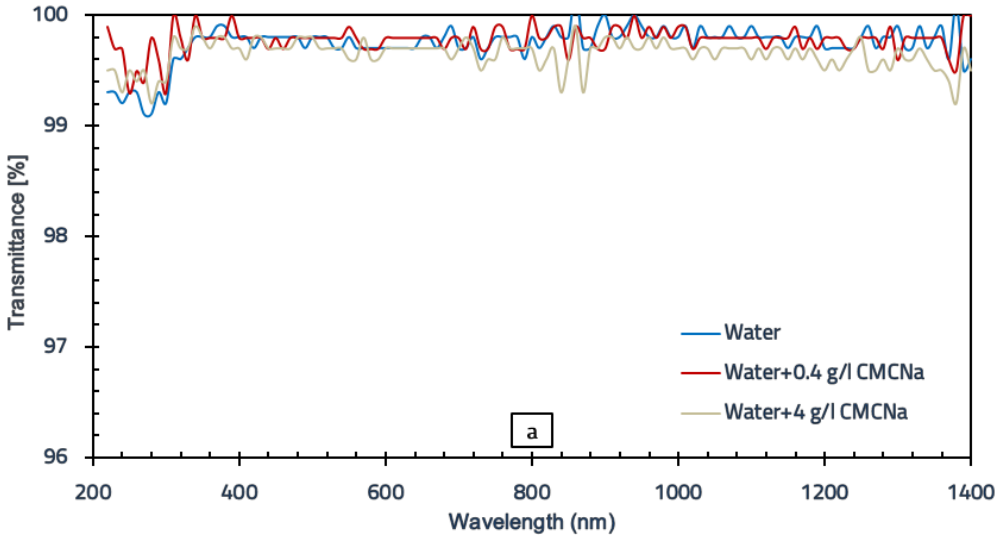

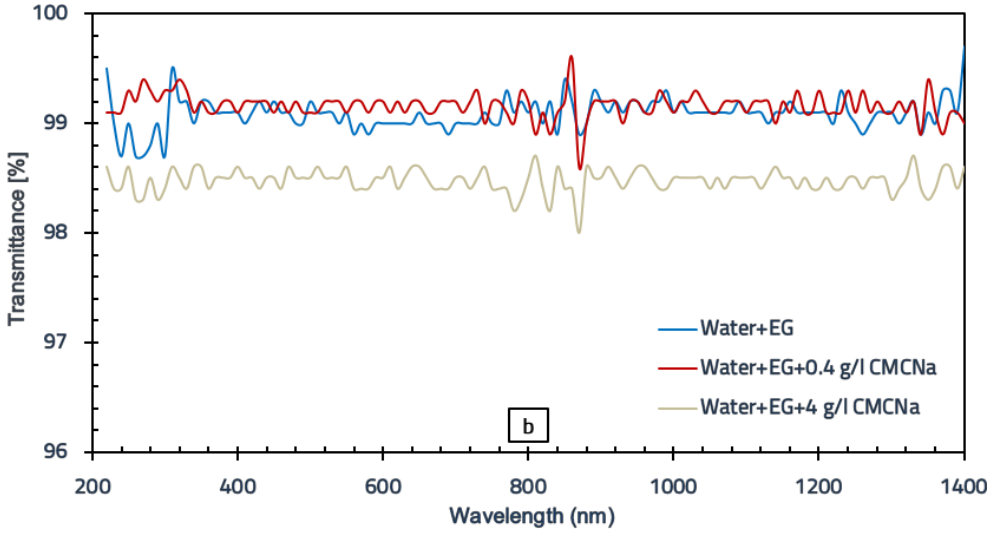

Figure 8.1. Transmittance for: a) water; b) water+EG (50%-50%) – 1 mm optical path.

In Figure 8.2, a decrease in transmittance is observed for both water and the water+EG mixture, with and without surfactant, for an optical path length of 10 mm. It can be concluded that transmittance is dependent on the optical path length and an increase in this length leads to a reduction in transmittance.

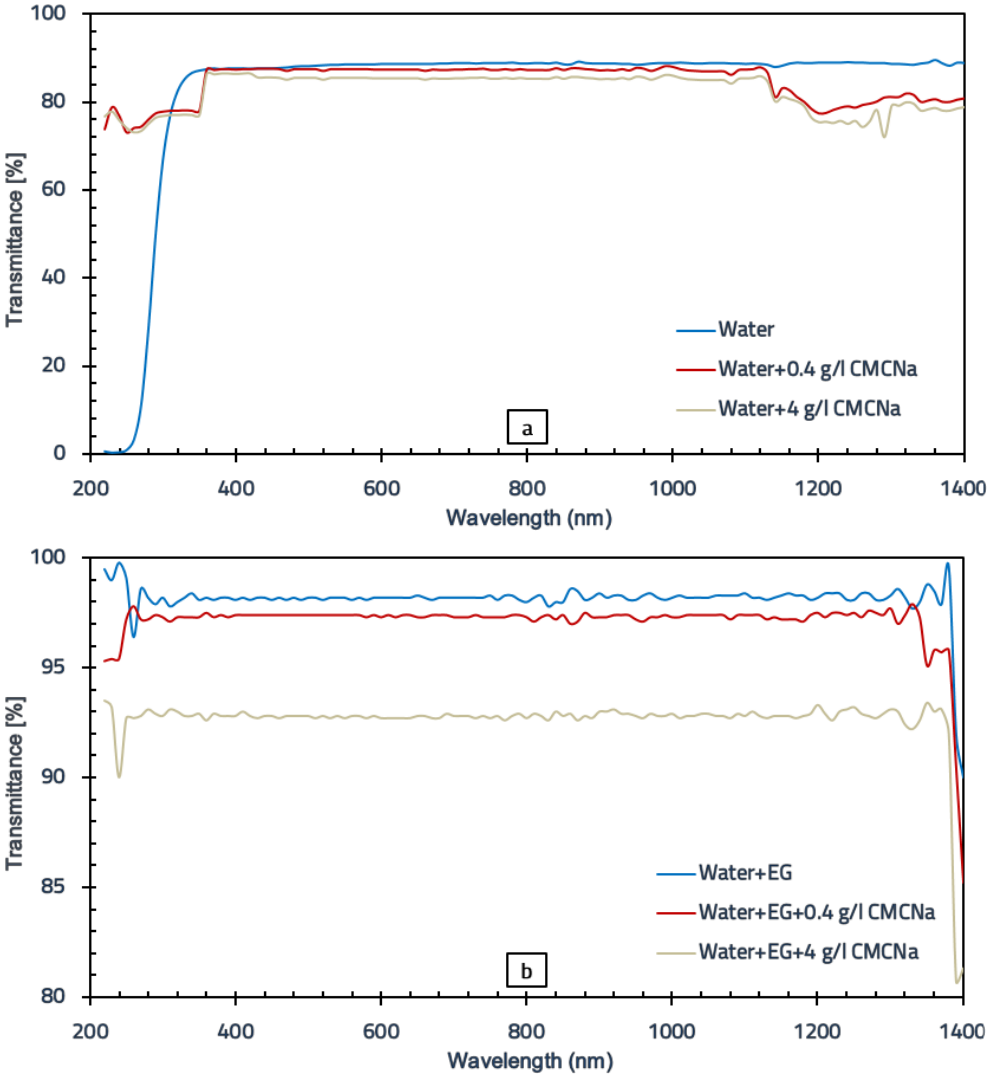

Figure 8.2. Transmittance for: a) water; b) water+EG (50%-50%) – optical path length of 10 mm

The following presents the optical properties of the multiphase fluids based on water and water+EG (1:1). A quartz cuvette with a 1 mm optical path length was used to measure the absorbance and transmittance of the multiphase fluids. The results of these measurements are shown in Figures 8.3-8.18.

8.3 Water-based multiphase fluids

8.3.1 Transmittance

The transmittance results for water-based multiphase fluids at different mass concentrations are presented in Figures 8.3-8.6.

Figure 8.3 shows the transmittance values for the Ag-rGO/water multiphase fluid at concentrations of 0.05, 0.075 and 0.1 wt%, compared to distilled water with 0.4 g/l CMCNa, which was used as the reference. The transmittance of the Ag-rGO/water multiphase fluid is very low (below 7%) in the near-infrared region after a wavelength of 800 nm, whereas distilled water maintains a transmittance of approximately 100% across the entire wavelength range [65]. However, the transmittance of the Ag-rGO/water multiphase fluid is high for wavelengths between 220-550 nm, reaching a maximum value of 44.53% at 390 nm for a concentration of 0.05 wt%. For concentrations of 0.075 and 0.1 wt%, the maximum transmittance values were 37.23% and 22.83%, at 390 nm and 340 nm, respectively. At 0.1 wt%, the transmittance is approximately 2% in the near-infrared region and decreases towards zero, indicating complete light absorption. The Ag and rGO nanoparticles endow the multiphase fluid with excellent optical absorption properties, suggesting its potential use as a working fluid in a DASC.

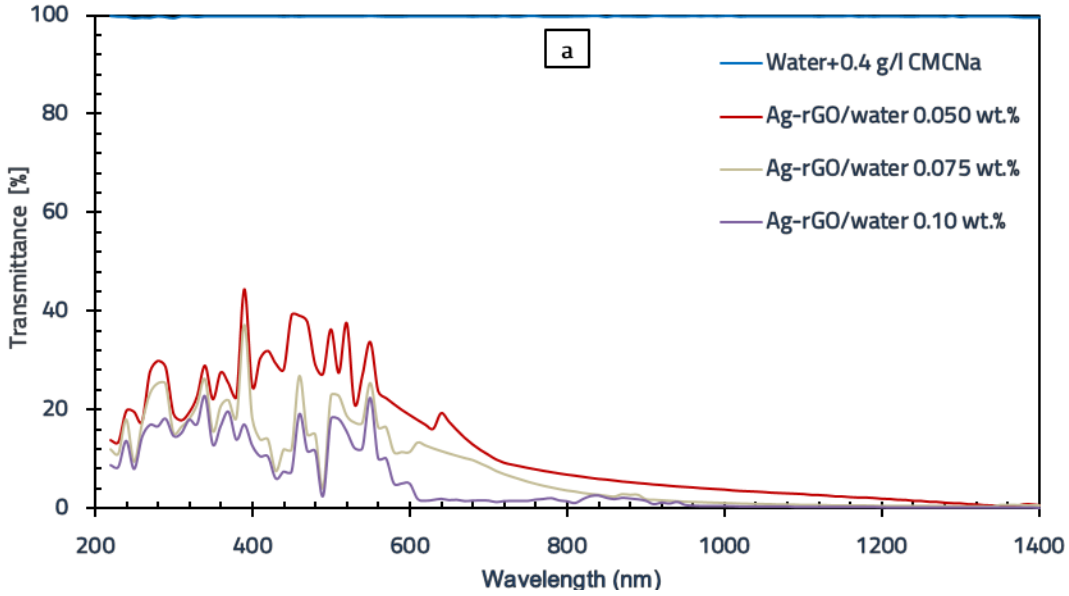

Figure 8.3. Transmission spectrum of water and the Ag-rGO/water multiphase fluid

Figure 8.4 shows the transmission spectra of the Ag-Fe_2O_3/water multiphase fluid at concentrations of 0.5, 0.75 and 1.0 wt%, compared to the reference sample (water + 4 g/l CMCNa). Water with 4 g/l CMCNa is transparent across the entire wavelength range. The Ag-Fe_2O_3/water multiphase fluid exhibits a maximum transmittance of 68.73% at 1400 nm for the 0.5 wt% concentration, which decreases to 64.16% for 0.75 wt% and 57.16% for 1 wt%. The fluid at 0.5 wt% shows high transmittance (64.83%-68.73%), indicating low absorption. A similar trend of increasing transmittance is observed for

the 0.5 and 0.75 wt% concentrations, while for 1 wt%, the increase is more pronounced, likely due to excessive nanoparticle aggregation and suspension instability.

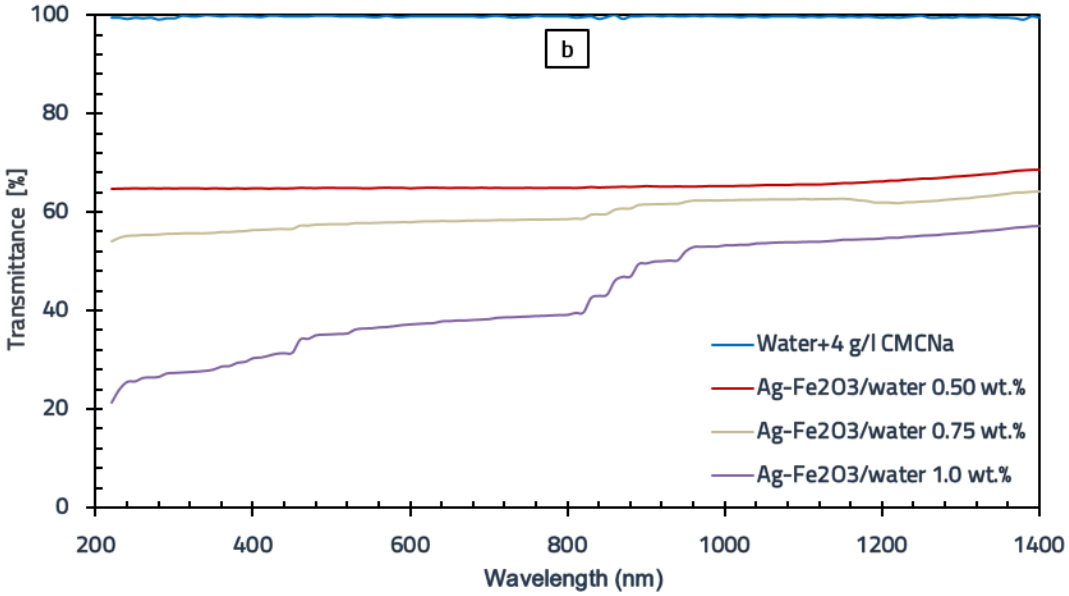

Figure 8.4. Transmission spectrum of water and the Ag-Fe_2O_3/water multiphase fluid

The transmission spectrum of the Ag-FeC/water multiphase fluid and the base fluid (water + 4 g/l CMCNa) in the UV, visible and near-infrared regions is shown in Figure 8.5. After a wavelength of 530 nm, the transmittance of the multiphase fluid for all studied concentrations drops below 11%. In the UV region, the multiphase fluid records a maximum transmittance value of 77.4% at a wavelength of 330 nm, for a concentration of 0.5 wt%. Particles or impurities in the material scatter the incident light, causing fluctuations in the transmission spectrum. The fluctuations in the transmission spectrum observed in the UV range correspond to variations in the amount of light transmitted through the multiphase fluid at different concentrations, depending on the wavelength. These fluctuations appear as peaks in the spectrum at certain wavelengths where the nanoparticles transmit light most efficiently. In the visible and near-infrared regions, the Ag-FeC/water multiphase fluid exhibits lower transmittance, suggesting more efficient light absorption in these regions.

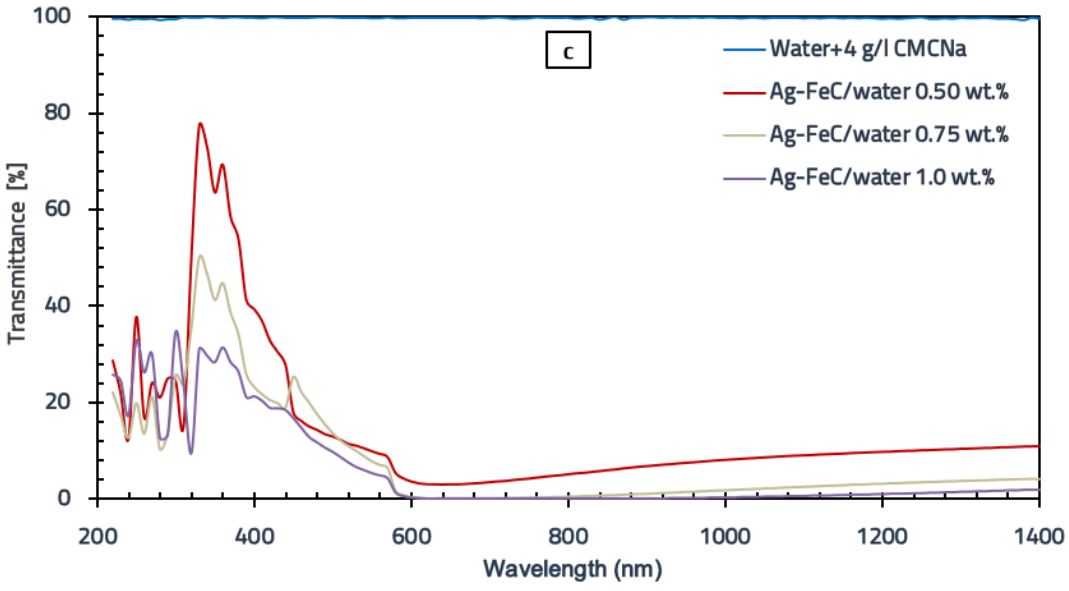

Figure 8.5. Transmission spectrum of water and the Ag-FeC/water multiphase fluid

The transmission spectrum of the Ag-TiO_2/water multiphase fluid (Figure 8.6) shows a similar trend for the three nanoparticle concentrations studied. It can be observed that after reaching a wavelength of 810 nm, the transmittance begins to stabilize, with no further variations in the transmission spectrum. Additionally, fluctuations are observed in the UV and visible ranges, corresponding to changes in the amount of light transmitted at different concentrations. For a concentration of 0.5 wt%, the maximum transmittance is 62.125%, which decreases to 61.3% and 56.15% for concentrations of 0.75 and 1.0 wt%, respectively, at a wavelength of 440 nm. At a wavelength of 810 nm, the multiphase fluid exhibits a surface plasmon resonance (LSPR) peak, where light is absorbed most efficiently.

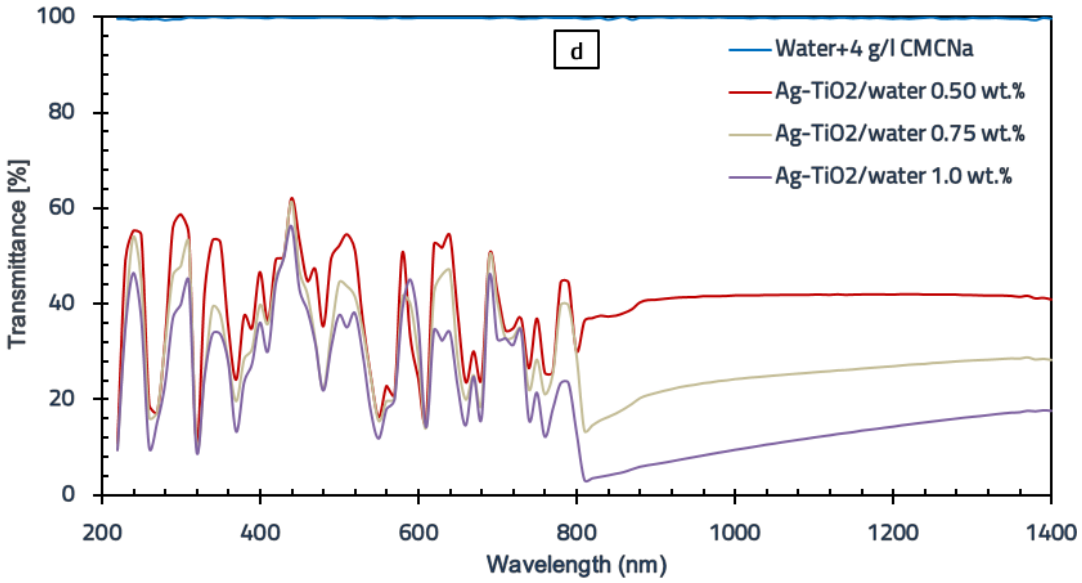

Figure 8.6. Transmission spectrum of water and the Ag-TiO_2/water multiphase fluid

The Ag-Fe_2O_3, Ag-FeC and Ag-TiO_2 water-based multiphase fluids show higher transmittance than the Ag-rGO/water fluid. This indicates that the Ag-rGO/water multiphase fluid, with a mass concentration of 0.1%, shows promising potential for use as a working fluid in a DASC.

8.3.2 Absorbance

Figures 8.7-8.10 show the variations in absorbance as a function of wavelength for the multiphase fluids Ag-rGO, Ag-Fe_2O_3, Ag-FeC and Ag-TiO_2, based on water with 0.4 and 4 g/l of CMCNa at different concentrations, compared to the reference sample.

The absorbance variation with wavelength for the multiphase Ag-rGO fluid with 0.4 g/l of CMCNa is shown in Figure 8.7. The maximum absorbance was 3.339 at a wavelength of approximately 1130 nm for a concentration of 0.1 wt%, while for concentrations of 0.05 and 0.075 wt%, the maximum values were 2.281 and 3.075 at wavelengths of 1300 and 1160 nm, respectively. The Ag-rGO/water multiphase fluid absorbs significantly more light in the visible and near-infrared regions. Increasing the nanoparticle concentration considerably improved the solar absorption of the base fluid (water with 0.4 g/l CMCNa), but the increase in absorbance was smaller between 0.075 and 0.1 wt% (7.15%), compared to the increase from 0.05 to 0.075 wt% (32.27%).

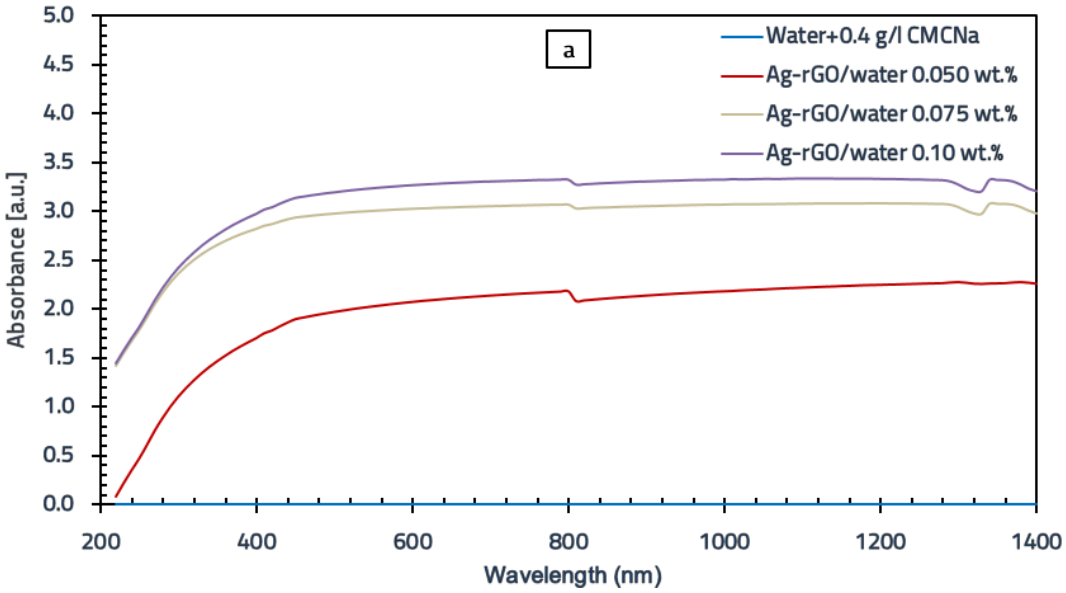

Figure 8.7. Absorption spectrum of water and the Ag-rGO/water multiphase fluid

Figure 8.8 shows the variation in absorbance as a function of wavelength for the Ag-Fe_2O_3 multiphase fluid in water with 4 g/l of CMCNa. As the concentration of the multiphase fluid increases from 0.5 to 1.0 wt%, the absorbance increases significantly, enhancing solar absorption. The maximum absorbance values are 0.202, 0.234 and 0.406 at a wavelength of 220 nm for concentrations of 0.5, 0.75 and 1.0 wt%, respectively. For concentrations of 0.5 and 0.75 wt%, the absorbance remains relatively constant around 0.195 and 0.215 across the entire wavelength range, while for 1.0 wt%, the absorbance decreases at longer wavelengths due to more efficient absorption at shorter wavelengths.

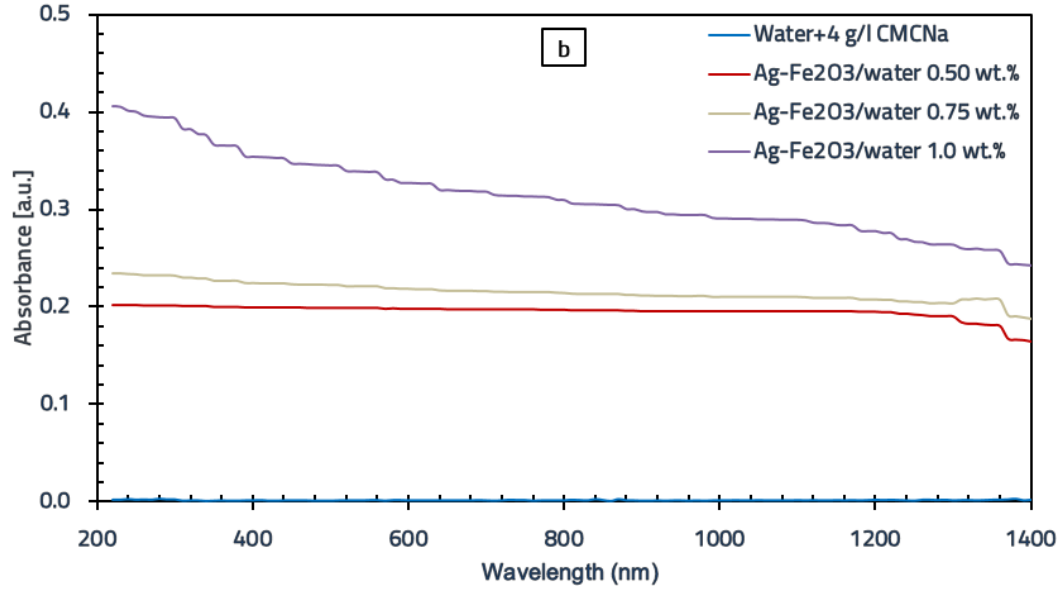

Figure 8.8. Absorption spectrum of water and the Ag-Fe_2O_3/water multiphase fluid

The UV, visible and near-infrared absorption spectrum of the Ag-FeC/water multiphase fluid and the base fluid (water with 4 g/l CMCNa) is shown in Figure 8.9. The absorption spectrum of the multiphase fluid with a concentration of 0.5 wt% exhibits a profile similar to that of the 0.75 and 1.0 wt% concentrations. For all concentrations studied, it can be observed that the absorbance increases up to wavelengths between 640 and 710 nm, after which it decreases as the wavelength increases. Thus, the maximum absorbance values are recorded around wavelengths of 640 nm, 650 nm and 710 nm

for concentrations of 0.5, 0.75 and 1.0 wt%, respectively. These absorption peaks can be attributed to the LSPR of Ag nanoparticles [66]. In the UV range, the multiphase fluid absorbs less light, but in the visible and near-infrared regions, the absorption increases significantly, indicating that this fluid could be a viable solution for use in solar applications.

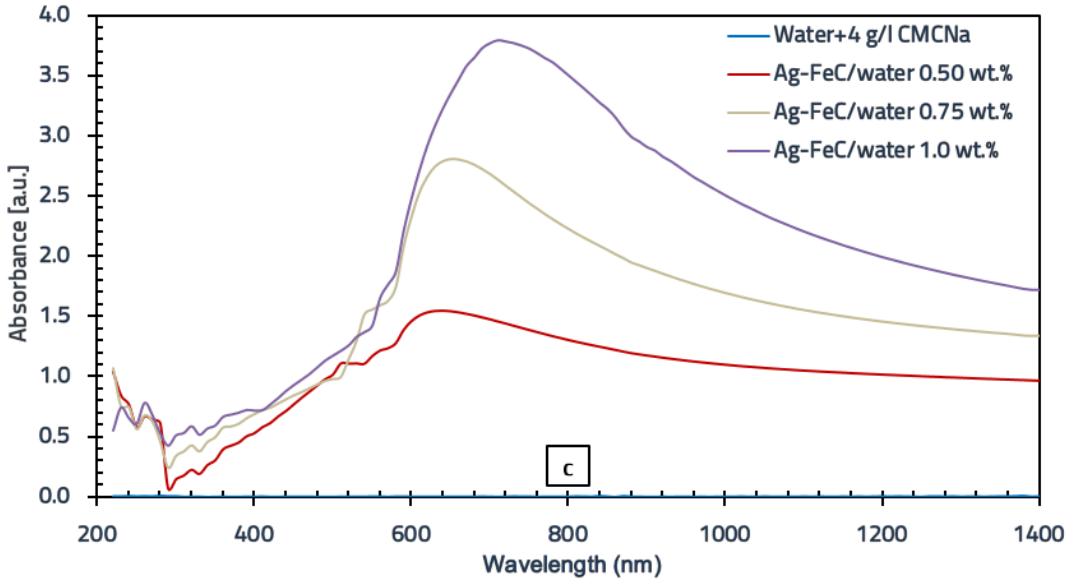

Figure 8.9. Absorption spectrum of water and the Ag-FeC/water multiphase fluid

Figure 8.10 shows the variation in absorbance of the Ag-TiO_2/water multiphase fluid as a function of wavelength for concentrations of 0.5, 0.75 and 1.0 wt%. The peaks in the spectrum correspond to wavelengths at which the nanoparticles absorb and scatter light most effectively. The maximum absorbance for the three concentrations (0.5, 0.75 and 1.0 wt%) occurs at a wavelength of approximately 570 nm, with values of 3.385, 4.147 and 4.431, respectively. In the UV region, the multiphase fluid absorbs more light than in the near-infrared. In the visible light range, from 380 to 650 nm, the Ag-TiO_2/water fluid exhibits significantly higher absorbance values, after which a decreasing trend in absorbance is observed around the wavelength of 950 nm. Between 950 and 1400 nm, the absorbance values for the three concentrations remain nearly constant.

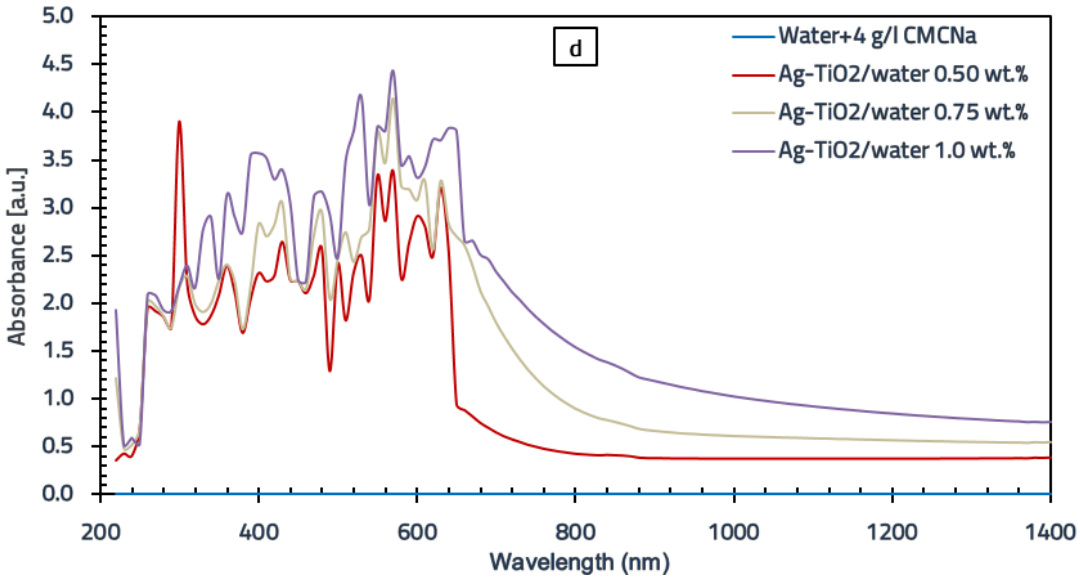

Figure 8.10. Absorption spectrum of water and the Ag-TiO_2/water multiphase fluid

8.4 Water+EG-based multiphase fluids

8.4.1 Transmittance

Figures 8.11-8.14 show the variation in transmittance as a function of wavelength for the multiphase fluids Ag-rGO, Ag-Fe_2O_3, Ag-FeC and Ag-TiO_2 at different concentrations, compared to the reference sample. The water+EG mixture with 0.4 and 4 g/l CMCNa is transparent across the entire studied wavelength range. Particles or impurities in the material scatter incident light, causing fluctuations in the transmission spectrum. These fluctuations often appear as peaks in the spectrum at specific wavelengths, where nanoparticles transmit light most effectively.

Figure 8.11 analyzes the transmittance of the Ag-rGO/water+EG multiphase fluid at concentrations of 0.05, 0.075 and 0.1 wt%. At a concentration of 0.05 wt%, the Ag-rGO multiphase fluid shows high transmittance in the near-infrared region, with a maximum value of 32.6% at a wavelength of 980 nm. At a concentration of 0.075 wt%, the maximum transmittance of 21.46% is achieved in the UV region at a wavelength of 360 nm. As the concentration increases to 0.1 wt%, the transmittance drops below 4.3% across the 220-1400 nm wavelength range. The Ag-rGO/water+EG multiphase fluid at 0.1 wt% exhibits significantly lower transmittance than the base fluid (water+EG with 0.4 g/l CMCNa), indicating exceptional optical absorption properties, especially in the visible region [65].

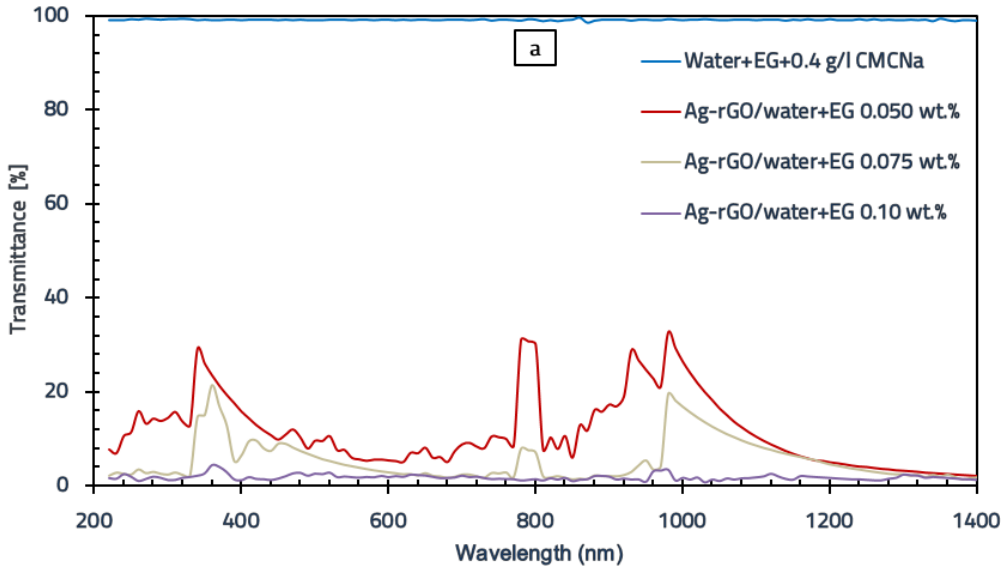

Figure 8.11. Transmission spectrum of the water+EG mixture and the Ag-rGO/water+EG multiphase fluid

For the Ag-Fe_2O_3/water+EG multiphase fluid (Figure 8.12), the maximum transmittance values were obtained in the UV region. For mass concentrations of 0.5%, 0.75% and 1.0%, the maximum transmittance peaks were 89.1%, 74.8% and 61.65%, occurring at wavelengths of 370 nm, 300 nm and 380 nm, respectively. It can be concluded that transmittance decreases with increasing nanoparticle concentration. For all concentrations studied, transmittance remains relatively high in the 220-490 nm wavelength range. In the visible region, at a wavelength of 510 nm, improved absorption is observed, highlighted by an LSPR peak, while for the 510-1400 nm range, a slight increase in transmittance is observed for all concentrations studied.

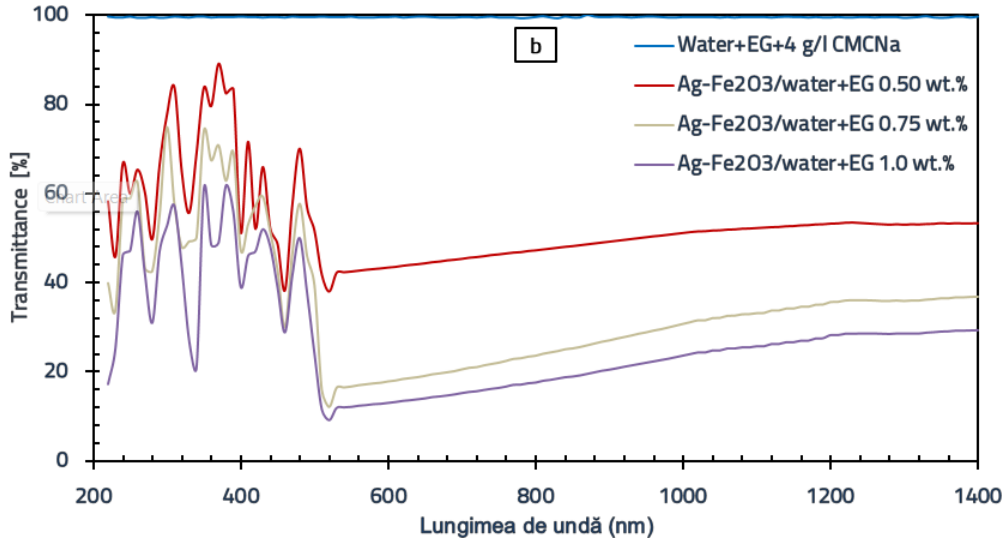

Figure 8.12. Transmission spectrum of the water+EG mixture and the Ag-Fe_2O_3/water+EG multiphase fluid

Figure 8.13 presents the transmittance values of the Ag-FeC/water+EG multiphase fluid at mass concentrations of 0.5%, 0.75% and 1.0%. The maximum transmittance peaks were 88.4% (780 nm), 60.6% (950 nm) and 42.3% (940 nm) for the three concentrations studied. Enhanced absorption was also observed in the visible region at a wavelength of 390 nm and in the near-infrared at wavelengths of 960 nm and 1070 nm, where LSPR peaks were recorded. Furthermore, improved absorption was observed in the 1150-1400 nm wavelength range for all concentrations studied.

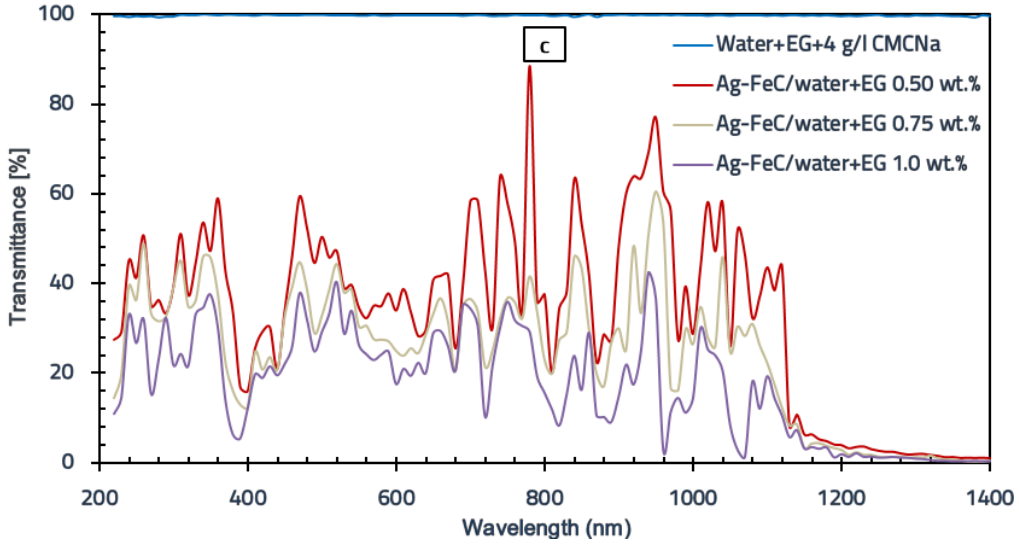

Figure 8.13. Transmission spectrum of the water+EG mixture and the Ag-FeC/water+EG multiphase fluid

The transmittance values for the Ag-TiO_2/water+EG multiphase fluid are presented in Figure 8.14. For concentrations of 0.5%, 0.75% and 1.0 wt%, the maximum transmittance peaks were 70.7% at 880 nm (near-infrared), 62.975% at 480 nm (visible) and 58.45% at 230 nm (UV). The results indicate improved absorption at 250 nm (UV) and 840 nm (near-infrared), marked by two LSPR peaks. Additionally, the Ag-TiO_2/water+EG multiphase fluid shows increased absorption in the 900-1400 nm wavelength range for the 0.75% and 1.0% wt concentrations.

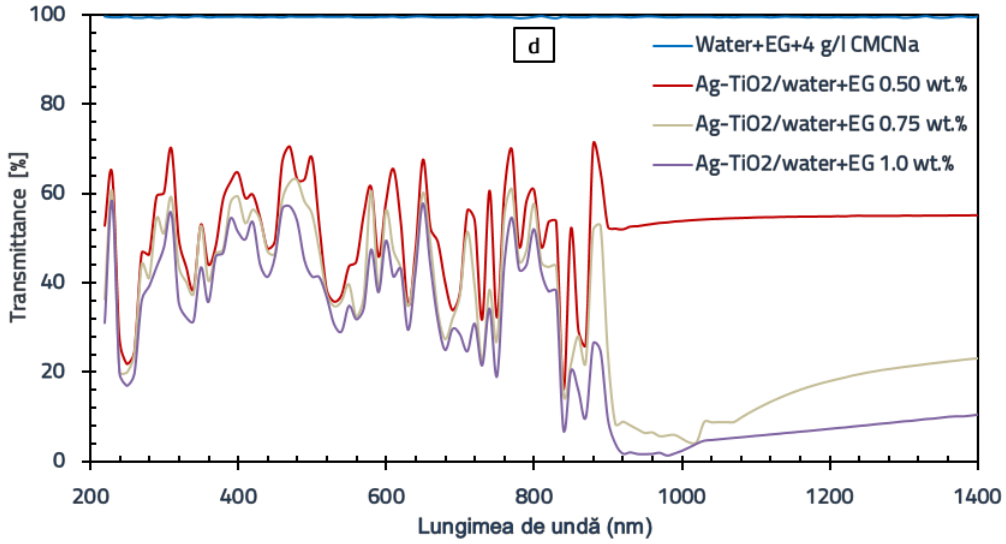

Figure 8.14. Transmission spectrum of the water+EG mixture and the Ag-TiO_2/water+EG multiphase fluid

8.4.2 Absorbance

Figures 8.15-8.18 show the variation in absorbance as a function of wavelength for the multiphase fluids Ag-rGO, Ag-Fe_2O_3, Ag-FeC and Ag-TiO_2 based on a water and EG mixture, at different mass concentrations and for the reference sample.

Figure 8.15 illustrates the variation in absorbance for the Ag-rGO/water+EG multiphase fluid as a function of wavelength. The chemical reactions between Ag nanoparticles and rGO alter the absorption characteristics of the base fluid, resulting in fluctuations in absorbance. These fluctuations are visible in the UV and visible regions, where as the concentration increases, the absorption band widens and shifts to a longer wavelength. In the near-infrared region, absorbance decreases between 860-920 nm and then increases in the range of 930-1400 nm. The maximum absorbance values were 3.295, 4.402 and 4.804 at a wavelength of 580 nm for the concentrations of 0.05%, 0.075% and 0.10% wt, respectively.

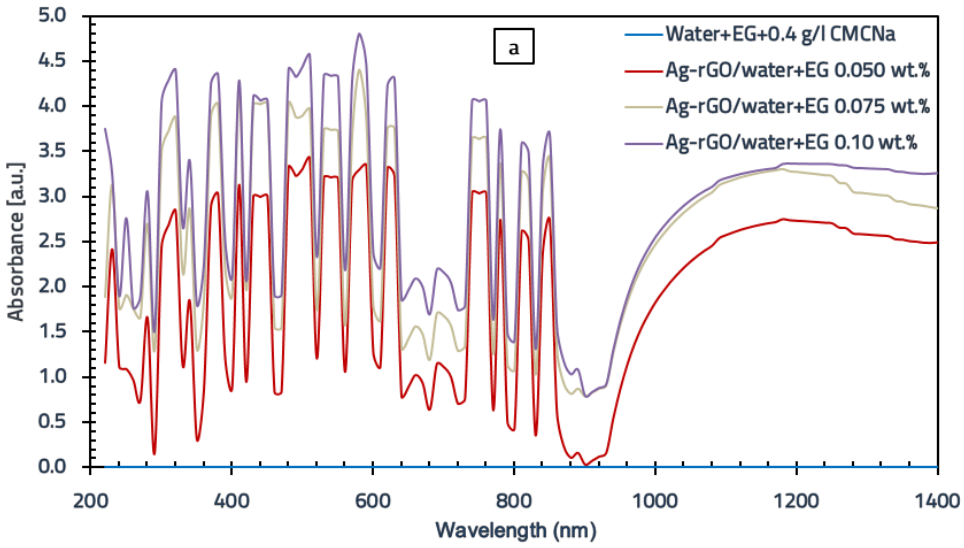

Figure 8.15. Absorbance spectrum of the water+EG mixture and the Ag-rGO/water+EG multiphase fluid

The absorbance of the Ag-Fe_2O_3/water+EG multiphase fluid (Figure 8.16) for concentrations of 0.75% and 1.0% wt is higher in the UV and visible spectrum and decreases as the wavelength increases. For the 0.5% wt concentration, the absorbance remains constant around 0.390. The maximum absorbance values for the 0.75% and 1.0% wt concentrations were 2.604 and 3.046 at wavelengths of 260 nm and 310 nm, respectively. Increasing the Ag-Fe_2O_3 concentration from 0.5% to 1.0% wt significantly enhances solar absorption in the UV and visible regions.

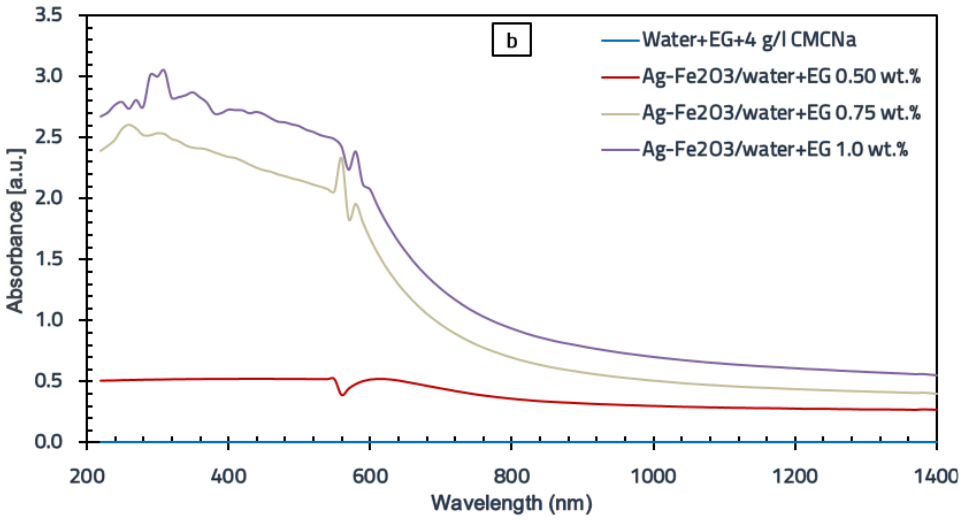

Figure 8.16. Absorbance spectrum of the water+EG mixture and the Ag-Fe_2O_3/water+EG multiphase fluid

The absorbance variation for the Ag-FeC/water+EG (Figure 8.17) follows the same trend in the UV and visible regions for all concentrations, while in the near-infrared, the 1.0% wt concentration shows a slight improvement. The absorption spectrum of the multiphase fluid features a strong absorption band at 830-870 nm and 1220-1270 nm for 1.0% wt, attributed to the LSPR of the Ag nanoparticles. The maximum absorbance values for 0.5%, 0.75% and 1.0% wt were 0.659, 0.939 and 2.80 at 1210 nm, 930 nm and 850 nm, respectively. The 1.0% wt multiphase fluid absorbs light most efficiently in the infrared region, while the increase from 0.5% to 0.75% wt results in an insignificant improvement.

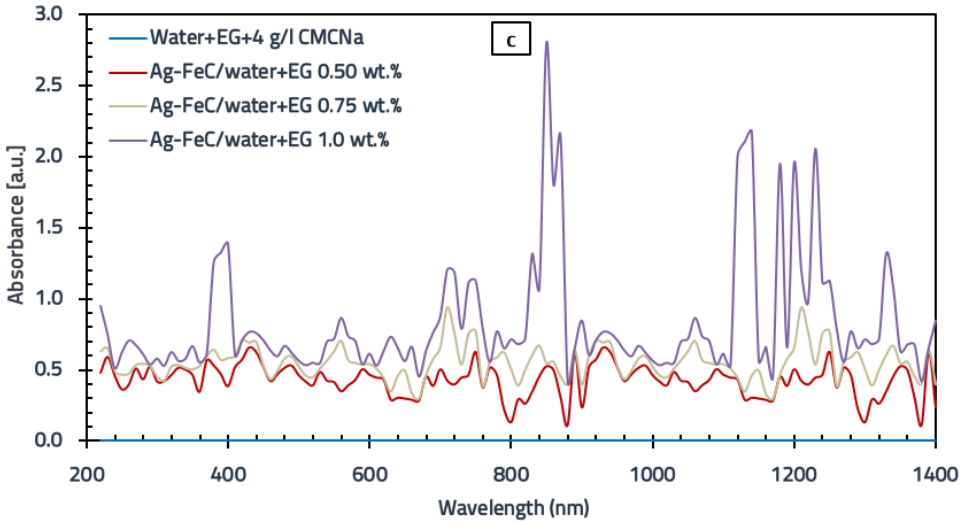

Figure 8.17. Absorbance spectrum of the water+EG mixture and the Ag-FeC/water+EG multiphase fluid

Figure 8.18 shows the variation in absorbance for the Ag-TiO_2/water+EG multiphase fluid. For the fluid with a concentration of 0.5 wt%, absorbance remains constant around 0.260 across the entire wavelength range. For concentrations of 0.75 and 1.0 wt%, the maximum absorbance values (1.465 and 3.086) are observed at 220 nm. The multiphase fluid with 0.75 and 1.0 wt% shows a decrease in absorbance as the wavelength increases, due to stronger absorption at shorter wavelengths. Increasing the concentration from 0.5 to 1.0 wt% leads to a significant improvement in the solar absorption of the water+EG mixture with 4 g/l of CMCNa.

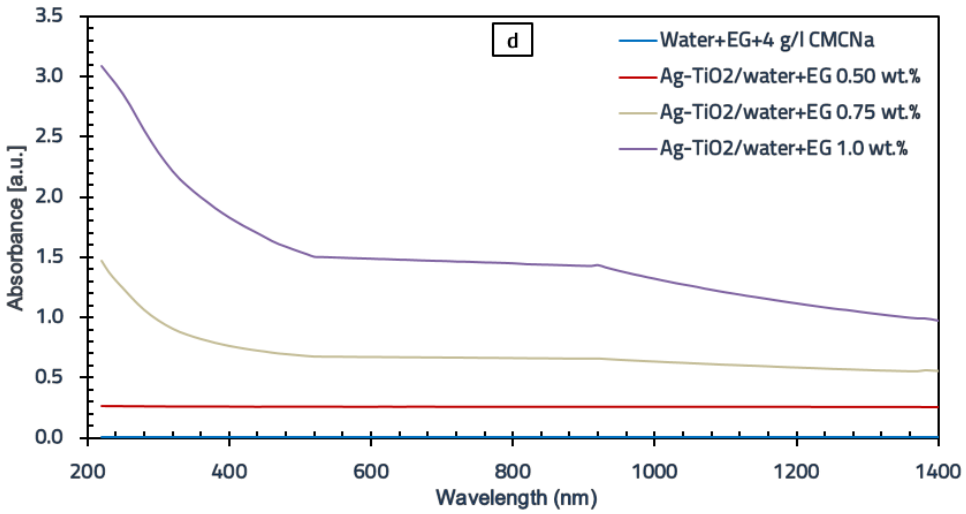

Figure 8.18. Absorbance spectrum of the water+EG mixture and the Ag-TiO_2/water+EG multiphase fluid

It is worth noting that the Ag-rGO multiphase fluid in a water+EG mixture with a concentration of 0.1 wt% showed the highest absorption across the examined wavelength range, compared to the Ag-Fe_2O_3, Ag-FeC and Ag-TiO_2 multiphase fluids, making it suitable as a working fluid in DASC.

8.5 Conclusions on the optical properties of multiphase fluids

- The results indicate an increase in the absorption of multiphase fluids compared to the base fluid, even at very low nanoparticle concentrations.
- The Ag-rGO multiphase fluid in water and in the water+EG mixture, at a concentration of 0.1 wt%, had three times higher absorption than the base fluid for a 1 mm optical path.
- The transmittance of all multiphase fluids decreased significantly, while their spectral absorption characteristics were superior to those of the base fluids.
- The Ag-Fe_2O_3 multiphase fluid with a concentration of 0.5 wt% achieved the highest average transmittance value of 65.99% in water and 52.82% in the water+EG mixture over the 220-1400 nm wavelength range.
- The optical properties of multiphase fluids are complex and varied and understanding them is crucial for the development and optimization of applications in fields such as optics, energy and cooling technologies.

9. PHOTOTHERMAL CONVERSION CHARACTERISTICS – EXPERIMENTAL RESULTS

This section analyzes the influence of concentration, temperature and irradiation time on the photothermal conversion efficiency.
The photothermal conversion efficiency was determined for the base fluids (water and water+EG, both with 0.4 g/l and 4 g/l CMCNa) and for the multiphase fluids (Ag-Fe_2O_3, Ag-FeC, Ag-rGO and Ag-TiO_2) with different mass concentrations (0.50%, 0.75% and 1.0%, respectively 0.05%, 0.075% and 0.1% for rGO) in water and water+EG (50:50).

9.1 Interpretation of results

At the beginning of testing, immediately after the solar simulator was activated, the working fluid absorbed the incident solar radiation and converted it into thermal energy, causing an increase in temperature. The fluid's temperature rose rapidly due to the low heat dissipation rate, as initially, the temperature difference between the fluid and the environment was negligible. The rate of temperature increase gradually slowed as the temperature difference grew larger, leading to a higher rate of heat dissipation. This phase can be referred to as the heating stage. Subsequently, the temperature reached an equilibrium point where the rate of heat dissipation equaled the rate of heat generation. This stage is called the equilibrium stage.
It is noteworthy that in all cases, the fluid temperature increased almost linearly with irradiation time due to the reduced heat loss [67].
Figure 9.1 shows the temperature rise on the upper surface of the base fluid samples (water and water+EG with 0.4 g/l and 4 g/l CMCNa, respectively), as well as the studied multiphase fluids, after 65 minutes of exposure to the irradiation source. The presence of Ag, Fe_2O_3, FeC, rGO and TiO_2 nanoparticles resulted in a greater temperature increase in all the multiphase fluids compared to the base fluid.
At the same irradiation time (65 minutes), the temperature difference between the upper and lower surfaces of the fluid sample is illustrated in Figure 9.2.
Figure 9.2 reveals that the temperature difference between the upper and lower surfaces of the fluid sample increases with the concentration of nanoparticles. All working fluids exhibit a relatively smaller temperature increase at the lower surface of the sample, as the absorption efficiency depends on the fluid layer thickness [67] (26 mm in this case).

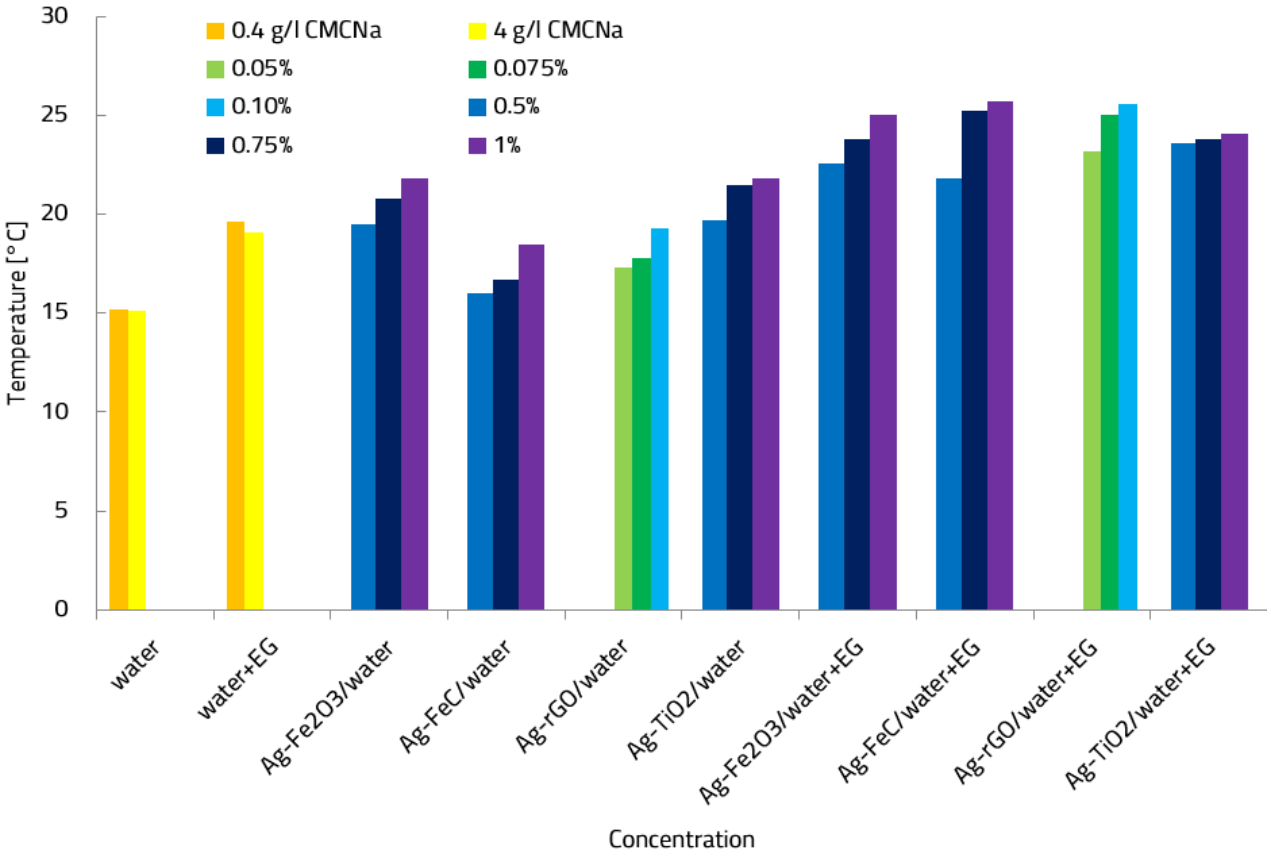

Figure 9.1. Temperature increase on the upper surface of the fluid sample after 65 minutes of irradiation

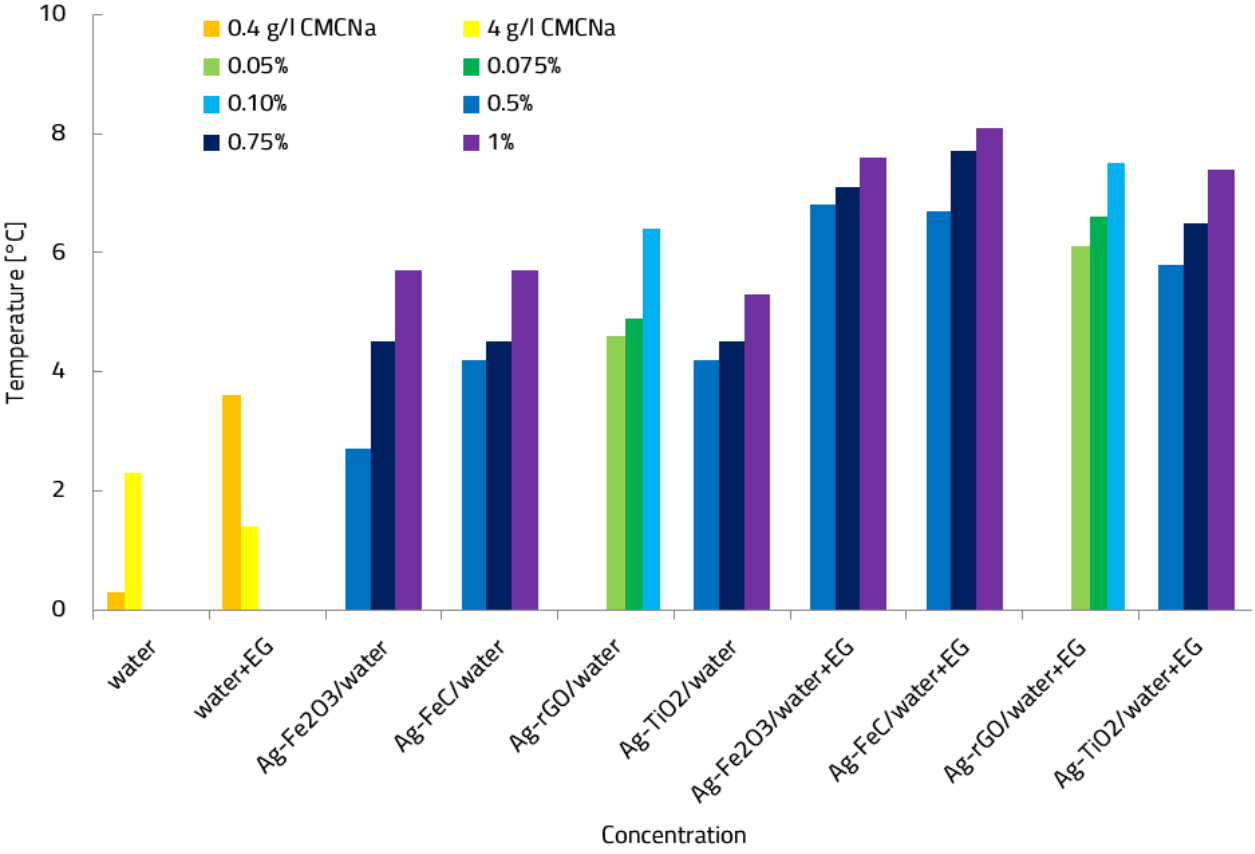

Figure 9.2. Temperature difference between the upper and lower surfaces of the fluid sample after 65 minutes of irradiation

The temperature variation throughout the entire testing process was recorded to assess the photothermal conversion properties of the multiphase fluids.
The total energy stored by the working fluid during the photothermal energy conversion experiment depends on the maximum temperature change, the mass and the specific heat of the working fluid. It is expressed as follows:

$$Q = m * c_p * (T_m - T_0) \quad (9.1)$$

where: T_0 și T_m represent the initial temperature and the average instantaneous temperature measured by two thermocouples, while m and c_p are the mass (with m=0.075 kg) and the specific heat capacity of the studied fluid. To determine the photothermal conversion capacity of the considered multiphase fluids, the efficiency was calculated using equation (9.2):

$$\eta = \frac{Q}{G_s * A * \Delta\tau} \quad (9.2)$$

unde: G_s-iradierea solară (618 W/m²), A-aria suprafeței expuse (0.00384 m²), $\Delta\tau$-timpul de iradiere
The efficiency of multiphase fluids in solar thermal applications largely depends on how temperature variation is influenced by irradiation time. The photothermal characteristics of the base fluid and the multiphase fluids are studied under similar solar irradiation conditions (618 W/m²).

9.2 Photothermal conversion performance of water-based multiphase fluids

The photothermal conversion efficiency of water with 0.4 and 4 g/L CMCNa and water-based multiphase fluids at various concentrations as a function of irradiation time is presented in Figure 9.3. According to the graphs in Figure 9.3, the photothermal conversion efficiency of the fluids decreased with irradiation time and increased with concentration in all the cases studied. This decrease can be attributed to the increased heat loss to the surrounding environment as the fluid temperature rises. The addition of nanoparticles to the base fluid improves the photothermal conversion efficiency in all cases studied, due to their excellent absorption properties.
Figure 9.3 (a) illustrates the photothermal conversion efficiency of the Ag-rGO/water multiphase fluid at three concentrations of 0.050, 0.075 and 0.1 wt%, showing increases of 78.91%, 82.76% and 86.72%, respectively, compared to the base fluid after 5 minutes of irradiation. After 65 minutes, these increases were 15.95%, 17.25% and 20.13%.
The photothermal conversion efficiency for the Ag-Fe_2O_3/water multiphase fluid is shown in Figure 9.3 (b). For mass concentrations of 0.5%, 0.75% and 1%, the photothermal conversion efficiency of the base fluid improved by 54.63%, 70.18% and 81.91%, respectively and by 45.30%, 50.18% and 54.58% after 5 and 65 minutes of irradiation, respectively.
The photothermal conversion efficiency of the Ag-FeC/water multiphase fluid (Figure 9.3 (c)), for the three concentrations analyzed (0.5%, 0.75% and 1.0 wt%), showed increases of 70.23%, 74.18% and 81.24% after 5 minutes and 25.20%, 35.34% and 41.97% after 65 minutes, compared to the base fluid.
According to the graph in Figure 9.3 (d), the photothermal conversion efficiency of the Ag-TiO_2/water multiphase fluid at three concentrations (0.5%, 0.75% and 1 wt%) showed improvements of 65.64%, 73.21% and 81.07% compared to the base fluid after 5 minutes of irradiation, while after 65 minutes, the improvements were 45.78%, 52.39% and 53.72%.

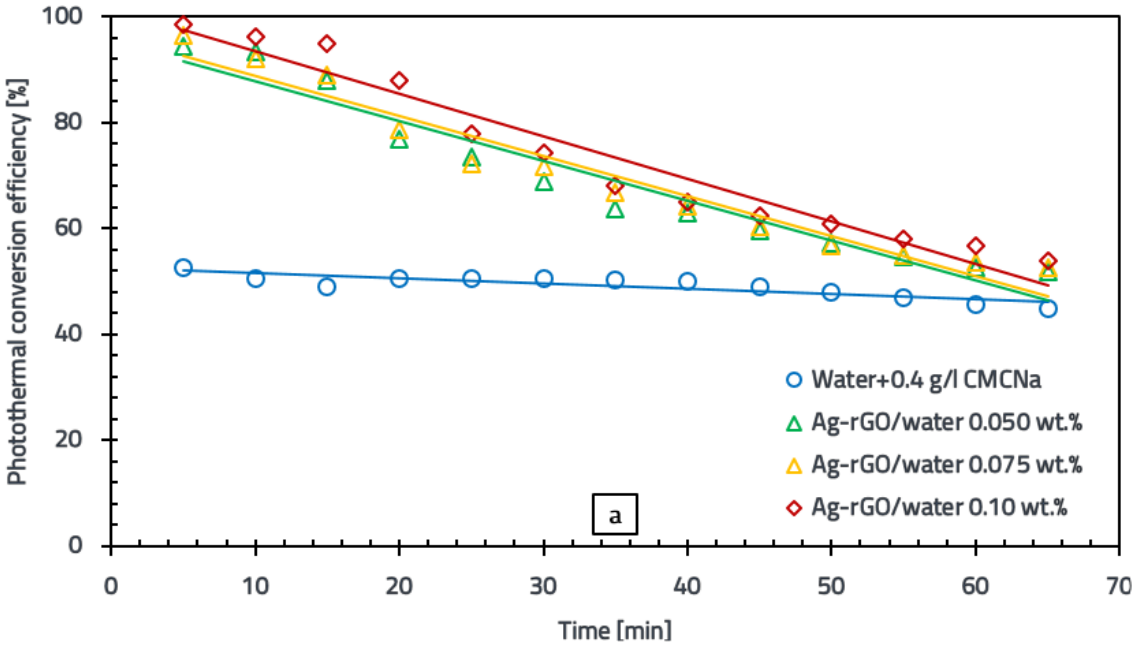
Photothermal conversion efficiency [%]
Time [min]
Water+0.4 g/l CMCNa
Ag-rGO/water 0.050 wt.%
Ag-rGO/water 0.075 wt.%
Ag-rGO/water 0.10 wt.%
a

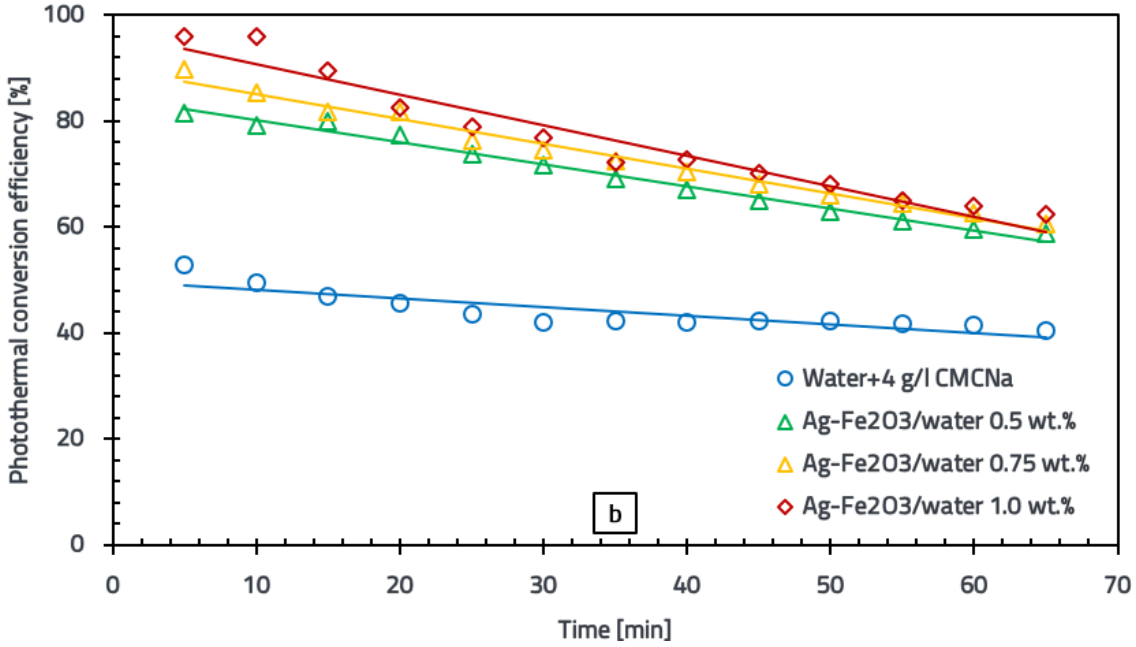
Photothermal conversion efficiency [%]
Time [min]
Water+4 g/l CMCNa
Ag-Fe2O3/water 0.5 wt.%
Ag-Fe2O3/water 0.75 wt.%
Ag-Fe2O3/water 1.0 wt.%
b

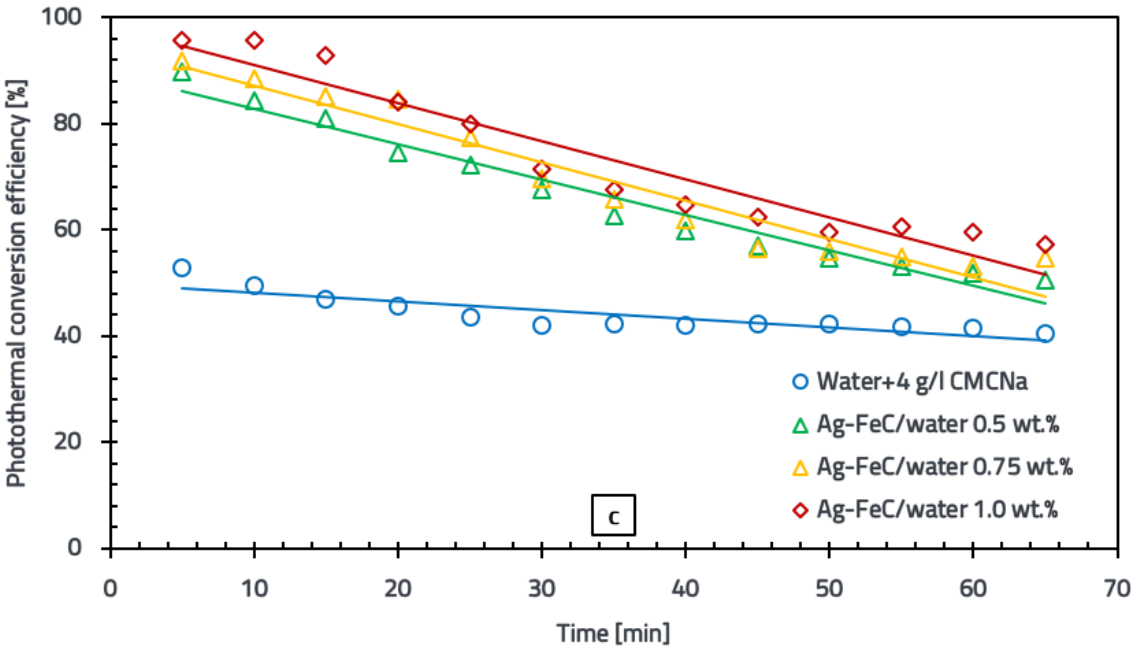
Photothermal conversion efficiency [%]
Time [min]
Water+4 g/l CMCNa
Ag-FeC/water 0.5 wt.%
Ag-FeC/water 0.75 wt.%
Ag-FeC/water 1.0 wt.%
c

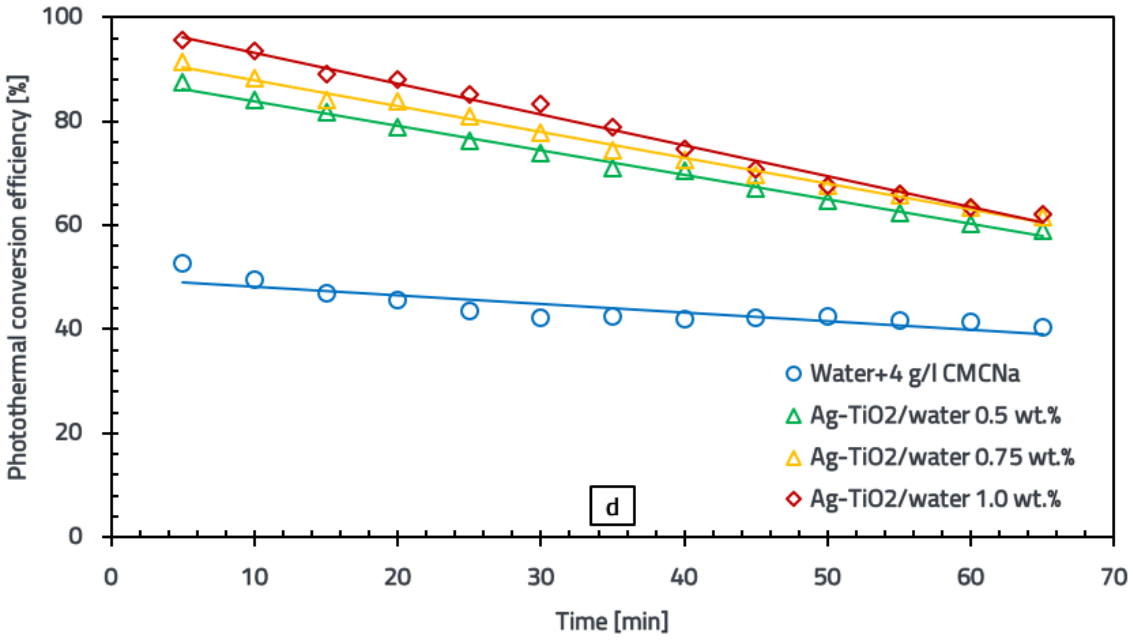

Figure 9.3. Photothermal conversion efficiency of water-based multiphase fluids: a) Ag-rGO; b) Ag-Fe_2O_3; c) Ag-FeC; d) Ag-TiO_2 as a function of irradiation time

The photothermal conversion efficiency of water with 0.4 and 4 g/l CMCNa, as well as that of water-based multiphase fluids at different mass concentrations as a function of temperature, is shown in Figure 9.4.

According to the graphs in Figure 9.4, it can be observed that the photothermal conversion efficiency of all fluids decreases as the temperature increases and increases with concentration.

For the Ag-rGO/water multiphase fluid (Figure 9.4 (a)), at a concentration of 0.1 wt%, the maximum photothermal conversion efficiency is 95.50% at 25 °C and 56.64% at 35 °C [65].

Figure 9.4 (b) shows that the Ag-Fe_2O_3/water multiphase fluid, at a concentration of 1.0 wt%, reaches a maximum photothermal conversion efficiency of 96.05% at 25 °C and 72.69% at 35 °C.

For a concentration of 1.0 wt%, the photothermal conversion efficiency of the Ag-FeC/water multiphase fluid (illustrated in Figure 9.4 (c)) is 95.70% at 25 °C and 57.35% at 35 °C.

According to the graph in Figure 9.4 (d), the photothermal conversion efficiency of the Ag-TiO_2/water multiphase fluid, at a concentration of 1 wt%, reaches a maximum value of 89.08% at 25 °C and 70.77% at 35 °C.

As heat loss through convection of the sample gradually increases with temperature, the photothermal conversion efficiency of all fluids decreases, indicating that heat loss is the key factor in improving photothermal properties.

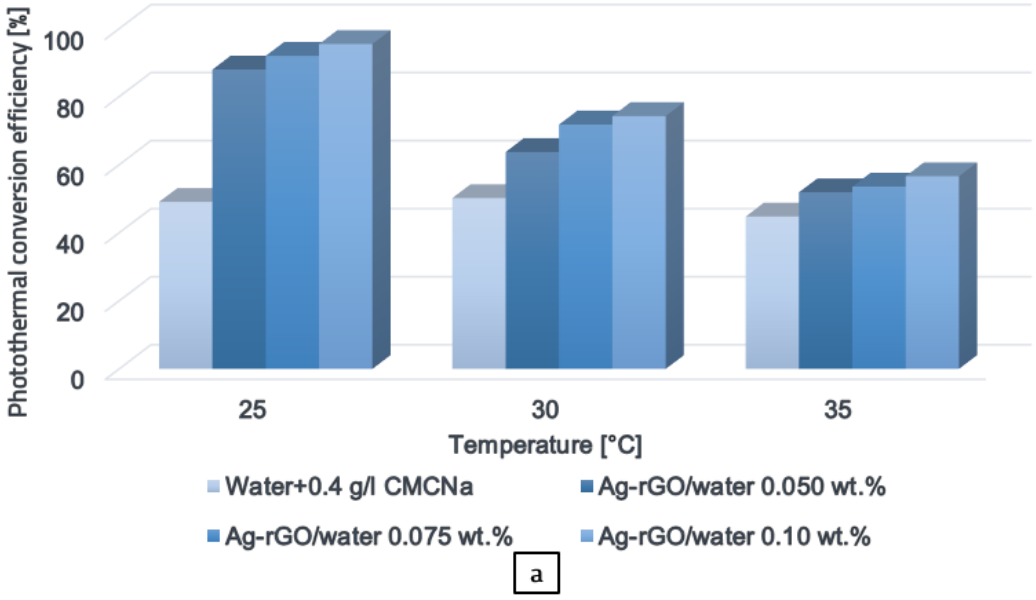
Photothermal conversion efficiency [%]
100
80
60
40
20
0
25
30
35
Temperature [°C]
Water+0.4 g/l CMCNa
Ag-rGO/water 0.050 wt.%
Ag-rGO/water 0.075 wt.%
Ag-rGO/water 0.10 wt.%

a

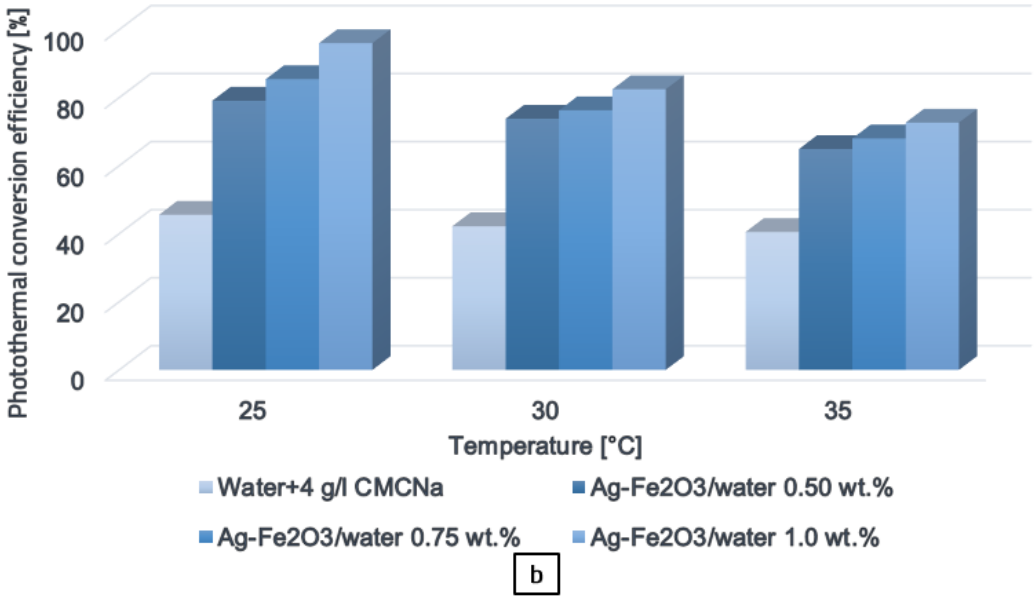
Photothermal conversion efficiency [%]
100
80
60
40
20
0
25
30
35
Temperature [°C]
Water+4 g/l CMCNa
Ag-Fe2O3/water 0.50 wt.%
Ag-Fe2O3/water 0.75 wt.%
Ag-Fe2O3/water 1.0 wt.%

b

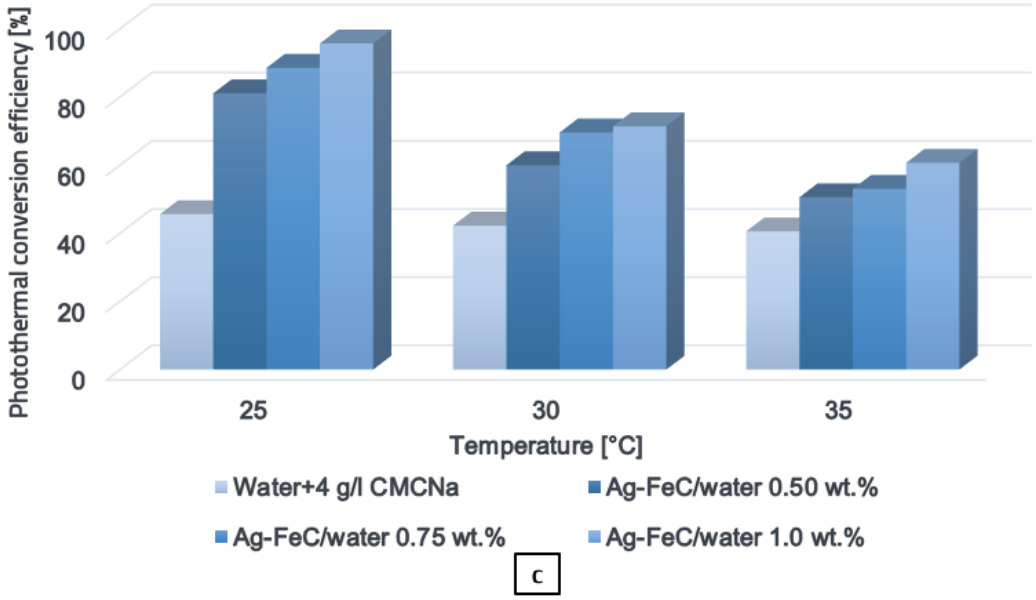
Photothermal conversion efficiency [%]
100
80
60
40
20
0
25
30
35
Temperature [°C]
Water+4 g/l CMCNa
Ag-FeC/water 0.50 wt.%
Ag-FeC/water 0.75 wt.%
Ag-FeC/water 1.0 wt.%

c

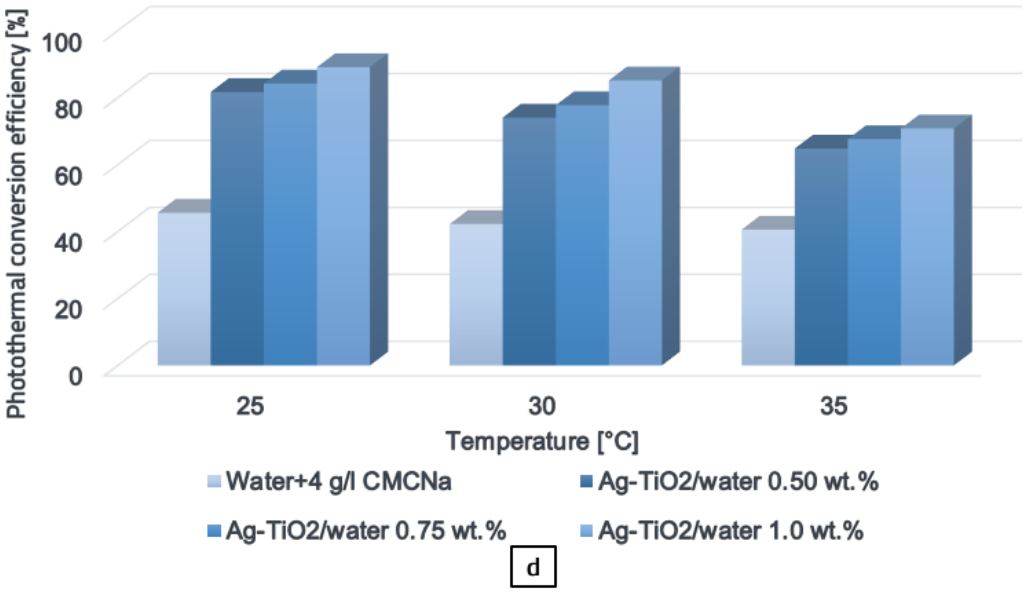

Figure 9.4. Variation of efficiency with temperature for water-based multiphase fluids: a) Ag-rGO; b) Ag-Fe_2O_3; c) Ag-FeC; d) Ag-TiO_2

9.3 Photothermal conversion performance of water+EG-based multiphase fluids

Figure 9.5 presents the photothermal conversion efficiency of the water+EG mixture with 0.4 and 4 g/l CMCNa, as well as the water+EG-based multiphase fluids at different concentrations, depending on the irradiation time. As shown in Figure 9.5, the photothermal conversion efficiency of all multiphase fluids is higher than that of the base fluid. It decreased during exposure to light and increased proportionally with nanoparticle concentration.

In Figure 9.5 (a), the photothermal conversion efficiency of the Ag-rGO/water+EG multiphase fluid at concentrations of 0.050, 0.075 and 0.1 wt% is shown, recording increases of 48.11%, 64.27% and 68.03% after 5 minutes and after 65 minutes, this increase was 20.29%, 23.37% and 29.93%, compared to the base fluid (water+EG with 0.4 g/l CMCNa).

For the Ag-Fe_2O_3/water+EG multiphase fluid (Figure 9.5 (b)), the increases were 56.29%, 61.77% and 64.34% after 5 minutes and 16.83%, 22.46% and 25.51% after 65 minutes, for concentrations of 0.5, 0.75 and 1.0 wt%, compared to the base fluid (water+EG with 4 g/l CMCNa).

The photothermal conversion efficiency of the Ag-FeC/water+EG multiphase fluid (Figure 9.5 (c)) at the analyzed concentrations (0.5, 0.75 and 1.0 wt%) showed increases of 41.93%, 59.15% and 65.34% after 5 minutes and 5.75%, 9.74% and 14.46% after 65 minutes.

For the Ag-TiO_2/water+EG multiphase fluid (Figure 9.5 (d)), improvements of 50.63%, 59.01% and 61.71% were observed after 5 minutes and 17.68%, 20.36% and 24.82% after 65 minutes, for concentrations of 0.5, 0.75 and 1.0 wt%.

Similar to the water-based multiphase fluids, it can be concluded that the main reason for the decrease in photothermal conversion efficiency with irradiation time is the increasing heat loss due to the growing temperature difference between the working fluid and the surrounding environment.

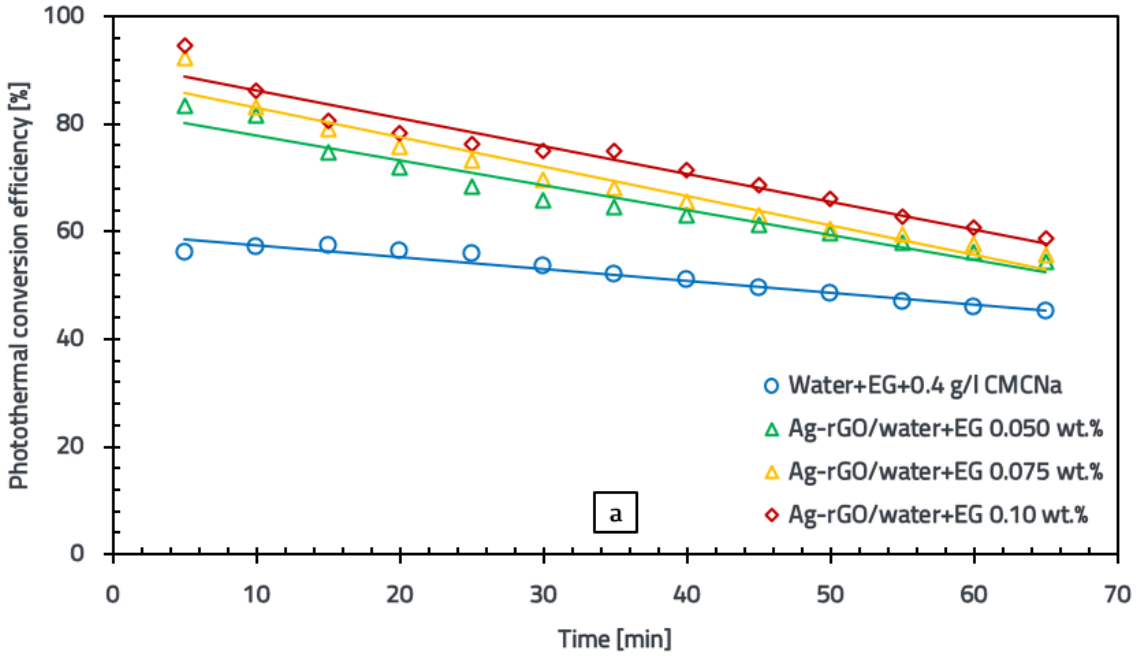
Photothermal conversion efficiency [%]
Time [min]
Water+EG+0.4 g/l CMCNa
Ag-rGO/water+EG 0.050 wt.%
Ag-rGO/water+EG 0.075 wt.%
Ag-rGO/water+EG 0.10 wt.%
a

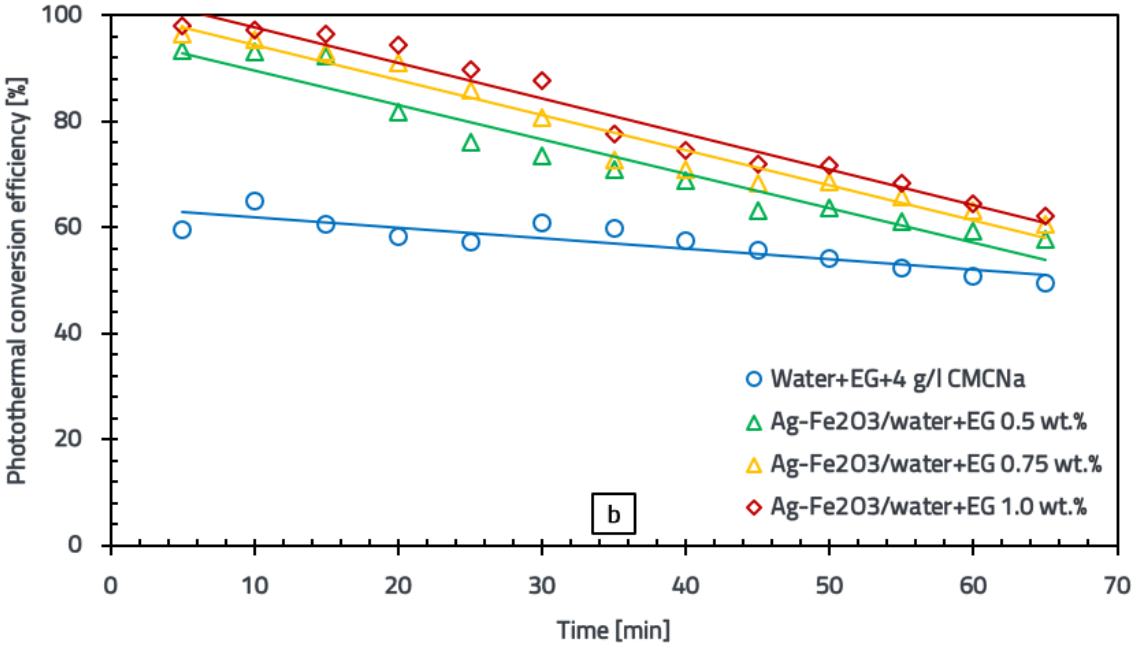
Photothermal conversion efficiency [%]
Time [min]
Water+EG+4 g/l CMCNa
Ag-Fe2O3/water+EG 0.5 wt.%
Ag-Fe2O3/water+EG 0.75 wt.%
Ag-Fe2O3/water+EG 1.0 wt.%
b

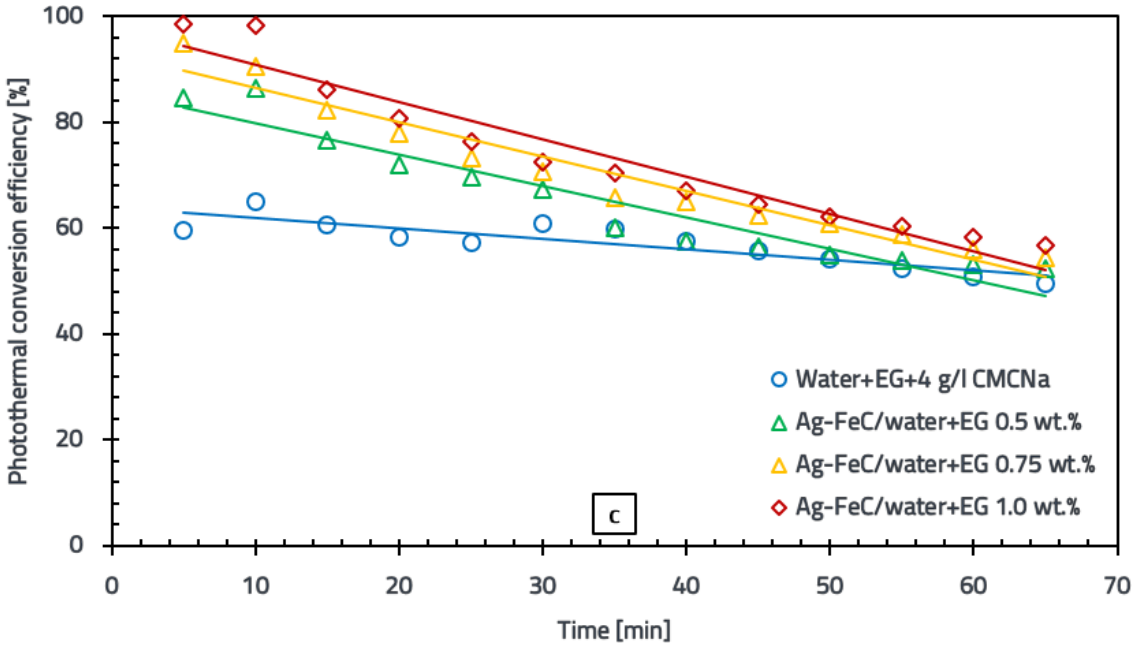
Photothermal conversion efficiency [%]
Time [min]
Water+EG+4 g/l CMCNa
Ag-FeC/water+EG 0.5 wt.%
Ag-FeC/water+EG 0.75 wt.%
Ag-FeC/water+EG 1.0 wt.%
c

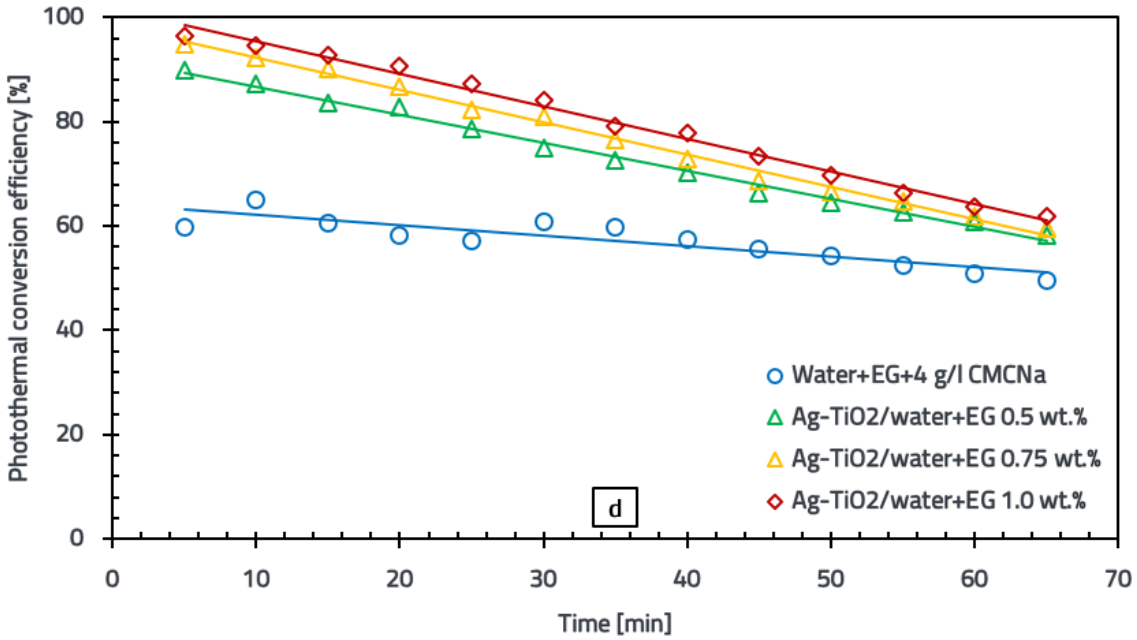

Figure 9.5. Photothermal conversion efficiency of water+EG-based multiphase fluids: a) Ag-rGO; b) Ag-Fe_2O_3; c) Ag-FeC; d) Ag-TiO_2 as a function of irradiation time

The photothermal conversion efficiency of the water+EG mixture with 0.4 and 4 g/l CMCNa, as well as the water+EG-based multiphase fluids at different concentrations as a function of temperature, is shown in Figure 9.6. In Figure 9.6 (a), it can be seen that the Ag-rGO/water+EG multiphase fluid at a concentration of 0.1 wt% presents a maximum efficiency value of 86.12% at 25°C and 62.57% at 40°C [65]. For the Ag-Fe_2O_3/water+EG multiphase fluid (Figure 9.6 (b)) at a concentration of 1.0 wt%, the maximum efficiency is 97.24% at 25°C and 71.60% at 40°C. The graph in Figure 9.6 (c) shows that the efficiency for Ag-FeC/water+EG at a concentration of 1.0 wt% reaches a maximum value of 98.35% at 25°C and 58.29% at 40°C. For a concentration of 1.0 wt%, the efficiency of the Ag-TiO_2/water+EG multiphase fluid (illustrated in Figure 9.6 (d)) is 94.47% at 25°C and 69.59% at 40°C.
All multiphase fluids demonstrate a higher photothermal conversion efficiency than the base fluid at the same temperatures, thus indicating improved properties in the photothermal conversion process.

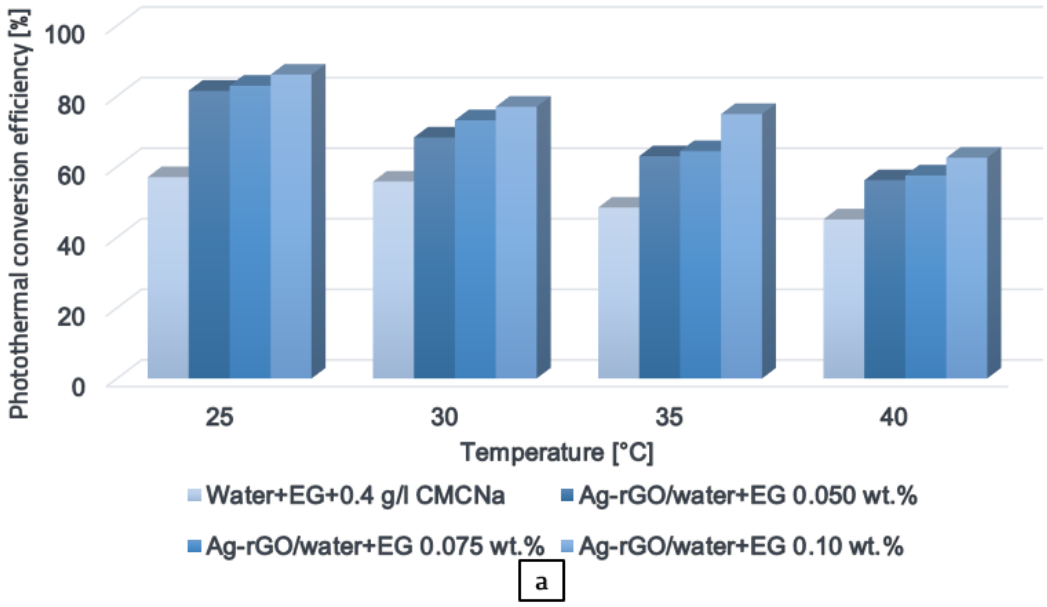

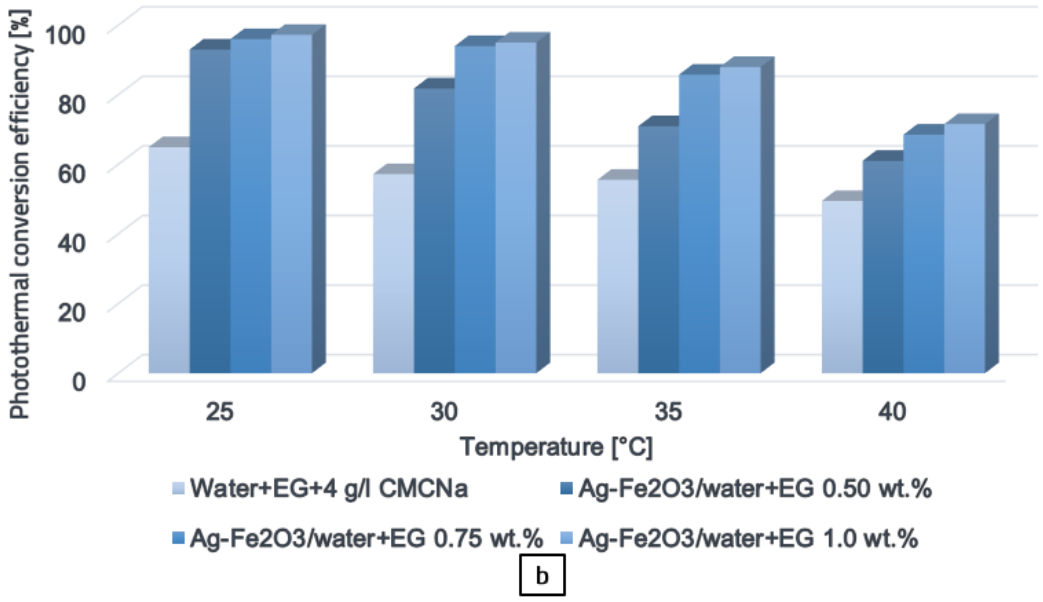

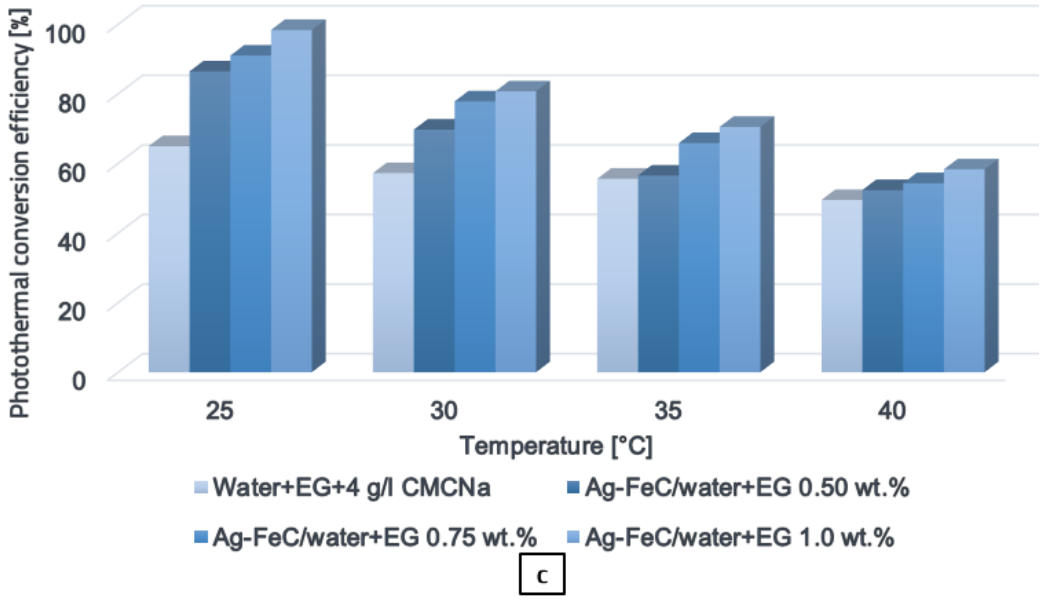

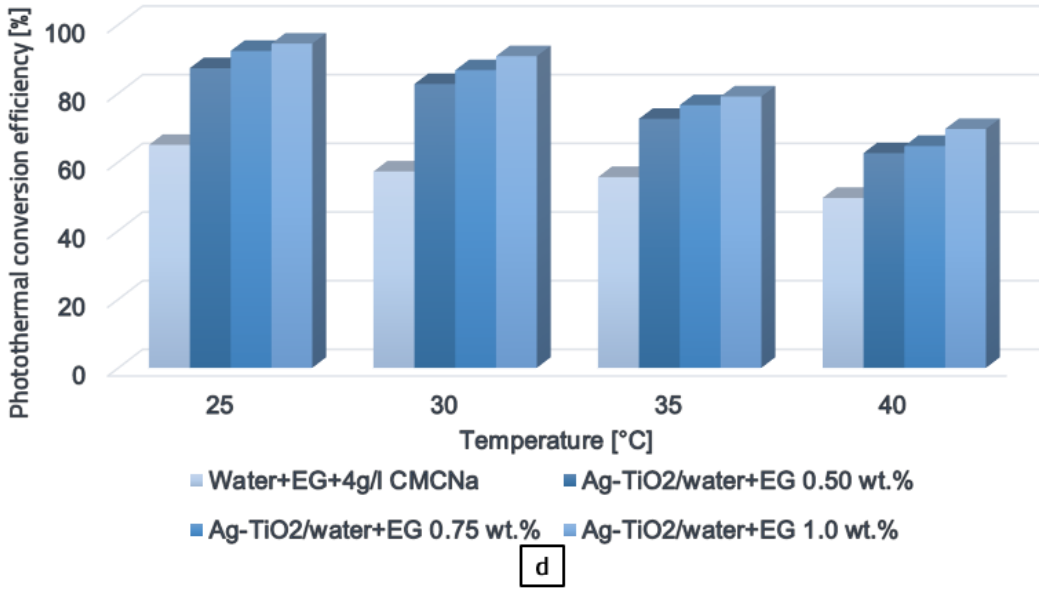

Figure 9.6. Variation of efficiency with temperature for water+EG-based multiphase fluids: a) Ag-rGO; b) Ag-Fe_2O_3; c) Ag-FeC; d) Ag-TiO_2

9.4 Conclusions on the photothermal conversion characteristics of multiphase fluids

Measurements were taken to determine the photothermal conversion efficiency for water, the water+EG (50:50) mixture and the multiphase fluids Ag-rGO/water, Ag-rGO/water+EG, Ag-Fe_2O_3/water, Ag-Fe_2O_3/water+EG, Ag-FeC/water, Ag-FeC/water+EG, Ag-TiO_2/water and Ag-TiO_2/water+EG at three mass concentrations (0.50, 0.75 and 1.0%) and (0.05, 0.075 and 0.1% for Ag-rGO) over a time range of 5-65 minutes. The results regarding the photothermal conversion characteristics of the multiphase fluids can be summarized as follows:

- As the mass concentration increased, the multiphase fluids exhibited higher photothermal conversion efficiency. The maximum photothermal conversion efficiency of 98.5% was achieved for the Ag-rGO/water fluid at a concentration of 0.1 wt% after 5 minutes, which was 86.72% higher than that of the water with 0.4 g/l CMCNa.
- The Ag-Fe_2O_3/water multiphase fluid at a concentration of 1 wt% achieved a photothermal conversion efficiency of 96.05% after 5 minutes, which was 81.91% higher than that of the base fluid (water with 4 g/l CMCNa).
- The Ag-rGO in water+EG with 0.4 g/l CMCNa, at a concentration of 0.1 wt%, recorded a maximum photothermal conversion efficiency of 94.4% after 5 minutes, which was 68.03% higher than that of the base fluid.
- For the water+EG fluids with 4 g/l CMCNa, Ag-FeC/water+EG at 1.0 wt% achieved the highest photothermal conversion efficiency of 98.69% after 5 minutes, which was 65.34% higher than that of the base fluid.

10. CONCLUSIONS, PERSONAL CONTRIBUTIONS and RESEARCH DIRECTIONS

This doctoral thesis primarily focused on enhancing the efficiency of solar collectors through the use of multiphase fluids. To achieve this, a detailed experimental study was conducted, during which the thermophysical properties, optical characteristics and photothermal conversion capabilities of these fluids were evaluated.

The main objective of the thesis was to develop new types of multiphase fluids that could contribute to improving the energy efficiency of solar collectors with direct absorption.

Multiphase fluids represent an innovation in national research, being a relatively new and rapidly expanding topic at the international level. In Romania, studies on multiphase fluids are still in their early stages, emphasizing the innovative nature of this work. This research marks an important step in advancing the knowledge base concerning multiphase fluids, being one of the first of its kind conducted at the national level.

Addressing this topic integrates elements from materials engineering, chemistry and physics. The research was conducted from both theoretical and experimental perspectives, aiming for a detailed analysis of the characteristics of these fluids. The results obtained highlighted the potential of multiphase fluids to bring significant improvements in energy efficiency, making them suitable for applications in the energy industry.

This work combines a thorough review of the specialized literature with the results of the author's own research. The findings presented in this doctoral thesis were obtained under the framework of the PN-III-P4-ID-PCE-2020-0353 project, CNCS-UEFISCDI, coordinated by Prof. Dr. Habil. Gabriela Huminic and have been published in prestigious journals, as listed in Annex 1. The research activity resulted in the publication of 7 articles in journals with an impact factor greater than 4, as well as the presentation of 2 papers at national and international conferences.

The main conclusions of the doctoral thesis are as follows:

Regarding the thermophysical properties of multiphase fluids, it can be concluded that for the three concentrations of nanoparticles added to the base fluids (water and water+EG), the following increases in the thermal conductivity of the multiphase fluids were observed:

- 6.14-10.69% for Ag-rGO/water; 9.12-13.02% for Ag-rGO/water+EG;
- 1.10-3.38% for Ag-Fe_2O_3/water; 1.56-4.70% for Ag-Fe_2O_3/water+EG;
- 6.61-8.92% for Ag-FeC/water; 2.23-5.89% for Ag-FeC/water+EG;
- 3.84-8.10% for Ag-TiO_2/water; 2.06-5.51% for Ag-TiO_2/water+EG;

For the dynamic viscosity of the studied multiphase fluids, the following increases were recorded:

- 0.29-18.77% for Ag-rGO/water; 62.43-141.56% for Ag-rGO/water+EG;
- 13.43-39% for Ag-Fe_2O_3/water; 3.64-13.65% for Ag-Fe_2O_3/water+EG;
- 8.44-16.34% for Ag-FeC/water; 7.16-18.08% for Ag-FeC/water+EG;
- 9.75-23.26% for Ag-TiO_2/water; 7.54-19.14% for Ag-TiO_2/water+EG;

For the density of the multiphase fluids, the following increases were recorded:

- 0.1-0.4% for Ag-rGO/water; 5.22-5.99% for Ag-rGO/water+EG;
- 0.1-0.9% for Ag-Fe_2O_3/water; 1.34-1.99% for Ag-Fe_2O_3/water+EG;
- 0.2-1.01% for Ag-FeC/water; 1.14-1.98% for Ag-FeC/water+EG;

- 0.4-1.2% for Ag-TiO_2/water; 1.15-2.18% for Ag-TiO_2/water+EG;

For the surface tension of the multiphase fluids, the following decreases/increases were recorded:

- Ag-rGO/water: At 0.05 and 0.075 wt%, it decreased by 5.00% and 3.38%. At 0.1 wt%, it increased by 5.01%.
- Ag-rGO/water+EG: It increased by 8.12%, 8.82% and 9.37% for 0.05, 0.075 and 0.1 wt%.
- Ag-Fe_2O_3/water: At 0.5, 0.75 and 1.0 wt%, it decreased by 11.95%, 10.02% and 8.74%.
- Ag-Fe_2O_3/water+EG: At 0.5 wt%, it decreased by 1.06%, while at 0.75 and 1.0 wt%, it increased by 1.25% and 4.73%.
- Ag-FeC/water: At 0.5 wt%, it decreased by 5.79%, while at 0.75 and 1.0 wt%, it increased by 9.81% and 14.14%.
- Ag-FeC/water+EG: It increased by 11.63%, 12.25% and 12.49% for 0.5, 0.75 and 1.0 wt%.
- Ag-TiO_2/water: At 0.5 wt%, it decreased by 9.32%, while at 0.75 and 1.0 wt%, it increased by 4.62% and 15.85%.
- Ag-TiO_2/water+EG: It decreased by 8.10%, 4.50% and 1.65% for 0.5, 0.75 and 1.0 wt%.

For the specific heat of the multiphase fluids, the following decreases were recorded:

- 0.01-0.72% for Ag-rGO/water; 4.97-5.67% for Ag-rGO/water+EG;
- 0.02-0.93% for Ag-Fe_2O_3/water; 1.33-1.96% for Ag-Fe_2O_3/water+EG;
- 0.21-1.02% for Ag-FeC/water; 1.13-1.96% for Ag-FeC/water+EG;
- 0.43-1.24% for Ag-TiO_2/water; 1.16-2.17% for Ag-TiO_2/water+EG;

Regarding the optical properties of the multiphase fluids, it can be concluded that the Ag-rGO multiphase fluid exhibited the best optical performance compared to the other studied fluids. It showed three times higher absorption than the base fluid, even at a low concentration of 0.1 wt%, both in water and in the water+EG mixture, for an optical path length of 1 mm. After the addition of nanoparticles, the transmittance of the Ag-rGO multiphase fluid decreased significantly and the average extinction coefficient reached a maximum value of 179.93 cm^{-1} in water and 178.70 cm^{-1} in water+EG, at a concentration of 0.1 wt%. Therefore, this multiphase fluid stands out as having the best optical properties for applications in optics and energy, compared to the other multiphase fluids analyzed.

Regarding the photothermal conversion properties:

Among all the multiphase fluids studied, the Ag-rGO/water multiphase fluid exhibited the best performance, achieving a maximum photothermal conversion efficiency of 98.5% at a concentration of 0.1 wt%. This remarkable result was achieved in just 5 minutes, which was 86.72% higher than the efficiency obtained for water with 0.4 g/l CMCNa. Therefore, Ag-rGO emerged as the most efficient multiphase fluid in terms of photothermal conversion, compared to the other multiphase fluids analyzed.

Based on the experimental results obtained, it can be concluded that the Ag-rGO/water multiphase fluid, at a concentration of 0.1 wt%, demonstrated the best performance among all the multiphase fluids analyzed. This fluid excelled in all essential aspects, both in terms of its thermophysical and optical properties, as well as its photothermal conversion capabilities, showing better behavior compared to the other studied multiphase fluids.

Given these results, the Ag-rGO/water multiphase fluid emerged as a viable solution for use in direct absorption solar collectors, due to its enhanced thermal, optical and photothermal conversion properties.

Personal contributions:

- This research represents the first international study of 8 types of multiphase fluids combining silver (Ag) with reduced graphene oxide (rGO), iron oxide (Fe_2O_3), iron carbide (FeC) and titanium dioxide (TiO_2) at three different concentrations (0.5, 0.75 and 1.0 wt% and 0.05, 0.075 and 0.1 wt% for Ag-rGO). These were dispersed both in water and in a 50:50 water+EG mixture.
- Experimental techniques were developed to characterize the thermophysical properties of silver-based multiphase fluids. A detailed database was created, which includes thermophysical parameters such as thermal conductivity, dynamic viscosity, density, surface tension and specific heat.
- Equations were developed to describe the dependence of thermal conductivity, dynamic viscosity, density and surface tension on temperature and the mass concentration of nanoparticles.
- Experimental techniques were developed to characterize the optical properties of multiphase fluids. A database was created, which includes essential optical properties such as transmittance, spectral absorption and extinction coefficients.
- A detailed evaluation of the photothermal conversion capabilities of multiphase fluids was conducted to understand and harness their potential for solar applications. The analysis focused on measuring and optimizing how multiphase fluids convert light energy into thermal energy, as well as enhancing the efficiency of solar systems.

The possible ***research directions*** resulting from this thesis are as follows:

- Intensifying research efforts to develop multiphase fluids with improved properties (especially by increasing thermal conductivity and reducing viscosity), so that they can be effectively used in DASC systems.
- Analyzing the impact of the composition and concentration of multiphase fluids on the performance of direct absorption solar collectors under real operating conditions.
- Developing theoretical models and numerical simulations to predict the thermal behavior of multiphase fluids in DASC systems, with the goal of optimizing the design of these systems and improving overall energy efficiency.
- Investigating the potential for integrating multiphase fluids into other renewable energy systems, as well as expanding research to explore new base fluids or surfactants that could enhance their properties.
- Analyzing the ecological effects of multiphase fluids in DASC systems by assessing potential environmental consequences and developing sustainable solutions to minimize natural resource consumption and carbon emissions.

References

[1] S. Choi, J.A. Eastman, Enhancing thermal conductivity of fluids with nanoparticles, Asme Fed, 66 (1995), pp. 99-105.

[2] S. Kakac, A. Pramuanjaroenkij, Review of convective heat transfer enhancement with nanofluids, Int. J. Heat Mass Transf., 52 (2009), pp. 3187-3196.

[3] Y. Xuan, Q. Li, Heat transfer enhancement of nanofluids, Int. J. Heat Fluid Flow, 21 (2000), pp. 58-64.

[4] R.P. Feynman,There's plenty of room at the bottom" at California institute of technology, Caltech Eng. Sci., 23 (1959), pp. 22-36.

[5] G. Huminic, A. Huminic, F. Dumitrache, C. Fleacă, I. Morjan, Study of the thermal conductivity of hybrid nanofluids: recent research and experimental study, Powder Technol., 367 (2020), pp. 347-357.

[6] P.K. Nagarajan, J. Subramani, S. Suyambazhahan, R. Sathyamurthy, Nanofluids for solar collector applications: a review, Energy Proc., 61 (2014), pp. 2416-2434.

[7] P. Alphonse, K. Muthukumarasamy, S. Elumalai, M. Kadamban, R. Dhairiyasamy, Optimization of heat transfer in heat pipes using nanofluids at various inclinations and filling levels, Case Stud. Therm. Eng., 65 (2024), Article 105624.

[8] R. Jibhakate, N. Nirwan, Y. Nandanwar, K.S. Rambhad, Thermal analysis of hybrid nanofluid flowing inside the automobile radiator, Mater. Today.: Proc., Available online 29 June 2023.

[9] H. Mehrarad, M.R.S. Emami, K. Afsari, Thermal performance and flow analysis in a brazed plate heat exchanger using MWCNT@ water/EG nanofluid, Int. Communicat. Heat Mass Transfer., 146 (2023), Article 106867.

[10] Y. Jia, G. Alva, G. Fang, Development and applications of photovoltaic–thermal systems: a review, Renew. Sustain. Energy Rev., 102 (2019), pp. 249-265.

[11] Y.A. Cengel, A.J. Ghajar, "Introduction and basic concept" in Heat and Mass Transfer Fundamental and Applications (5th ed.), McGraw-Hill Education, New York, NY, USA (2015), pp. 7-10.

[12] F. Selimefendigil, D. Okulu, H.F. Oztop, Application of ternary nanofluid and rotating cylinders in the cooling system of photovoltaic/thermoelectric generator coupled module and computational cost reduction, Appl. Therm. Eng., 250 (2024), Article 123436.

[13] Y.A. Cengel and J.M. Cimbala, Properties of fuids, in Fluid Mechanics: Fundamentals and Applications, McGraw-Hill (2014), pp. 37-73.

[14] Y.A. Cengel, M.A. Boles, Thermodynamics: an engineering approach (fourth ed.), McGraw-Hill (2002)

[15] A.W. Adamson, A.P. Gast, Physical Chemistry of Surfaces, Interscience Publishers, New York (1967), p. 150

[16] A. Aziz, A. Agha, S. Anwer, E. Abu-Nada, A. Alazzam, Numerical and experimental investigation of optimized triangular microchannels using mxene-based nanofluids for enhanced microfluidic thermal performance, Int. J. Thermofluids, 26 (2025), Article 101074.

[17] F.P. Incropera, D.P. DeWitt, Fundamentals of heat and mass transfer, John Wiley and Sons, New York, NY, USA (1996).

[18] F. Ren, Q. Li, P. Wang, Optimizing heat transfer in phase change thermal energy storage systems: A bionic method using alveolar vessel fins and nanofluids, Appl. Therm. Eng., 266 (2025), Article 125668.

[19] T.P. Otanicar, P.E. Phelan, J.S. Golden, Optical properties of liquids for direct absorption solar thermal energy systems, Sol. Energy, 83 (2009), pp. 969-977.

[20] N. Brekke, J. Dale, D. DeJarnette, P. Hari, M. Orosz, K. Roberts, E. Tunkara, T. Otanicar, Detailed performance model of a hybrid photovoltaic/thermal system utilizing selective spectral nanofluid absorption, Renew. Energy, 123 (2018), pp. 683-693.

[21] R. Taylor, T. Otanicar, Y. Herukerrupu, F. Bremond, G. Rosengarten, E. Hawkes, X. Jiang, S. Coulombe, Feasibility of nanofluid-based optical filters, Appl. Opt., 52 (7) (2013), pp. 1413-1422.

[22] Z. Meng, D. Wu, L. Wang, H. Zhu, Q. Li, Carbon nanotube glycol nanofluids: photo-thermal properties, thermal conductivities and rheological behavior, Particuology, 10 (2012), pp. 614-618.

[23] P.G. Kumar, V. Kumaresan, R. Velraj, Stability, viscosity, thermal conductivity and electrical conductivity enhancement of multi-walled carbon nanotube nanofluid using gum Arabic, Fullerene Sci. Technol., 25 (2017), pp. 230-240.

[24] A. Karthikeyan, S. Coulombe, A.M. Kietzig, Wetting behavior of multi-walled carbon nanotube nanofluids, Nanotechnology, 28 (2017), Article 105706.

[25] L. Wang, M. Wu, D. Wu, C. Zhang, Q. Zhu, H. Zhu, Optical absorption and photo-thermal conversion properties of CuO/H2O nanofluids, J. Nanosci. Nanotechnol., 15 (2015), pp. 3178-3181.

[26] M.U. Sajid, H.M. Ali, Thermal conductivity of hybrid nanofluids: a critical review, Int. J. Heat Mass Transf., 126 (2018), pp. 211-234.

[27] J. Sarkar, P. Ghosh, A. Adil, A review on hybrid nanofluids: recent research, development and applications, Renew. Sustain. Energy Rev., 43 (2015), pp. 164-177.

[28] N.A.C. Sidik, I.M. Adamu, M.M. Jamil, G.H.R. Kefayati, G. Najafi, Recent progress on hybrid nanofluids in heat transfer applications: a comprehensive review, Int. Commun. Heat Mass Transf., 78 (2016), pp. 68-79.

[29] J. Qu, R. Zhang, Z. Wang, Q. Wang, Photo-thermal conversion properties of hybrid CuO-MWCNT/H_2O nanofluids for direct solar thermal energy harvest, Appl. Therm. Eng., 147 (2019), pp. 390-398.

[30] J.E. Minardi, H.N. Chuang, Performance of a "black" liquid flat-plate solar collector, Sol. Energy, 17 (1975), pp. 179-183.

[31] NIST Reference Fluid Thermodynamic and Transport Properties Database (REFPROP), http://www.nist.gov/srd/nist23.cfm (2007) (accessed on 22 November 2024).

[32] ASHRAE Handbook: Fundamentals, American Society of Heating, Refrigerating and Air-Conditioning, Engineers Inc., Atlanta, GA (2017).

[33] ***A. Vărdaru***, G. Huminic, A. Huminic, C. Fleaca, F. Dumitrache, I. Morjan, Aqueous hybrid nanofluids containing silver-reduced graphene oxide for improving thermo-physical properties, Diam. Relat. Mater., 132 (2023), Article 109688.

[34] G. Huminic, A. Huminic, ***A. Vărdaru***, F. Dumitrache, C. Fleacă, Experimental investigation on Ag NPs-rGO-water/ethylene-glycol hybrid nanofluids used in solar applications, Diam. Relat. Mater., 143 (2024), Article 110851.

[35] M. Chereches, ***A. Vărdaru***, G. Huminic, E.I. Chereches, A.A. Minea, A. Huminic, Thermal conductivity of stabilized PEG 400 based nanofluids: An experimental approach, Int. Commun. Heat Mass Transf, 130 (2022), Article 105798.

[36] P. Kanti, K.V. Sharma, R.S. Khedkar, Tauseef-ur Rehman, Synthesis, characterization, stability and thermal properties of graphene oxide based hybrid nanofluids for thermal applications: experimental approach, Diam. Relat. Mater., 128 (2022), Article 109265.

[37] G. Huminic, ***A. Vărdaru***, A. Huminic, C. Fleacă, F. Dumitrache, I. Morjan, Water-based graphene oxide–silicon hybrid nanofluids—experimental and theoretical approach, Int. J. Mol. Sci., 23 (2022), p. 3056.

[38] ***A. Vărdaru***, G. Huminic, A. Huminic, C. Fleacă, F. Dumitrache, I. Morjan, Synthesis, characterization and thermal conductivity of water based graphene oxide–silicon hybrid nanofluids: An experimental approach, Alexan. Eng. J., 61 (12) (2022 Dec 1), pp. 12111-12122.

[39] H. Yarmand, S. Gharehkhani, G. Ahmadi, S.F.S. Shirazi, S. Baradaran, E. Montazer, et al., Graphene nanoplatelets silver hybrid nanofluids for enhanced heat transfer, Energy Convers. Manage., 100 (2015), pp. 419-428.

[40] S. Askari, et al., Rheological and thermophysical properties of ultra-stable kerosene-based Fe3O4/graphene nanofluids for energy conservation, Energy Convers. Manag., 128 (2016), pp. 134-144.

[41] S.N. Shoghl, J. Jamali, M.K. Moraveji, Electrical conductivity, viscosity and density of different nanofluids: an experimental study, Exp. Thermal Fluid Sci., 74 (2016), pp. 339-346.

[42] R.S. Vajjha, D.K. Das, B.M. Mahagaonkar, Density measurement of different nanofluids and their comparison with theory, Pet. Sci. Technol., 27 (6) (2009), pp. 612-624.

[43] O. Mahian, A. Kianifar, S. Wongwises, Dispersion of ZnO nanoparticles in a mixture of ethylene glycol-water, exploration of temperature-dependent density and sensitivity analysis, J. Clust. Sci., 24 (4) (2013), pp. 1103-1114.

[44] B. Saleh, L.S. Sundar, Entropy generation and exergy efficiency analysis of ethylene glycol-water based nanodiamond + Fe3O4 hybrid nanofluids in a circular tube, Powder Technol., 380 (2021), pp. 430–442.

[45] L.S. Sundar, S. Mesfin, E.V. Ramana, Z. Said, A.C. Sousa, Experimental investigation of thermo-physical properties, heat transfer, pumping power, entropy generation and exergy efficiency of nanodiamond+ Fe3O4/60: 40% water-ethylene glycol hybrid nanofluid flow in a tube, Thermal Sci. Eng. Prog., 21 (2021), Article 100799.

[46] G. Huminic, A. Huminic, ***A. Vărdaru***, C. Fleacă, F. Dumitrache, I. Morjan, Surface tension of rGO-Ag based hybrid nanofluids, J. Mol. Liq., 390 (2023), Article 123002.

[47] J.J. Jasper, Surface Tension of Pure Liquid Compounds, J. Phys. Chem. Ref. Data, 1 (1972), pp. 841-1009.

[48] A.K. Connors, L.J. Wright, Dependence of Surface Tension on Concentration of Binary Aqueous-Organic Solutions, Anal. Chem., 61 (1989), pp. 194-198.

[49] A.R. Harikrishnan, P. Dhar, P.K. Agnihotri, S. Gedupudi, S.K. Das, Effects of interplay of nanoparticles, surfactants and base fluid on the surface tension of nanocolloids, Eur. Phys. J. E, 40 (2017), pp. 53-67.

[50] D. Cabaleiro, et al., Dynamic viscosity and surface tension of stable graphene oxide and reduced graphene oxide aqueous nanofluids, J. Nanofluids, 7 (2018), pp. 1081-1088.

[51] G. Huminic, A. Huminic, F. Dumitrache, C. Fleaca, Ion Morjan, Experimental study of thermo-physical properties of nanofluids based on γ-Fe2O3 nanoparticles for heat transfer applications, Heat Transfer Eng., 38 (2017), pp. 1496-1505.

[52] A. Huminic, G. Huminic, C. Fleaca, F. Dumitrache, I. Morjan, Thermal conductivity, viscosity and surface tension of nanofluids based on FeC nanoparticles, Powder Technol., 284 (2015), pp.78-84.

[53] S. Zhang, X. Han, Y. Tan, K. Liang, Effects of hydrophilicity/lipophilicity of nano-TiO_2 on surface tension of TiO_2-water nanofluids, Chem. Phys. Lett., 691 (2018), pp. 135-140.

[54] I. Fazeli, M.R. Sarmasti Emami, A. Rashidi, Investigation and optimization of the behavior of heat transfer and flow of MWCNT-CuO hybrid nanofluid in a brazed plate heat exchanger using response surface methodology, Int. Commun. Heat Mass Transf., 122 (2021), Article 105175.

[55] I.M. Shahrul, I.M. Mahbubul, S.S. Khaleduzzaman, R. Saidur, M.F.M. Sabri, A comparative review on the specific heat of nanofluids for energy perspective, Renew. Sustain. Energy Rev., 38 (2014), pp. 88-98.

[56] M. Devarajan, et al., Thermophysical properties of CNT and CNT/Al2O3 hybrid nanofluid, Micro Nano Lett., 13 (2018), pp. 617-621.

[57] Y. Gao, Y. Xi, Y. Zhenzhong, A. Sasmito, A. Mujumdar, L. Wang, Experimental investigation of specific heat of aqueous graphene oxide Al2O3 hybrid nanofluid, Therm. Sci., 25 (1B) (2021), pp. 515-525.

[58] N. Ahammed, L.G. Asirvatham, S. Wongwises, Entropy generation analysis of graphene–alumina hybrid nanofluid in multiport minichannel heat exchanger coupled with thermoelectric cooler, Int. J. Heat Mass Transf., 103 (2016), pp. 1084-1097.

[59] L.S. Sundar, M.K. Singh, A.C.M. Sousa, Enhanced heat transfer and friction factor of MWCNT-Fe3O4/water hybrid nanofluids, Int. Commun. Heat Mass Transf., 52 (2014), pp. 73-83.

[60] E.C. Okonkwo, I. Wole-Osho, D. Kavaz, M. Abid, T. Al-Ansari, Thermodynamic evaluation and optimization of a flat plate collector operating with alumina and iron mono and hybrid nanofluids, Sustain. Energy Technol. Assessments, 37 (2020), Article 100636.

[61] H. Yarmand, et al., Study of synthesis, stability and thermo-physical properties of graphene nanoplatelet/platinum hybrid nanofluid, Int. Commun. Heat Mass Transf., 77 (2016), pp. 15-21.

[62] G.M. Moldoveanu, A.A. Minea, Specific heat experimental tests of simple and hybrid oxide-water nanofluids: Proposing new correlation, J. Mol. Liq., 279 (2019), pp. 299-305.

[63] S. Kannaiyan, C. Boobalan, A. Umasankaran, A. Ravirajan, S. Sathyan, T. Thomas, Comparison of experimental and calculated thermophysical properties of alumina/cupric oxide hybrid nanofluids, J. Mol. Liq., 244 (2017), pp. 469-477.

[64] V.V. Wanatasanappan, M.Z. Abdullah, P. Gunnasegaran, Thermophysical properties of Al2O3-CuO hybrid nanofluid at different nanoparticle mixture ratio: An experimental approach, J. Mol. Liq., 313 (2020), Article 113458.

[65] G. Huminic, ***A. Vărdaru***, A. Huminic, C. Fleacă, F. Dumitrache, Broad-band absorption and photo-thermal conversion characteristics of rGO-Ag hybrid nanofluids, J. Mol. Liq., 408 (2024), Article 125347.

[66] Z.Y. Sun, N.N. Dong, K.P. Wang, D. Konig, T.C. Nagaiah, M.D. Sanchez, et al., Ag-stabilized few-layer graphene dispersions in low boiling point solvents for versatile nonlinear optical applications, Carbon, 62 (2013), pp. 182-192.

[67] R. Zhang, J. Qu, M. Tian, X. Han, Q. Wang, Efficiency improvement of a solar direct volumetric receiver utilizing aqueous suspensions of CuO, Int. J. Energy Res., 42 (2018), pp. 2456-2464.

APPENDIX 1. Research results presented in papers published in scientific journals or presented at conferences

Published articles in Web of Science-indexed journals with impact factor (IF):

[1] M. Chereches, ***A. Vărdaru***, G. Huminic, E.I. Chereches, A.A. Minea, A. Huminic, Thermal conductivity of stabilized PEG 400 based nanofluids: An experimental approach, Int. Commun. Heat Mass Transf, 130 (2022), Article 105798, IF = 6.4.

[2] G. Huminic, ***A. Vărdaru***, A. Huminic, C. Fleacă, F. Dumitrache, I. Morjan, Water-based graphene oxide–silicon hybrid nanofluids—experimental and theoretical approach, Int. J. Mol. Sci., 23 (2022), p. 3056, IF = 4.9.

[3] ***A. Vărdaru***, G. Huminic, A. Huminic, C. Fleacă, F. Dumitrache, I. Morjan, Synthesis, characterization and thermal conductivity of water based graphene oxide–silicon hybrid nanofluids: An experimental approach, Alexan. Eng. J., 61 (12) (2022 Dec 1), pp. 12111-12122, IF = 6.2.

[4] ***A. Vărdaru***, G. Huminic, A. Huminic, C. Fleaca, F. Dumitrache, I. Morjan, Aqueous hybrid nanofluids containing silver-reduced graphene oxide for improving thermo-physical properties, Diam. Relat. Mater., 132 (2023), Article 109688, IF = 4.3.

[5] G. Huminic, A. Huminic, ***A. Vărdaru***, C. Fleacă, F. Dumitrache, I. Morjan, Surface tension of rGO-Ag based hybrid nanofluids, J. Mol. Liq., 390 (2023), Article 123002, IF = 5.3.

[6] G. Huminic, A. Huminic, ***A. Vărdaru***, F. Dumitrache, C. Fleacă, Experimental investigation on Ag NPs-rGO-water/ethylene-glycol hybrid nanofluids used in solar applications, Diam. Relat. Mater., 143 (2024), Article 110851, IF = 4.3.

[7] G. Huminic, ***A. Vărdaru***, A. Huminic, C. Fleacă, F. Dumitrache, Broad-band absorption and photo-thermal conversion characteristics of rGO-Ag hybrid nanofluids, J. Mol. Liq., 408 (2024), Article 125347, IF = 5.3.

Papers presented at conferences:

[8] ***A. Vărdaru***, G. Huminic și A. Huminic, Thermal conductivity of water based silver-graphene oxide hybrid nanofluids, The 10th International Conference on Advanced Concepts in Mechanical Engineering ''ACME 2022'', June 6-7, 2022, Iași, Romania.

[9] ***A. Vărdaru***, G. Huminic și A. Huminic, Study of hybrid nanofluids used in direct absorption solar collectors, XXIIIrd National Conference on Thermodynamics with International Participation "NACOT 2023", May 11-13, 2023, Galați, Romania.